UNIVERSIDAD AUTÓNOMA DE MADRID

DEPARTAMENTO DE BIOQUÍMICA

PHYSIOLOGICAL AND PHARMACOLOGICAL MODULATION OF K_V7 CHANNELS

Alicia de la Cruz Fernández

Madrid 2017

DEPARTAMENTO DE BIOQUÍMICA

FACULTAD DE MEDICINA

UNIVERSIDAD AUTÓNOMA DE MADRID

PHYSIOLOGICAL AND PHARMACOLOGICAL MODULATION OF K_V7 CHANNELS

Alicia de la Cruz Fernández

Licenciada en Bioquímica

Directoras de Tesis:

Dra. Carmen Valenzuela Miranda, Investigador Científico del Consejo Superior de Investigaciones Científicas (CSIC)

Dra. Teresa González Gallego, Investigador Ramón y Cajal de la Universidad Autónoma de Madrid

Departamento de Bioquímica, Facultad de Medicina, UAM

Instituto de Investigaciones Biomédicas "Alberto Sols" (CSIC-UAM)

Madrid 2017

Carmen Valenzuela Miranda, Investigador Científico del Consejo Superior de Investigaciones Científicas y **Teresa González Gallego** Investigadora Ramón y Cajal de la Universidad Autónoma de Madrid, en el Instituto de Investigaciones Biomédicas "Alberto Sols" (CSIC-UAM) de Madrid,

CERTIFICAN que

Alicia de la Cruz Fernández, Licenciada en Bioquímica por la Universidad Autónoma de Madrid ha realizado bajo su dirección el trabajo de investigación titulado:

"Physiological and pharmacological modulation of K_V7 channels"

y consideran que el trabajo realizado reúne todas las condiciones requeridas por la legislación vigente, así como la originalidad y calidad científica necesarias, para poder ser presentado y defendido con el fin de optar al grado de Doctor por la Universidad Autónoma de Madrid.

Y para que así conste y surjan los efectos oportunos, firman el presente certificado en Madrid a 11 de mayo de 2017.

Firma Directora de la Tesis Doctoral
Dra. Carmen Valenzuela Miranda
Investigador Científico del CSIC

Firma Directora de la Tesis Doctoral
Dra. Teresa González Gallego
Investigadora Ramón y Cajal

El trabajo descrito en la presente Tesis Doctoral ha sido llevado a cabo en el departamento de modelos experimentales de enfermedades humanas del Instituto de Investigaciones Biomédicas “Alberto Sols” (CSIC-UAM) y ha sido financiado por los siguientes proyectos de investigación.

Red Temática de Enfermedades Cardiovasculares RECAVA. Instituto de Salud Carlos III. FIS (RD06/0014/0006).2007-2012. Investigador principal: Lisardo Boscá

Modulación adrenérgica de los canales K_V1.5-K_Vβ1.3 expresados en diferentes tipos de células cardiovasculares. CICYT (SAF2010- 14916). 2011-2013. Investigador principal: Carmen Valenzuela Miranda

Red Temática de Enfermedades Cardiovasculares RECAVA. Instituto de Salud Carlos III. FIS (RD12/0042/0019). 2013-2015. Investigador principal Carmen Valenzuela Miranda

Canalosoma de K_V1.5: Papel de Lgi1-4 Sig-1R. Consecuencias Farmacológicas. CICYT (SAF2013-45800-R). 2014-2016. Investigador principal Carmen Valenzuela Miranda y Teresa González Gallego

“La mente es como un paracaídas, sólo funciona si se abre”

Albert Einstein (1879 – 1955)

A mis padres,

a los que admiro casi tanto como quiero.

"Hay que hacer de la vida un sueño; y de un sueño, una realidad"

Georges Benjamin Clemenceau (1841 – 1929)

A Dani

"Es preciso sacudir enérgicamente el bosque de las neuronas adormecidas: es menester hacerlas vibrar con la emoción de lo nuevo e infundirles nobles y elevadas inquietudes"

Santiago Ramón y Cajal (1852 – 1934)

Parece mentira que hayan pasado casi 6 años desde que entré en el laboratorio. Por un lado, parece que fue ayer, y por otro es como si hubiera pasado toda mi vida allí. Aunque por supuesto han pasado cosas buenas y malas, en general estos años han sido muy buenos. Mi entrada en el laboratorio no fue lo que yo esperaba, empezó siendo más duro de lo que yo podía imaginar, incluso cuando mi ilusión y motivación estaban al máximo. Por no tener resultados especialmente fructíferos y por perder las ganas de estar allí, esa ilusión y motivación fueron apagándose. Sin embargo, tras hablar con la Dra. Carmen Valenzuela, la cual me dijo literalmente "Alicia, tienes que coger al toro por los cuernos", todo cambió, lo cogí. A partir de ahí todo fue mejorando, la relación con la gente del laboratorio mejoró y mi motivación e ilusión volvieron.

A Carmen, quiero agradecerle que me diera la oportunidad de trabajar en su laboratorio y que contrato tras contrato confiara en mí. Quiero agradecerle todo lo que me ha enseñado de ciencia en general y concretamente de electrofisiología (la cual creo que es la ciencia más bonita). También quiero agradecerle otras enseñanzas, como que el trabajo duro se ve recompensado, como que es necesario tener una actitud positiva en la vida para afrontar todos los baches que vayan viniendo y como que todo, por poco que sea, hay que celebrarlo. Creo que, por el resultado de estos casi 6 años, aquel día en el que me entrevistaste, las dos acertamos. Por otro lado, quiero agradecer a la Dra. Teresa González, haberme enseñado la técnica de patch-clamp y electrofisiología. Y también que a los "duendes" del patch se les vence con paciencia y perseverancia.

Quiero agradecer su trato cercano y amabilidad a Ana Pérez, Rosario Perona, Leandro Sastre, Ángel Pascual y Ana Aranda.

Quisiera agradecer a Toño (marido de Carmen), que llamara a Carmen para que fuese a cenar a casa, cuando ya era tarde, y así poder irme yo a casa también. Pero sobretodo quiero agradecerle que desde el primer día me tratara con tanto cariño.

Por orden (más o menos) cronológico, quisiera agradecer a Cristina y Álvaro, mis primeros compis del laboratorio, todos aquellos momentos de risas que pasamos juntos mientras yo hacía mis primeros experimentos. Recuerdo aquellos tiempos como muy divertidos, aunque supongo que ellos no porque estaban acabando la tesis y la presión va en aumento. A Cris, me gustaría agradecerle que me enseñara a hacer patch-clamp con parche perforado y que me enseñara que el trabajo en equipo en un laboratorio siempre da buenos resultados para todos. También quiero agradecerle todos los buenos momentos fuera del laboratorio, tanto de cenas y teatros, como de congresos. A Álvaro, que aparte de enseñarme cosas de patch, me enseñara lo que es el "verdadero gitaneo" y todas las risas subyacentes. Poco después llegó Ángela (estábamos las dos en la misma fase de la tesis). Desde mi punto de vista, Ángela y yo nos complementábamos perfectamente. Trabajar con ella codo con codo durante aproximadamente dos años, fue un verdadero placer, porque además de trabajadora es una gran persona. Poco después vino una época un poco más solitaria en el labo. Pero, como de hasta de lo malo algo bueno se puede sacar, en esa época empecé a conocer mejor a mi querido "Laboratorio amigo 1.9". Allí estaban/están Jose, Marina y Sandra. ¡¡Qué decir de ellos!!, que aparte de estar siempre dispuestos a ayudar a un científico perdido, son la alegría de la huerta!!! Gracias por estos años de cafés, marujeos y risas máximas!!!. Durante estos años también me apoyé mucho en María y Eva. A Eva, agradecerle todas aquellas comidas tan entretenidas y toda su ayuda con experimentos que se me atravesaban. Y a Mery, lo primero agradecerle que con Jose (1.9, o twitero-fiestero máximo del iib) volvieran a traer las fiestas de Navidad al instituto (esas fiestas donde agradeces que el vecino vaya igual de borracho que tú, para que no se acuerde de lo que le contaste…) y después, que por cosas del destino, estos últimos años hemos estado juntas, y que por mi parte ha sido un verdadero placer, tanto en lo intelectual como en lo personal. De aquella época, no me quiero olvidar de gente como Mario, que aunque se fue hace bastante tiempo también eran muy divertidas las comidas gracias a él. Y a Toño, con el cual he disfrutado y disfruto mucho hablando de casi cualquier tema, pero sobretodo de ciencia y de política.

No sé si simultáneamente, o poco después, vino una avalancha de estudiantes al labo. Allí se juntaron Pilar, Lucía y Diego. Que vinieran, fue como volver a la primera época, donde había muy buen ambiente en el laboratorio. A Pilar y a Lucía, me gustaría agradecer el buen rollo y la alegría que trajeron al labo. Aunque duró poco, fue intenso. A Diego, bueno no, a Don Diego Peras(z)a Péres(z), por traer la alegría de nuevo al laboratorio, y por estar siempre

dispuesto a aprender y a ayudar, y por todo lo que me ha enseñado. Pero sobretodo, por conseguir sacarme una sonrisa cuando el estrés del laboratorio sacaba lo peor de mí.

Esta última época, por necesidad de la crisis (cada vez había menos gente en el instituto) nos arrejuntamos a comer con "nueva" gente…Muy nueva no era porque a María (Tiana) la conozco desde aquellas tardes en la biblioteca de ciencias donde nos juntábamos a marujear sobre nuestros novios (hoy, menos mal, exs).
De ahí quisiera agradecer su buen rollo y el haberme acogido a Gemma, Chus, Diego, María, Asun y Toño (de nuevo). De ese grupo surgió algo muy muy divertido "las mujeres fetén en chochorts" Donde además de las locas de las Merys está Asun, un auténtico fichaje (que pretende disimular por haber ido a un colegio de monjas) Laura (boluda) divertida como pocas, y Alba, que es un auténtico encanto de persona. A mis mujeres fetén, agradecerlas este año de risas sin parar y aprendizaje de la vida máximo. Y por muchos más días de conquistar el mundo, ya sea en un bar o una terraza.

Quisiera también mencionar a los nuevos fichajes del labo, a mari-Alba, q no!!! A Alba, nuevo super-fichaje, y a los estudiantes pasados y futuros como Pablo, María y Javi. Ha sido un placer conoceros y compartir labo con vosotros.

Para ir acabando con la gente del iib agredecer a Guti y a Alex todas sus enseñanzas de informática (aunque es mejor llamarles, que vienen, te lo arreglan y encima te echas unas risas) y a Carlos y a Diego. A Diego por darme siempre los buenos días de buen humor y dejarme la luz encendida del pasillo cuando me voy a las 21:30 del iib. Y a Carlos, por gruñirme cada día, y por hacerme todos los favores que le pido, incluso abrirme la puerta cuando se me olvida la tarjeta.

Por supuesto a todos los labos amigos como el labo de Ángel y Paco o el de Antonio Felipe en Barcelona (por todas aquellas biofísicas y RECIs juntos). También en general a toda la gente del iib con la que he compartido estos casi 6 años.

Respecto a la parte de mi vida personal, en estos 6 años han pasado muchas cosas, intentaré resumir. Primero quisiera agradecer que comenzaran y siguieran en mi viaje por la biología, todos mis queridos biolok@s, a los que quiero de manera diferente, porque cada uno de ellos es único, y mis vivencias con cada uno de ellos también: Sólo contando todo lo que hemos vivido durante estos 12 años, podría escribir otra tesis. Por tanto, y sin seguir ningún orden en especial, gracias a Alfonso, Ana, Andrés, Belén, Blanca, Cande, Caselles, Helen, Ceci, Javi, Laura, Luis, Martis, Pili y Soledad por formar parte de mi vida. Sin vosotros, el viaje no hubiera merecido tanto la pena.

Quisiera agradecer a mi amigo Javi y a mi amiga Kei el que estéis en mi vida, me siento muy afortunada por teneros y espero que nuestra amistad dure muchos años más!

También quiero agradecer a mis samberos todo lo que me habéis enseñado y aportado estos últimos años. He disfrutado y disfruto mucho con vosotros. Gracias a Jorge, Roi, Tonino, Laura. Hairen, Chabi, y ahora también Noa.

Quisiera agradecer a mi amiga Eunate, el que después de toda una vida siga ahí, para cuando la necesito. Nos conocimos con 6 años y aquí seguimos. Esto es amor del bueno! Ánimo con tu Tesis! Nuestro "colmo" sería presentarla el mismo día!

También quería agradecer a Lore todos los momentos geniales que hemos pasado juntas, en este nuestro barrio, el Barrio del Pilar. Por todas nuestras aventuras de post-próxima adolescencia, nuestros viajes y nuestra amistad.

Un huequito grande en mi corazón es para mis "Rusas", desde que os conocí, mi vida cambió, y he de decir que si ya era difícilmente mejorable, mejoró. Orgullosa de ser capitana de un equipo tan grande de personas (porque el voleibol se nos da de aquella manera). Gracias a todas por celebrar los éxitos y los fracasos juntas y por aguantarme en mis épocas pre-tésicas con una sonrisa. Gracias a Luci, Belu, Eva, Luci Suazo, Malena, Antía, Mariu, y especialmente a las veteranas Natasha, Vero, Soni, Babel, Montsita y Noe. Haré mención especial a la libero, Vero; porque aunque todo lo que tiene de pequeña lo tiene de tocapelotas, es una gran persona y me alegro mucho tanto de haberla conocido como de tenerla a mi lado (el puesto sólo será tuyo cuando yo me vaya). A Soni, la cual es un portento científico, digno de estudio, bien conservado por el etanol. Todo en ella es bueno y bonito. Y a su "patillas" por ser el mejor embajador y profesor, y regalarnos tardes tan divertidas. Y a Noe y Montsita, que lo

siento, pero sois un pack. De hecho, un maravilloso pack, no sólo habéis sido las protagonistas de varios de los mejores viajes de mi vida sino que además sois un claro ejemplo de simpatía, fortaleza, inteligencia y actitud. Yo de mayor quiero ser como vosotras. Gracias por haber sacado a la "loquilla" que llevo dentro. Gracias por estar siempre. Y sobre todo porque mi vida sin vosotras sería mucho más aburrida. Por supuesto por contribuir en este trabajo, os tendría que haber puesto en las citas. Labor edición Mon, Labor diseño Noe. Aprovechando la coyuntura, quisiera agradecer a Laura y Juanito, otros dos viajeros, el haberme siempre tratado con cariño, y decir que lo viajes no hubieran sido lo mismo sin vosotros!!!. Por muchas más aventuras juntos!!!

Quisiera agradecer a toda mi familia, mís tíos, Cristina y Jose, Concha y Sonsoles, el haber estado siempre ahí unidos, y apoyándome. A mis primas Laura, Jime y Lucía por todo lo que me enseñan día a día (aunque yo sea la mayor), y porque son un claro ejemplo de fortaleza. Gracias por vuestro cariño. Y a los chicos, Dani (sin palabras ;) y Alex.

Quisiera agradecer especialmente a mi amiga-prima (con acento niña de la mía bosnia), "lorito" el estar siempre ahí. El poder contar con ella para todo, pero sobre todo por todos esos momentos que me ha regalado y me regala día a día. Un sabio dijo una vez, que la familia no se la elige, y por tanto no hay que quererla. Yo te elijo y te quiero!!! También agradecer a su actual pareja, Edu; todo lo que hemos vivido juntos, y el trato tan amable y cariñoso que me ha dado siempre.

Por ir acabando, mis incondicionales. A mi hermana Paula, para la cual no tengo palabras, ella ya sabe cuánto de especial es. A Tim, del que diré que me alegro mucho de que estés en nuestras vidas, contigo nos enriquecemos. A mis bichillos (Ciro y Emilia) que son todo amor y ternura. Y a mis padres, a los que dedico esta Tesis, porque gracias a ellos, a su esfuerzo, a su perseverancia y a no tirar nunca jamás la toalla hoy en día soy la mujer que soy. Gracias por habérmelo dado TODO, pero sobretodo cariño incondicional y apoyo.

Por último, a Dani, que aunque cuando comencé la Tesis no te conocía, has conseguido que estos dos últimos años a tu lado fueran inmejorables. Gracias por tu amor. Gracias por enseñarme a ser mejor persona y sacar lo mejor de mí. Gracias por tu respeto y apoyo en absolutamente todo lo que hago. Y gracias por todos los momentos, buenos y malos, que hemos pasado juntos y que nos hacen disfrutar y avanzar como personas. Espero poder compartir el camino contigo.

No soy una persona a la que le gusten los cambios, y ahora empieza un camino desconocido para mí. Si soy una persona optimista, así que con optimismo afrontaré esta nueva etapa y todo lo que el futuro me quiera deparar.

“El hombre que ha perdido la facultad de maravillarse, es un hombre muerto”

Pierre Curie (1859 – 1906)

Los canales de potasio dependientes de voltaje (K_V) son proteínas de membrana involucradas en diversos procesos fisiológicos y patológicos tales como la respuesta inmune y la función cardiovascular. Nuestro primer objetivo fue determinar el posible papel que los canales heterotetraméricos $K_V7.1/K_V7.5$ en músculo liso vascular. Para ello, estudiamos los niveles de expresión de ambos canales en diferentes miocitos vasculares. Se estudió la interacción de ambos canales tanto en un sistema de expresión heterólogo como en células nativas de aorta de rata. Los canales $K_V7.1$ se localizan en dominios enriquecidos de lípidos en las membranas celulares. La presencia de canales $K_V7.5$ modula su localización en estos dominios y por tanto su regulación fisiológica. En aquellos tejidos donde ambas isoformas están presentes, la localización de canales en membrana es fuera de las balsas lipídicas. Gracias a la técnica de patch-clamp se determinó que los canales $K_V7.1/K_V7.5$ eran canales funcionales. El resultado obtenido de la activación de los canales $K_V7.1/K_V7.5$ fueron corrientes fenotípicamente intermedias entre las obtenidas para cada uno de los canales por separado. Además, se demostró que, en presencia de subunidades reguladoras (KCNE1 Y KCNE3), los canales muestran características electrofisiológicas y farmacológicas propias. Retigabine es un fármaco (activador) ampliamente usado en el estudio de los canales K_V7. Los canales $K_V7.1/K_V7.5$ son susceptibles de regulación por retigabine. Por último, se estudió la implicación de estos canales en la regulación del tono vascular. Se midió la capacidad de relajación de arterias coronarias, pre-constreñidas con bloqueantes de canales K_V7. Se determinó que los canales $K_V7.1/K_V7.5$ están presentes en dichas arterias e involucrados en la regulación del tono vascular. Por otro lado, se estudió el canal $K_V7.1$, junto con la subunidad reguladora, KCNE1, con la que forma una de las corrientes más importantes de la fase de repolarización del potencial de acción cardíaco (I_{Ks}). Se analizaron los efectos de la aplicación aguda y crónica de ácidos grasos poliinsaturados (AGPIs), DHA y AA, en la corriente generada por $K_V7.1$/KCNE1 expresados en células COS-7 mediante la técnica de patch-clamp. La perfusión aguda de DHA y AA aumentó la magnitud de la corriente de los canales $K_V7.1$/KCNE1. DHA, pero no AA, hizo más lenta la cinética de activación de la corriente. Ambos, aceleraron la corriente de cierre de los canales. La aplicación crónica de estos compuestos, no aumentó la magnitud de la corriente. Sin embargo, DHA desplazó la dependencia de voltaje de los canales a valores más electronegativos del potencial de membrana, e hizo más rápida la cinética de activación y la cinética de cierre de los canales. La aplicación crónica de AA ralentizó la cinética de activación y aceleró la cinética de cierre. Además, DHA crónico disminuyó la expresión de $K_V7.1$ pero no de KCNE1, e indujo una redistribución de $K_V7.1$ en la membrana celular. El efecto producido por los ácidos grasos sobre los canales $K_V7.1$/KCNE1, depende tanto de la naturaleza del compuesto, n-3 o n-6 AGPIs, como del modo de administración, agudo o crónico. Los mediadores lipídicos derivados de AGPIs n-6 y n-3, como lipoxinas y resolvinas (cuya producción aumenta tras la ingesta de aspirina), han surgido como nuevos y potentes agentes que regulan la inflamación aguda promoviendo la resolución. Los canales iónicos juegan un papel esencial en la fisiología de los macrófagos. Por ello, se estudió los efectos de estos derivados lipídicos tanto en macrófagos derivados de médula ósea (MDMO) cuya activación se relaciona con los canales $K_V1.3/K_V1.5$, como en los canales $K_V7.1$/KCNE1 donde se habían previamente estudiado los efectos de los AGPIs. Las lipoxinas, pero no las resolvinas, revertieron la activación de los macrófagos inducida por el lipopolisacárido (LPS). Sin embargo, la resolvina D1 bloqueó de una manera mucho más potente los canales $K_V7.1$/KCNE1.

Voltage-dependent potassium channels are spanning-membrane integral proteins involved in several and diverse physiological and pathological processes such as immune response or cardiovascular function. The first goal of this study was to elucidate the role of $K_V7.1/K_V7.5$, as a heterotetramer complex, in vascular smooth muscle. To that end, we studied the expression levels of both channels in rat vascular myocytes, as well as their interaction in both a heterologous system and in aorta artery cells. $K_V7.1$ channels targets lipid-enriched domains in plasma membrane. The presence of $K_V7.5$ channels modulates $K_V7.1$ channels-targeting and, indeed, their physiological regulation. In those tissues where $K_V7.1$ channels are the only ones expressed, as in the heart, $K_V7.1$ channels are targeting lipid rafts. However, when both isoforms are expressed together, as in aorta artery and cava vein, the distribution of both channels throughout the membrane changes. Using patch-clamp technique we demonstrated that $K_V7.1/K_V7.5$ channels were functional, and we studied their electrophysiological and pharmacological properties. The activation of the channels generated a phenotypically intermediate current, which properties were between both the homotetrameric channels alone. In addition, electrophysiological characteristics of the channels were studied in the presence of different regulatory subunits (KCNE1 and KCNE3). In the presence of regulatory subunits $K_V7.1/K_V7.5$ channels showed their own electrophysiological properties. Retigabine is an activator drug of $K_V7.2$-7.5 channels. $K_V7.1/K_V7.5$ channels can be regulated by retigabine as $K_V7.5$ channels. We studied the possible role of these channels in the control of the vascular tone. To that end, we measured the relaxant response of coronary arteries induced by retigabine in constricted arteries by different blockers of K_V7 channels. We demonstrated that $K_V7.1/K_V7.5$ are involved in the control of the vascular tone. Otherwise, we studied the K_V7 first member, the $K_V7.1$ channel, with the KCNE1 regulatory subunit. Together, they form one of the most important current of the repolarization phase of the cardiac action potential (I_{Ks}). We analyzed, using the patch-clamp technique, the acute and chronic exposition of polyunsaturated fatty acids (PUFAs), DHA and AA, in $K_V7.1$/KCNE1 channels expressed in COS-7 cells. Also, in DHA analysis, we used western blot and isolation lipid rafts techniques. Acute DHA and AA exposition increased the magnitude of $K_V7.1$/KCNE1 currents. DHA but not AA slowed the activation kinetics. However, both PUFAs accelerated the deactivation kinetics. Chronic exposition to these compounds did not modify the magnitude of the currents. However, DHA shifted the activation curve toward more negative membrane potentials and accelerated the activation and deactivation kinetics of the channels. On the contrary, AA slowed the activation whereas it accelerated the deactivation process. Chronic exposure to DHA, decreased the $K_V7.1$ but not KCNE1 protein expression. Also, it induced a redistribution of $K_V7.1$ channels in the plasma membrane. PUFAs effects on $K_V7.1$/KCNE1 channels depends on both the compound's chemical nature, n-3 or n-6 PUFAs, as well as the time of exposure, which might be acute or chronic. It has been described that enriched PUFAs diet has anti-inflammatory properties. Moreover, n-3 or n-6 PUFAs lipid-derived mediators such as lipoxins and resolvins (which levels are increased by the consumption of aspirin), have been emerged as potent anti-inflammatory agents that promote the resolution phase of the inflammation process. Ion channels, and specially potassium ion channels, play an essential role in macrophages physiology. Accordingly, we studied the lipid-derived mediators effects on both bone marrow derived macrophages (BMDM), which LPS-dependent activation are related with the increased of $K_V1.3/K_V1.5$ expression, and in $K_V7.1$/KCNE1 channels where the PUFAs effects have been studied. Lipoxins, but not resolvins, could reverse the LPS-activated macrophages. However, resolvins $K_V7.1$/KCNE1 block were much more potent.

Content

Figure List

Suplemental Figures

Table list

Abbreviations Index

AA	Arachidonic Acid, Eicosa-5Z,8Z,11Z,14Z-tetraenoic acid
AF	Atrial fibrilation
AKAP79/150	A-Kinase anchoring protein 79/150
AKAP-Yotiao	A-Kinase anchoring protein Yotiao
AMME syndrome	Alport Syndrome, mental retardation midface hypoplasia, and elliptocytosis
AP	Action Potential
APCs	Antigen presenting cells
BMDM	Bone Marrow Derived Macrophages
CaM	Calmodulin protein
CHO cells	Chinese Hamster Ovary cells
Chromanol 293B	trans-N-[6-Cyano-3,4-dihydro-3-hidroxy-2,2-dimethil-2H-1-benzopyran-4-yl]-N-methyl
CNS	Central Nervous System
COX	Cyclooxygenase
DHA	Cis-4,7,10,13,16,19-Docosahexaenoic acid
DMEM	Dulbecco´s Modified Eagle´s Medium
e-LXA_4	5(S),6(R),15(R)-trihydroxy-7E,9E,11Z,13E-eicosatetraenoic-acid ethanesulfonamide
FBS	Fetal bovine serum
GYG	Glycine-Tyrosine-glycine amino acids
HETEs	Hydroxyeicosatetranoic acid
IP_3	Inositol triphosphate
I-V relationship	Current-Voltage relationship
K_V	Voltage-dependent potassium channels
LC20	20-kDa light chain myosin
Linopirdine	1,3-Dihydro-1-phenyl-3,3-bis(4-pyridinylmethyl)-2H-indol-2-one
LO or LOX	Lipoxygenase
LQTS	Long QT syndrome
LT- Leukotriene	
LXA_4	5S,6R,15S-trihydroxy-7E,9E,11Z,13E-eicosatetraenoic acid or 5(S),6(R),15(S)-triHETE
MβCD	Metil-beta-ciclodextrin
MES	2-(*N*-morpholino)ethanosulfonic-acid

MLCK	Myosin light chain kinase
NT	Normotensive
PG	Prostaglandin
PGD	Pore gating domain
PIP_2	Phosphatidylinosotol 4,5-biphosphate
PKA	Protein kinase A
PKC	Protein kinase C
RTG	Retigabine ([ethyl N-[2-amino-4-[(4-fluorophenyl)methyl] amino] phenyl] carbamate]
Rv	Resolvins
RvD1	17(S)-Resolvin D1, 7S,8R,17S-trihydoroxy-4Z,9E,11E,13Z,15E,19Z-docosahexaenoic acid
s	Slope
ser19	Serine 19
SHRs	Spontaneously hypertensive rats
SPMs	Specialized pro-resolving mediators
TCR	T-Cell Receptor
TEA	Tetraethylammonium
TM	Transmembrane domain/ segment
TX	Thromboxane
VDCCs	Voltage dependent Ca^{2+} channels
VG	Voltage-gated
V_h	Half voltage of channels activation
Vm	Cellular membrane potential
VSD	Voltage sensor domain
VSM	Vascular smooth muscle
VSMC	Vascular smooth muscle cells
VSP	Voltage sensing phosphatasas
WB	Western blot
XE991	(4-pyridinylmethyl)-9-(10H)- anthracenone dihydrochloride

1. INTRODUCTION

1.1 ION CHANNELS

Ion channels represent one of the main mechanisms of cellular signaling of almost all live cells. Our ability to do gymnastic, to perceive a colorful world and to process language relies on rapid communication among cells. Such signaling, the fastest in our bodies, involves electrical fluxes produced when ion channels open and close (1). Fast electrical signaling is made possible by the homeostatic mechanisms that establish the standard environment and content of animal cells: high Na^+ concentration [Na^+] in the blood and extracellular fluid, and high [K^+] (but low [Na^+] and [Ca^{2+}]) in the cytoplasm. Gradients are established and maintained by active transporters and pumps, which prepare the way for rapid changes in membrane voltage to be produced by passive transport through ion channels. These pore-forming proteins allow ions to flow only "downhill", as dictated by their electrochemical gradients, but they do it rapidly (the rate of passage of ions through one open channel is often more than 106 ions per second) and selectively. Opening a Na^+ or Ca^{2+} selective channel permits Na^+ or Ca^{2+} to flow down its gradient into a cell, making the intracellular voltage more positive. Opening a K^+ selective channel permits K^+ to flow from the cell and restores the voltage to a negative value. The dimensions of a typical cell and its membrane allow the voltage to be changed rapidly back and forth many times, with relatively small changes in concentration. This is essentially how all cellular electrical signaling is produced (1, 2).

These ion channels are spanning-membrane integral proteins that allow the flux of ions across them, promoted by their electrochemical gradients. The movement of charged ions generates electrical currents. The measure of how these currents flow through the membrane is known as conductance or membrane conductance.

The fundamental properties of currents mediated by ion channels were analyzed by the British biophysicists Alan Hodgkin and Andrew Huxley as part of their Nobel Prize-winning research on the action potential (AP), published in 1952 (3, 4). The existence of ion channels was confirmed in the 1970s by Bernard Katz and Ricardo Miledi using noise analysis (5). It was afterwards shown more directly with an electrical recording technique known as the "patch clamp", which led to a Nobel Prize to the German researchers Erwin Neher and Bert Sakmann, the technique's inventors (6). Thousands of researchers continue to pursue a more detailed understanding of how these proteins work. More recently, the Nobel Prize in Chemistry for 2003 was awarded to two American scientists: Roderick MacKinnon for his studies on the physico-chemical properties of ion channel structure and function, including x-ray crystallographic structure studies, and Peter Agre for his similar work on aquaporins (7, 8).

There are more than 75 genes whose expression is related with potassium channels subunits in humans. For this reason, K_V channels are the most extensive and diverse group of ion channels (9). K_V channels are constituted by 4 pore-forming subunits (α-subunits), each formed by six transmembrane domains, TM, (S1-S6) with intracellular N- and C-terminus. S1 to S4 conform the voltage sensing domain (VSD), whereas S5-S6, connected by the P-loop, form the central cavity of the ion pore (10). Based on this oligomeric organization, it is considered that K_V channels belong to a family of cation channels, not necessarily activated by voltage, that includes Na_V and Ca_V channels (formed by only one subunit with four similar repeats of six TM segments) (11, 12),Ca^+-activated K^+ channels, cyclic

nucleotide-activated channels (13), hyperpolarization activated cation channels (14), inward-rectifier K^+ channels (15, 16), two-pore K^+ channels (17, 18), TRP channels and glutamate-activated channels (19) (Figure 1)

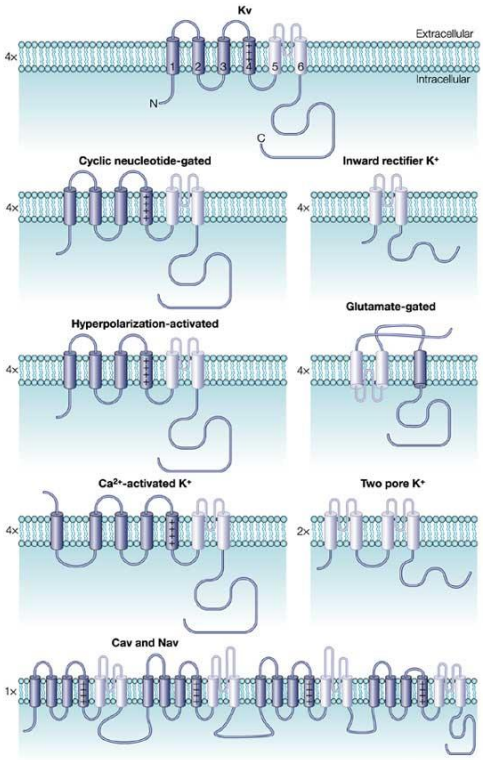

Figure 1: Schematic representation of the TM spanning segments of K_V channels and cation related channels. The white background represents the extracellular side of the plasma membrane. Light blue segments represent the TM segment that conforms the ion conduction pore. Taken from: Swartz et al., (2004) **Nature Rev Neurosci** 5:905-916.

1.2 VOLTAGE-GATED POTASSIUM CHANNELS

Voltage-gated ion channel protein superfamily is formed by more than 140 members and it is one of the largest groups of signal transduction proteins able to change their structural conformation as a consequence of changes in the membrane electrical field (20). These conformational changes promote the transition from the closed to the open and/or inactivated states (20-25). Excitable tissues generate action potentials (APs), without the need of any external stimuli, after the activation of Na^+ and/or Ca^{2+} channels. The AP is controlled by the coordinated activation of K_V, Na_V and Ca_V channels. Thus, K_V channels are involved in the maintaining of the resting membrane potential, the AP duration, the heart contraction, neuronal signaling, as well as other processes such as the immune activation, neurohormonal secretion, cell proliferation or cell volume regulation (26-29). At hyperpolarized membrane voltages, the open probability (p_o) of K_V channels is very low (~ 10^{-9}); but, after depolarization, K_V channels increase their open probability with a very high precision (~ 1) (23). K_V channels comprise a big and diverse family among human potassium channels, with 12 known subfamilies (K_V1-K_V12) (30). Activation of K_V channels generates potassium currents with different biophysical properties. K_V1-4 α-subunits can interact (between members of the same subfamily) and form homo- and heterotetramers (Figure 2). Subunits belonging to K_V5, K_V6, K_V8 and K_V9 subfamilies are known as “silent channels” that do not form homotetramers. They can heterotetramerize with other α-subunits. Usually, they interact with K_V2 subunits, generating functional K_V2/K_VS channel complexes in which the K_VS subunits modulate the K_V2 current (31-33). K_V7 channels can form homotetramers and heterotetramers channels, but

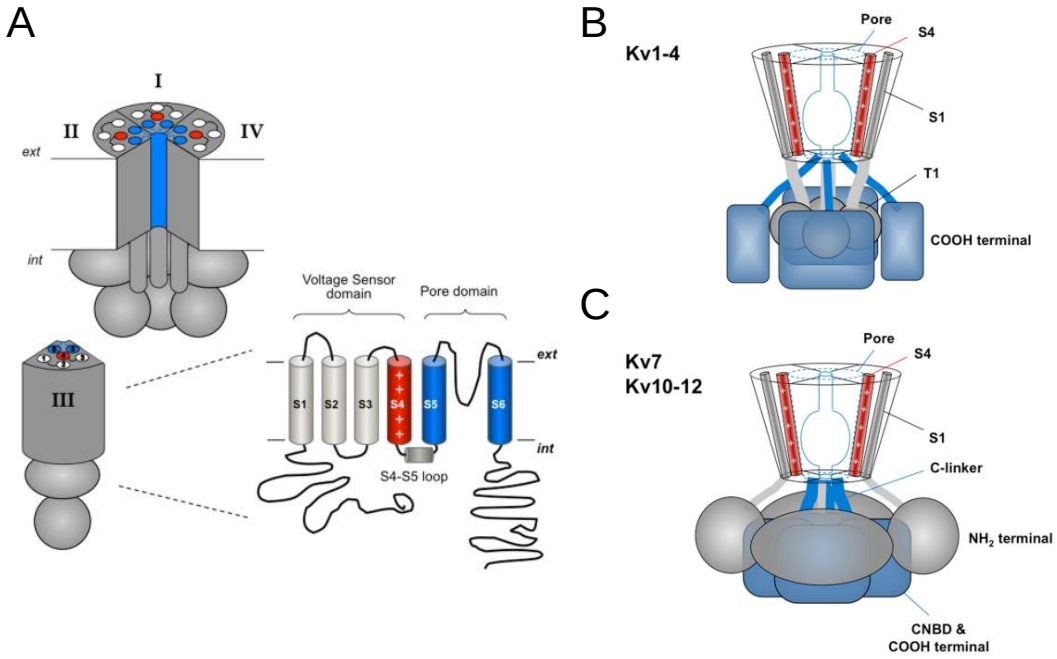

Figure 2: **Summary of structural components of K_v channels. (A)** Schematic representation of the tetrameric organization of a K_v channel. A structural folding model of one of the four α subunits is shown on the right. **(B)** General organization of the K_v1–K_v4 channels group with the T1 "tetramerization domains" hanging centrally below the transmembranal core and attached to it through four linkers continued from the first transmembrane helices. In this case, the C-terminus structures probably track to the periphery surrounding T1 and extending to its bottom. **(C)** General architecture of the K_v7 and K_v10–K_v12 channels characterized by a C-terminus (i.e., the C-linker/cyclic nucleotide-binding domain (CNBD) region of the K_v10–K_v12 channels or the A–D helical regions of the K_v7 channels) forming a compact tetrameric structure in a central position immediately below the cytoplasmic pore opening. In this case the N-terminus probably surrounds the C-terminus and extends to its bottom establishing extensive contacts with its top and side surfaces. Note that in both models the initial N-termini structures are likely to interact with the gate surroundings in the transmembrane core. S4 segment is also depicted as a reference. Taken from: Barros et al., (2012). **Front Pharmacol.** 3:49.

structurally are more similar to K_V10-12 subfamilies (34). Additional intracellular domains and/or accessory subunits modulate the gating properties of K_V channels (35-37). Taking in mind the structure of the K_V channels, we can divide them in two groups. All K_V channels belonging to each group share homology in the pore region and they exhibit very low matches in other regions. On the one hand, K_V1-4 channels exhibit an N-terminal that has a tetramerization domain (T1), dangling centrally below the TM core, which determines different functional characteristics and allow the assembly of K_V monomers as well as the assembly of regulatory subunits (Figure 2B) (38). On the other hand, K_V7 and K_V10-12 subfamilies, are characterized by the absence of an N-terminal T1 domain (Figure 2C), have a long C-terminal domain forming a compact tetrameric structure in a central position immediately below the cytoplasmic pore opening. These channels are characterized by a very big cytoplasmic region (almost 80% of total protein), although structural details of this region is still unknown (39). However, it is known that the gating properties are strongly influenced by cytoplasmic domains. In both K_V structures, the N- and C- termini encircle the main terminal, which are likely to interact with the surroundings in the transmembrane (TM) core (Figure 2BC). Due to their accessibility, the cytoplasmic regions of the channels are targets for cell-physiological control of the channel function

(i.e. β-regulatory subunits, KCNEs, syntaxin, G β-gamma proteins, SNARE complex, Ca^{2+}/calmodulin, PIP_2, PKC, PKA, etc.).

1.2.1 Ion pore and selectivity filter of K_V channels

The role of all K^+ channels is to conduct K^+ ions with a high selectivity over other cations across the cell membrane. The differences between Na^+ ion and K^+ ion are practically undetectable, the atomic radius are 0.95 Å and 1.33 Å for Na^+ and K^+ ions, respectively. However, this difference in size is managed with a very high precision (1000:1) by K^+ channels to select K^+ and not Na^+ ions. This high selectivity does not compromise the rates of conduction for K^+ ions, which is similar to the diffusion limit value (40, 41). The fact that the rates of conduction will not be affected by electrostatic repulsion is due to several properties of the ion pore. The first K^+ channel crystalized was the bacterial KcsA channel at a 3.2 Å resolution (7). This channel is a tetramer, with four identical subunits arranged symmetrically around a central ion pore. Each subunit consists of two transmembrane α-helices connected by a P-loop; the inner (closer to the ion pore) and the outer (closer the membrane), which are equivalent to S5 and S6 in K_V channels (subsequently confirmed in Long SB et al., 2005 (42)) (Figure 3). From external side (extracellular medium) to internal side (cytosol) of the channel model, it can be considered two regions, the broad region (upper region) and the narrowest region (inner region). The upper region of the ion pore is the K^+ selectivity filter region, because is where is located the selectivity filter. (marked in yellow in Figure 3A) In the inner region, the pore is lined by inner helices and is considered as gating part (Figure 3A). This configuration is known as the inverted teepee. Just inside the upper region of the pore, the selectivity filter is between the extracellular medium and the central water-filled cavity, where the hydrated K+ ions remain suspended within the crystal structure (41). The inner helices converge to a hole and there is the amino acid sequence (TVGYG) considered the selectivity filter of K^+ channels. This amino acid sequence is highly conserved in nature and is also known as K^+ channel signature sequence (7, 41). Their side chains do not point into the pore, but the strongly dipolar carbonyl groups of α carbons do. The presence of water-filled cavity and the oriented α-helices helps the moving of ions, into the low dielectric membrane environment (Figure 3C). Thus, K^+ ions remain hydrated at the membrane center and it will be stabilized there thanks to the C-terminal negative ends-charge of α-helices (43). K^+ ions confront with evenly spaced layers of carbonil oxygen atoms and a single layer of threonine hydroxyl oxygen atoms. This disposition gives rise to 4 numbered spaces (1 to 4), in the selectivity filter, where the K^+ ion will be surrounded by four oxygen atoms above and four oxygen atoms below (red circles, Figure 3B). This arrangement of the oxygen atoms in the selectivity filter surrounding K^+ ions, mimics the water that is held in the central cavity. Therefore, K^+ ions can diffuse from the selectivity filter to the central cavity being energetically compensated (40). The passage model suggests that K^+ occupies two of the four spaces and that between them there is a water molecule (Figure 3). In summary, the selectivity filter has several binding sites for K^+ ions that mimic hydrated K^+ ions breastplate. They achieve right conductions rates due to the electrostatic repulsion compensation, and by coupling the selectivity filter conformation to the binding of the K^+ ions (41). A few years later, the crystal structure of the first K_V channel (K_V1.2) was performed (42). The pore structure of K_V channels differs from that of the non-voltage-gated bacterial K^+ channel KcsA due to a sharp-bend in the S6 helices (equivalent to the

inner helices of the KcsA channel) This bend occurred at a Pro-X-Pro sequence that is conserved in K_V channels (44).

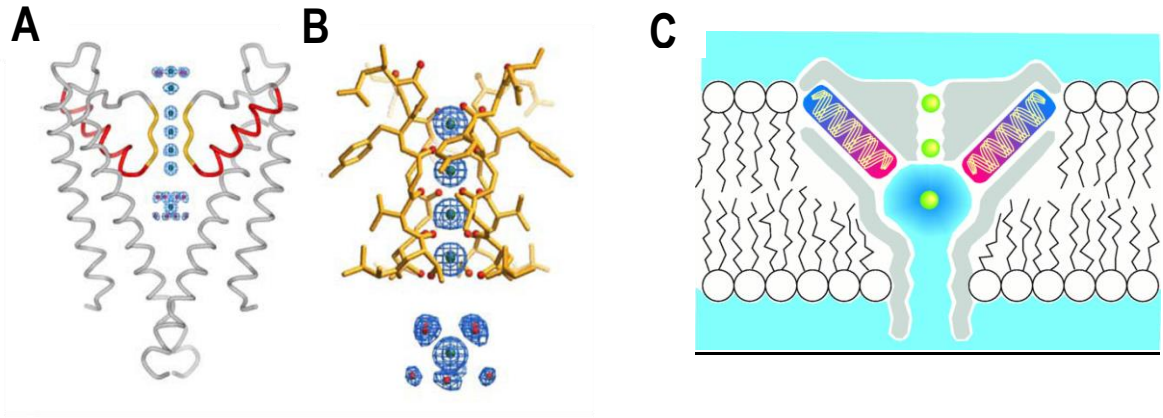

Figure 3: The ion conduction pore of K^+ channels. **(A)**: Two of the four subunits from the KcsA pore are shown with the extracellular side on top. Each subunit contains an outer helix close to the membrane, an inner helix close to the pore, a pore helix (red) and a selectivity filter (gold). Blue mesh shows electron density for K^+ ions and water along the pore**. (B)** Close-up view of the selectivity filter with dehydrated K^+ ions at positions 1 through 4 (external to internal) inside the filter and a hydrated K^+ ion in the central cavity below the filter. **(C)** Schematic view of the stabilizing mechanism of K^+ channels. Central cavity water-filled and oriented helices pointed their partial negative charge (red) toward the cavity where a cation (green) is located. Adapted from: Doyle et al., (1998). **Science**. 280(5360):69-7 and Mackinnon et al.,(2003). **FEBBS Lett**. 27;555(1):62-5

1.2.2 Voltage-sensor domain of K_V channels

K_V channels sense and change their conformation depending on the membrane potential. Different studies reported that the voltage sensor domain (VSD) of K_V channels resides in the S1-S4 segments (45-47). In particular, the S4 is rich in positively charged basic residues and, thus, it represents the major component of the voltage sensor. The movement of these charged amino acids through the membrane (gating charges) provides the energy necessary to promote the channels to open. In addition, negative charges in S1, S2 and S3 also contribute to this process (20, 23-25, 48, 49). S3 is formed by two helices named S3a and S3b (Figure 4C). In the crystal structure of K_V1.2 (42), S3b forms, together with S4, a helix-turn-helix structure called the voltage-sensor paddle (42). Membrane depolarization produces an outward movement of the S4 inducing further conformational changes that results in the opening of the channel pore leading to selective K^+ permeation. This movement has been monitored electrically as the gating current or by voltage-clamp fluorometry(50-53).

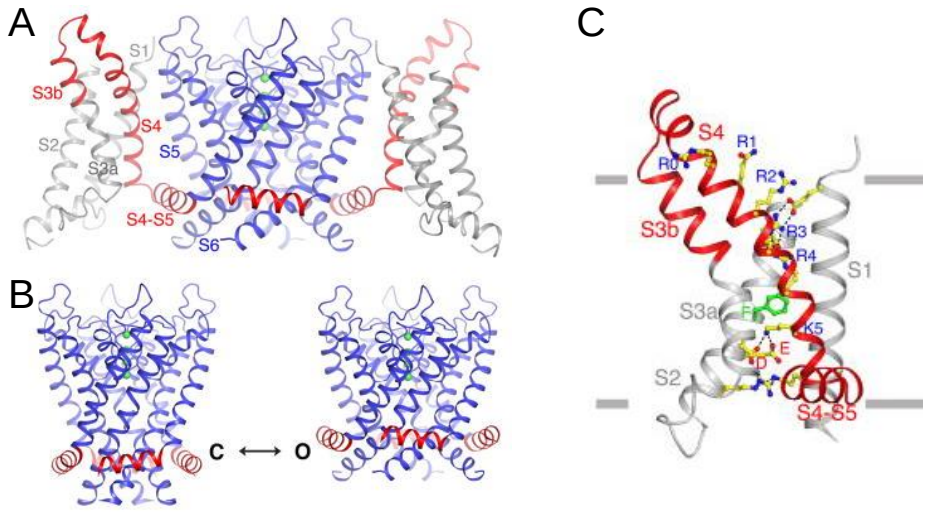

Figure 4*:* Schematic view of the voltage-sensor of K^+ channels. (A) Ribbon representation of the transmembrane region of K_v2.1 paddle–K_v1.2 chimera channel tetramer ($K_v$chim, viewed from the side, and oriented with the extracellular solution above. The pore is colored blue; the voltage sensor paddle (S3b and S4) and the linker helix (S4-S5) between voltage sensor and the pore in red; and S1, S2, and S3a gray. The voltage sensor closest to the viewer was removed for clarity. K^+ ions in the selectivity filter are shown as green spheres. **(B)** Ribbon representation of the pore and S4-S5 linkers in the hypothetical closed conformation (C) from a model constructed from the $K_v$chim and KcsA structures and in the open conformation (O) from the crystal structure of $K_v$chim. In the hypothetical closed state, based on the closed conformation of KcsA, the S4-S5 linker helices are pushed down to maintain their same contacts with the pore. **(C)** View of the voltage sensor and S4-S5 linker helix of the open conformation from $K_v$chim. Side chains of the positively charged residues on S4 (labeled as R0, R1, R2, R3, R4, and K5) and the negatively charged residues forming ionizing hydrogen bonds (dashed black lines) with the positive charges, as well as those of the three residues (labeled F, E, and D) forming an occluded binding site in the voltage sensor, are shown as sticks and colored according to atom types (yellow, carbon; blue, nitrogen; red, oxygen; and green, phenylalanine). Taken from: Tao et al., (2010) **Science** 2;328(5974):67-73.

1.2.3 K_V channels gating

K_V channels are mostly intracellular being their TM segments essentially in contact with the lipid bilayer to sense voltage membrane and respond to its changes. Moreover, both C- and N- termini face to the cytosolic medium and are widely regulated by the different protein and lipids present in the cytosol. The comparison of the structures of K^+ channels trapped in the open conformation, MthK, K_VAP and K_V1.2 (42, 54, 55), and channels kept in the closed conformation, KcsA and KirBac1.1 (7, 56), suggests that the K_V gate opening is linked to a conformational change of the S6 helix. The S6 helix of K_V channels has a high conserved sequence PXP motif. Results of accessibility studies (44, 57, 58) suggest that the opening of the S6 bundle takes place at the PVP motif of K_V1 channels. The crystal structure of the rat K_V1.2 (59) supports this view and shows that widening of the S6 occurs because of a bend at the PVP motif. Opening of the gate is associated with the bending of the S6 helix which can occur at either a glycine or a PVP motif. Several studies on different channels suggest the S4-S5 linker and the end of S6 are involved in coupling (60-62). The crystal structure of K_V1.2 demonstrates this interaction clearly. The distal end of the S4-S5 linker comes close to the internal end of S5 below the PVP motif, with extensive contacts between side chains of the two regions. This structural picture of the activated conformation suggests that to close the gate, the S4-S5 linker would have to

move inward, shutting down the S6 gate (42). Therefore, the S4-S5 linker and C-terminus end of S6 are critical for coupling between voltage-sensor movement and channel opening.

1.3 K_V1 SUBFAMILY CHANNELS

This subfamily is constituted by 8 members (K_V1.1 – K_V1.8). In the present Doctoral Thesis we have focused on two of them, K_V1.3 and K_V1.5, and a brief description of their electrophysiological characteristics are given in this section.

1.3.1 K_V1.3 channels

The expression of KCNA3 gene generates a 575 amino acid protein. K_V1.3 traffics very efficiently to the cell membrane (63). It is activated after membrane depolarization and has a slow and cumulative inactivation (64-66). K_V1.3 also targets nuclear membrane, mitochondrial membrane and Golgi apparatus (67, 68). K_V1.3 channels are involved in several processes like cell volume regulation, maintaining of the resting membrane potential and apoptosis. K_V1.3 is mostly expressed in neurons and in immune cells, being significantly important in hypothalamus and olfactory bulb, and in T and B lymphocytes, macrophages and dendritic cells (69, 70). K_V1.3 alterations are related to several autoimmune diseases (71). K_V1.3 has also been studied in other tissues where its role appears less relevant such as kidney, smooth muscle, colon epithelia and testes (72-74). It is also involved in processes related to the insulin response, where the glucose transporter, GLUT4, is involved (75, 76). Moreover, K_V1.3 channels are being described as possible targets for obesity (77, 78). Therefore, K_V1.3 is considered a putative therapeutic target for several diseases.

1.3.2 K_V1.5 channels

K_V1.5 (KCNA5) was cloned for the first time from a human ventricle library (79). In the human heart K_V1.5 channels are responsible for the rapid repolarizing phases of the AP (phases 1 and 3 of atrial APs). However, this current could not be recorded from human ventricular cardiac myocytes (80-83). K_V1.5 channels are mostly expressed in atria, where they generate the so-called ultra-rapidly activating delayed outward-rectifying K^+ current (I_{Kur}) (84-87). K_V1.5 is considered as a potential molecular target for antiarrhythmic drugs useful in the treatment of supraventricular arrhythmias (86, 87). Also K_V1.5 channels have been described in other tissues but in a lesser extent, such as GABAergic neurons, human fetus, skeletal and smooth muscle, and immune cells.

Like, K_V1.3 channels, K_V1.5 are also expressed in cells from the immune system. In fact, they play crucial roles in cells from the immune system and proliferation (88, 89).

1.3.3 Bone marrow derivate macrophages express K_V1.5 and K_V1.3 channels

Macrophages are highly regulated cells of the immune system. They can be involved in several actions, among them, acting as antigen presenting cells (APCs), taking part in T-signaling and/or regulating cytokine release. The molecular signals leading the different activation programs in macrophages i.e. proliferation, activation, resolution or tolerance proceed from the extracellular medium and they will determine the direction of the immune response,

driving it to inflammation or resolution (90). K_V channels play a pivotal role in the regulation of macrophages. Indeed, the electrophysiological properties of macrophages depend on their state of functional activation (91). Thus, changes in membrane potential that occur as a consequence of the modulation of ion channels are among the earliest events after macrophage activation (92, 93). Hence, the expression of $K_V1.3$ channels is increased as a consequence of the macrophage activation by lipopolysaccharide (LPS) and proliferation, whereas K_{ir} channel expression is reduced under these conditions. Previous reports demonstrate that macrophages K_V outward current is generated after the activation of $K_V1.3$/$K_V1.5$ heterotetrameric channels (91, 94). It is also known that the innate activation increases the $K_V1.3$:$K_V1.5$ ratio of these heteromeric channels. On the contrary, alternative activation of macrophages leads to a decrease in the $K_V1.3$:$K_V1.5$ ratio (94). The influx of extracellular Ca^{2+} is an essential requirement for the activity of many cellular processes (92, 95, 96). Therefore, $K_V1.3$ and the Ca^{2+}-activated K^+ ($K_{Ca}3.1$) channels regulate Ca^{2+} influx through the Ca^{2+} release-activated Ca^{2+} (CRAC) channel, which consists of the Ca^{2+}-sensor stromal interaction molecule 1 (STIM1) and the pore-forming protein CRACM1 (Orai1) (97-100). In T cells, this crucial influx of Ca^{2+} is only possible if they can keep their membrane potential negative by a counterbalance of K^+ efflux through $K_V1.3$ and/or $K_{Ca}3.1$ (101, 102) and both channels are regarded as targets for immunosuppression (101). Interestingly, inflammation is involved in several cardiovascular pathologies, from atrial fibrillation or atherosclerosis to myocardial infarction or heart failure (103-106).

1.4 K_V7 CHANNELS

The K_V7 subfamily of potassium channels ($K_V7.1$-$K_V7.5$) plays a crucial role on cardiac, neuronal, cochlear and vascular function (107, 108). These channels are constituted by homo- or heterotetramers of K_V7 subunits (108). Each K_V7 member exhibits a characteristic tissue expression pattern. Thus, $K_V7.1$ is mainly expressed in cardiac tissue (where they are responsible, together with the regulatory subunit KCNE1, of the cardiac I_{Ks}). $K_V7.2$ to $K_V7.5$ are predominantly distributed throughout the CNS and peripheral nerves and are therefore referred to as neuronal K_V7 channels (109). In fact, the activation of $K_V7.2$, $K_V7.5$, $K_V7.2$/$K_V7.3$ and $K_V7.5$/$K_V7.3$ channels generates the so-called M-current, crucial for the control of neuronal excitability (108, 110). In addition, $K_V7.4$ is also expressed in sensory cells of the cochlea. K_V7 channels are a subfamily of K_V channels of great physiological importance also in the kidney, gastro-intestinal tract, inner ear, testis, skeletal and smooth muscle(111). In fact, $K_V7.1$, $K_V7.4$ and $K_V7.5$ channels are also highly expressed in vascular smooth muscle where they are important regulators of the vascular tone in veins and arteries.

Mutations in K_V7 channels may trigger cardiac arrhythmias, deafness and epilepsy (112-115), displaying a prominent role in human disease (110). The diversity and complexity of K_V7 channels is further increased by the interaction of the channels with different types of KCNE subunits.

As it was described, K_V pore and voltage sensor domains are well-conserved structures within K_V channels (7, 42). K_V7 channels are characterized by the largest C-terminal that, besides being the tetramerization domain, it has several domains for modulation (38).

1.4.1 Role of C-terminal in K_V7 channels

The C-terminal domain in K_V7 channels is much longer (300-500 residues) than in other K_V channels, playing a critical role in assembling, trafficking and gating (116). The secondary structure predicts four helices (A-D helices), which are present in all members of the K_V7 subfamily. Schematically, C-terminus is subdivided in two parts: i) the proximal region, susceptible of PIP_2 regulation and constitutively associated with calmodulin (CaM), and ii) the distal part mediating tetramerization due to tandem coiled-coil (CaM) (Figure 5).

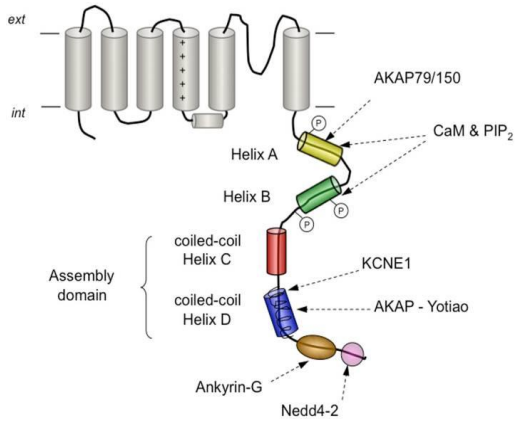

Figure 5: Schematic representation of C-Terminal of K_V7 channels. Grey cylinders represent the TM segment of the subunit. Green and yellow cylinders represent Helix B and Helix A respectively, which are the structures recognize as binding site for CaM and PIP_2. Phosphorylation sites by Src Kinase and by PKC are indicated by encircled P. For $K_V7.2$ are represented the AKAP79/150. Blue cylinder represents the conserved site for the auxiliary β -subunit KCNE1 and the AKAP-Yotiao in $K_V7.1$ and in brown and purple are represented ankyrin-G (in $K_V7.2$-$K_V7.3$) and ubiquitin protein ligase Nedd4-2 (in $K_V7.1$, $K_V7.2$, and $K_V7.3$), respectively. Taken from: Barros et al., (2012). **Front Pharmacol.** 3:49.

CaM is a constitutively tethered to the C- terminal of K_V7 channels both in the presence and in the absence of Ca^{2+} (117-119), and thus, the C-terrminus acts as a Ca^{2+} sensor necessary for the gating, folding and trafficking of these channels (116). Also, the proper function of K_V7 channels requires the tethering of PIP_2 to a binding site that overlaps with that of CaM (120-122). It has been described that $K_V7.1$ channels are activated by both PIP_2 and Ca^{2+}/calmodulin mediating I_{Ks} current, and mutations that alter PIP_2 or Ca^{2+}/calmodulin binding site yield different forms of Long-QT syndrome (123-126). Furthermore, K_V7 channels are targets of signaling cascades in which different protein kinases (PKC, PKA, Src Kinase, SGK1.1) are involved (127-130). Some of these kinases act through the interaction with AKAP proteins (128, 131). In the $K_V7.1$ C-terminus, there is a leucine zipper that acts as scaffold, recruiting a signaling complex of proteins such as proteinphosphatase 1 or PKA, which is essential for the regulation of this channel via β-adrenergic receptor (132, 133). The two tandemly arranged coiled-coil helices C and D are the structures that make possible the tetrameric assembly (also known as A-domain). Analyses of the helix C confirm that it is dimeric and undergoes self-association to form dimer of dimers and confirm that are absolutely necessary to form functional channels (134). In the most distal part of C-terminal there are two binding sites for two different regulatory proteins. Below helix D, it is located the Nedd4-2 ubiquitin ligase binding-site, which ubiquitinates K_V7 and, thus, modulates K_V7 channel density in the plasma membrane. This interaction seems to be crucial in cell excitability and in several pathophysiological conditions such as cardiac ischemia, epilepsy, Alzheimer´s disease or chronic pain (116). $K_V7.2$ and $K_V7.3$ channels are also regulated by Ankiryrin-G that binds to a site at the distal part of C-terminus known as C3-motif. The role of this protein is to anchor the C-teminus with other TM protein complexes and to connect it with the cytoskeleton via actin-spectrin proteins (135).

1.4.2 KCNE regulatory subunits

Ion channels are present, in different tissues, forming signaling complexes or channelosomes. In the past decade a myriad of protein-protein interactions involved in intracellular signaling have been described (131, 136). KCNE family is encoded by *KCNE* genes consisting in 5 known members (*KCNE1-5*) (137, 138). The KCNE structure consists in a single TM domain with the N-terminus facing the extracellular medium and a cytosolic C-terminus, which interacts with C-termini of the α-subunits (137, 139). Each one of these KCNE proteins can modulate multiple K_V channel α-subunits (72, 138, 140). KCNE1-5 proteins modulate membrane targeting of K_V7 channels, single-channel conductance, voltage-dependence, gating kinetics, ion selectivity and pharmacology (137, 164).

$K_V7.1$ channels interact with all KCNE family members. KCNE2 almost abolished the $K_V7.1$ current. KCNE3 subunit generates constitutively active $K_V7.1$ channels (110, 141, 142). These interactions between KCNE3 and $K_V7.1$ appear to stabilize the activated "up" state configuration of S4, which the authors propose as a prerequisite for full opening of the $K_V7.1$ channel activation gate (143). KCNE4 and KCNE5, at physiological membrane voltages, reduce the magnitude of $K_V7.1$ current (144).

$K_V7.5$ channels interact with all KCNE family members, but only KCNE1 and KCNE3 induce changes in the current. KCNE1 enhance $K_V7.5$ currents and slow their activation kinetics while KCNE3 drastically inhibits $K_V7.5$ currents (137).

1.4.3 $K_V7.5$ channels

$K_V7.5$ was cloned simultaneously by two laboratories (145, 146). $K_V7.5$ subunit is a protein formed by 897-932 amino acids (depending on the splicing variant) with a predicted molecular mass of ~99-102 kDa. The homology between $K_V7.5$ and other members can be summarized as $K_V7.5$ ~ $K_V7.4$ (65%) > $K_V7.3$ = $K_V7.2$ (50%) > $K_V7.1$ (40%) (137, 145, 146) (Figure 6).

Figure 6: Dendrogram of KCNQ (K_V7 channels) using the ClustalX program. Taken from: Schroeder et al., (2000). **J Biol Chem**. 275:24089-24095.

$K_V7.5$ channel exhibits the longest C-terminus of all the K_V7 subfamily members. It shares well-conserved sites with other members, i.e. structural regions susceptible to be phosphorylated by PKC. However, $K_V7.5$ channel lacks the N-terminal consensus site for cAMP-dependent phosphorylation that is present in $K_V7.1$ and $K_V7.2$ (147). $K_V7.5$ channel is mostly expressed in different areas of the brain, as well as in skeletal and smooth muscle (137, 145, 146). $K_V7.5$ channel is inhibited by the activation of M1 muscarinic receptor, suggesting that $K_V7.5$ are playing a specific role in generating "M-current" in different locations of nervous system (145, 146, 148).

In vascular smooth muscle, $K_V7.5$ channels play a crucial role maintaining the resting membrane potential (149-151). $K_V7.5$ and all KCNE subunits are expressed in rat skeletal muscle and vascular smooth muscle. However, the physiological role of the interactions between them remains unclear (137, 145, 146).

K_V7.5 currents were firstly studied in *Xenopus* oocytes. K_V7.5 currents activate very slowly, being not fully activated after 3-s test pulses, displaying a delay in the activation, like other K_V7 currents. K_V7.5 currents exhibit faster activation than K_V7.4, but slower than K_V7.2 currents, and much slower than K_V7.1 currents (145, 146, 152, 153). After applying depolarizing pulses to potentials positive to +40 mV, K_V7.5 currents accumulate, indicating a fast inactivation. The activation midpoint is ~ -46 mV (145, 146). Finally, K_V7.5 channels display a marked inward rectification at potentials positive to 0 mV (145, 146).

1.4.4 K_V7.1 channels

K_V7.1 channels have been previously known as K_VLQT1 or KCNQ1 channels. It was previously described by Wang and colleagues in 1996. They first described K_V7.1 channels when they reported a disorder of cardiac repolarization that led to long QT syndrome (LQTS) type 1. This LQTS type 1 was produced by an autosomal dominant mutation in the *KCNQ1* gene (112, 113). K_V7.1 channels are an essential part of cardiac I_{Ks} (K_V7.1 channels are the α-subunit of the cardiac slowly activating delayed-rectifier K^+ current) (152, 153).

K_V7.1 channels exhibited distinct biophysical properties in the absence and in the presence of KCNE1. K_V7.1 channels expressed alone activate and deactivate slowly, compared with others K_V channels (154). However, the activation process is faster than in other members of K_V7 channels. Depolarization of K_V7.1 channels elicits outward K^+ currents at membrane potentials positive to-70 mV. The I-V relationship showed a steady-state at high positive potentials (+40 mV- +60mV) (155).

After depolarization, and the characteristic activation, K_V7.1 channels rapidly inactivate. This inactivation process can be observed in the tail currents, which shows a “hook” (a little current increased with a subsequent slow decay) (156). A possible explanation for the non-linear I-V relationship is the inactivation process. This “hook” tail is also observed in K_V11.1 channels (HERG channels), it seems to be that the deactivation process is slower than the recovery of the fast inactivation of the channels (157).

An important regulator for K_V7.1 channels is PIP_2, which promotes the channels to open. The rundown observed when recording K_V7.1 currents, is a consequence of PIP_2 depletion. In fact, same results are observed with the activation of lipid-phosphatases (for instance with voltage sensing phosphatases, VSP) (26). Importantly, recent studies suggest that PIP_2 serve as a cofactor that mediate “voltage sensing domain-pore gating domain” coupling in K_V7.1 channels

Aside from heart, K_V7.1 channels are also expressed in pancreas, adrenal and thymus gland, placenta, intestine, brain, inner ear, kidney, smooth and skeletal muscle (133, 152).

1.4.4.1 K_V7.1/KCNE1 channels

The assembly of K_V7.1 and KCNE1 represents the cloned counterpart of the cardiac I_{Ks} current (152, 153). Although in the human heart KCNE1 is the highly expressed, it has been described the presence of several KCNEs in this tissue (142).

The slowly activating delayed-rectifier K^+ current, I_{Ks}, modulates the repolarization of cardiac action potentials. This was described, at the same time, by Sanguinetti and colleagues and Barhanin and colleagues, in 1996. Sanguinetti and colleagues used CHO cells as heterologous expression system (Barhanin and colleagues achieved the same conclusions using COS-7 cells). Thus, they expressed the cDNA of $K_V7.1$ channels (K_VLQT1) and KCNE1 (mink) in those cells. KCNE protein family was also named minK-related peptides (MiRPs). This name was assigned to this family protein because the first member KCNE1 was called minK (from "minimal K^+ channel") because it was thought that it generated K^+ channels by itself (158). In fact, when regulatory subunit was transfected into *Xenopus* oocytes, that endogenously express $K_V7.1$ channels, it assembles with them generating the slowly activated K^+ current (see below I_{Ks} current) (152, 153).

The $K_V7.1$/KCNE1 current did not saturate after long depolarization pulses, contrary to what was observed for $K_V7.1$ channels alone (i.e. the I-V relationships are completely different)(155). KCNE1 protein not only delayed the activation process, but also increases the amplitude of the currents and right-shifts the voltage-dependence of the channels. KCNE1 eliminates the inactivation observed in $K_V7.1$ channels (72, 146, 152, 153, 159-161).

There is still controversy about the stoichiometry between α- and KCNE subunits (i.e. 4:4 or 4:2 subunits) (162-165). The available data suggest that KCNE1 could be inserted into the lipid-filled space between two adjacent VSD (166). It seems that KCNE1 directly interacts with regions located in S1, S4 and S6 TM domains (166-169). $K_V7.1$/KCNE1 channels are highly regulated by PIP_2 and PKA protein. This regulation is very important, it is related to the activation mechanism of the channels and specifically related to heart rates (see below).

$K_V7.1$/KCNE1 channels are not only expressed in the heart, where this current plays a crucial role in the repolarization of the cardiac AP, but also in the endolymph of the inner ear, playing a crucial role in the homeostasis of the K^+, in the brain acting on the neuronal electrical signal, pancreas and kidney (133, 170).

1.4.5. K_V7 channels pharmacology

The main K_V7 channels activators are; i) retigabine (RTG) and its analog, flupirtine (activators of $K_V7.2$-7.5 channels) (174); ii) meclofenamic acid, a non-steroidal anti-inflammatory acid that activates $K_V7.2$ and $K_V7.3$ but not $K_V7.1$ channels (175); and finally iii) R-L3 and mefanamic acid, specific activators of $K_V7.1$ channels (176, 177).

XE991 and linopirdine are potent blockers of all members of K_V7 subfamily, but they do not discriminate between individual isoforms (171, 172). Chromanol 298B is a selective blocker of $K_V7.1$ channels (173).

KCNE regulatory subunits modulate the pharmacology of K_V7 channels (86). In such a way, the effects of blockers and activators in $K_V7.1$ channels can be either enhanced or decreased by the presence of KCNE1. The anti-inflammatory mefanamic acid (activator), tetraethylammonium (TEA) and chromanol 293B exhibited lower potency on $K_V7.1$ channels than in $K_V7.1$/KCNE1 channels (176, 177). The modulation produced by KCNE1 seems to be allosteric, i.e. facilitating the binding of the drugs to the $K_V7.1$ channels (178). However, when the effects of XE991 (K_V7 blocker) were tested in *Xenopus* oocytes, block-induced was greater in $K_V7.1$ than in $K_V7.1$/KCNE1 channels, being the effects time- and voltage- dependent (172).

1.5 PHYSIOLOGICAL ROLE OF K_V7 CHANNELS

1.5.1 Role of K_V7 channels vascular in smooth muscle (VSM)

The smooth muscle contractility depends on the increase of intracellular Ca^{2+}. Schematically, after an increase in intracellular Ca^{2+} concentration, this ion binds to calmodulin activating MLCK that phosphorylates the 20-kDa light chain myosin protein (LC20) at Ser19. The LC20 phosphorylation is essential for the cross-bridge between actin and myosin and therefore, for contraction (179). The maintenance of the contractility force is due to other proteins such as Rho or PKC, which inhibit the myosin light chain phosphatase. There are two main mechanisms by which Ca^{2+} can be increased: i) entering from the extracellular media, or ii) being released from intracellular stores. On the one hand, the Ca^{2+} release from sarcoplasmic reticulum (the main intracellular Ca^{2+} store) is produced via IP_3-dependent mechanism. On the other hand, the increase of Ca^{2+} from the extracellular media is produced through VDCCs or via nonselective cation channels. The activity of VDDCs depends on the V_m, in such a way that more positive potentials promote a higher open probability of these channels. Potassium channels are the main responsible of the hyperpolarization of the cell membranes. Thus, their activity will determine the open probability of VDDCs and indirectly the smooth muscle contraction (Figure 7).

Among others, K_V7 channels are involved in the control of the vascular tone. They control the resting membrane potential of vascular smooth muscle cells (VSMC) and therefore the contractility in several rodent and human arteries (180-182). Vascular musculature mostly expresses $K_V7.1$, $K_V7.4$, and $K_V7.5$ channels. However, a relationship between functional currents and specific genes has not been established (111). Homo- and heterotetramerization of K_V7 isoforms shapes K^+ currents in VSMC. It has been described that $K_V7.4$ and $K_V7.5$ channels form functional heterotetrameric channels that are involved in the regulation of contractility in VSM. This complexity is further increased by KCNE regulatory subunits. The main expression of different types of K_V7 channels and the combination with the KCNEs regulatory subunits are quite variable and depend on the type of vascular bed. KCNEs mRNAs are relatively abundant in aorta, carotid and femoral artery (111).

K_V7 channels are involved in different signaling pathways that lead to relaxation and vasodilatory actions, or to contractility and vasoconstriction (Figure 7). In the endogenously pathways, the Gs- and Gq-coupled receptor are involved. On the one hand, Gs-coupled receptor is activated by adenosine or isoprenaline (relaxant mediators, as in β-adrenergic regulation) and activates PKA, via AMPc, which promotes the activation of the channels and therefore the vasorelaxation. On the other hand, Gq-coupled receptor mediates activation of PKC that promotes the inhibition of the channels, favoring contractility (Figure 7).

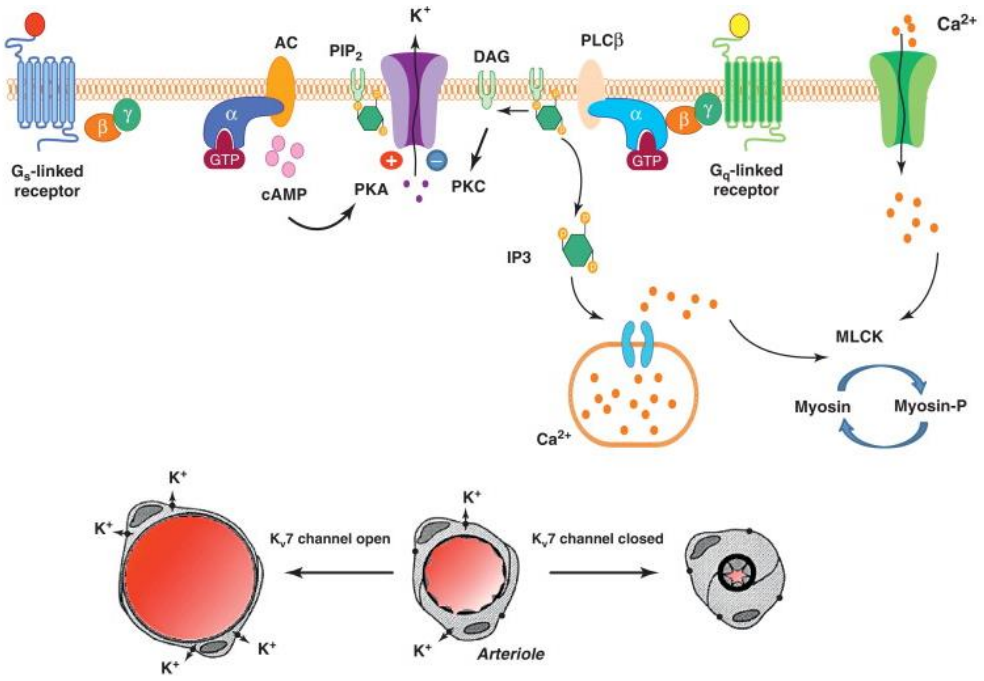

Figure 7: K_V (K_V7) channels signaling pathway involved in contractile state of smooth muscle. Activation of channels results in relaxation and vasodilation while block of them implies contraction and vasoconstriction. K_V (K_V7) channels are highly regulated by Gs- and Gq-coupled receptor signaling. Vasodilatoy actions induced by adenosine and isoprenaline are mediated y Gs-coupled receptor via AMPc. Gq-coupled receptor negatively modulates vasoconstrictor actions via PKC. Taken from: Stott et al., (2014). **Drug Discov. Today** 19:413-424.

Because it is established that activators of K_V7 channels lead to relaxation and vasodilatory actions, whereas blockers produce contractility and vasoconstriction, several pharmacological tools were used to determine the role of K_V7 channels on VSM. However, the presence of heteromeric channels (and their regulation by KCNEs subunits) makes difficult to properly interpret the results obtained using these pharmacological tools. It has been observed that $K_V7.1$ channels are the most abundant in portal veins and they are also expressed in pulmonary arteries. There are discrepant studies concerning the role of $K_V7.1$ in coronary arteries, due to the pharmacological effects observed (183-185).

1.5.2 Role of K_V7 channels in the heart

The heart is the organ responsible for pumping blood to the rest of the body. The electrical and mechanical mechanisms that underlies this process are fine-tune regulated and coupled. Na_V, Ca_V and K_V channels play a critical role in the generation, maintenance and repolarization of the cardiac action potential. In general terms, the ventricular cardiac action potential is divided in 5 phases. "Phase 0" is determined by Na_V channels activation (I_{Na}), which leads the generation of cardiac AP. Afterwards, during "Phase 1" there is a fast and short repolarization promoted by I_{to} (K_V channels) followed by a stable state of depolarization carried out by Ca_V channels (I_{CaL}). During the "Phase 2" or "plateau" a massive entry of Ca^{2+} ions is produced (with a slight exit of K^+ ions), which is coupled with the contraction process of ventricular cardiac muscle. "Phase 3" or "repolarization phase" is due to the outward currents I_{Kr}, and I_{Ks} (also I_{Kur} in atria). These K^+ currents promote the total repolarization of cell membrane.

The maintaining of the resting potential of cardiac myocytes is due to the activity of NaK- and Na-Ca ATPase as well as the activity of inward K^+ current (I_{K1}). This is "Phase 4" (Figure 8).

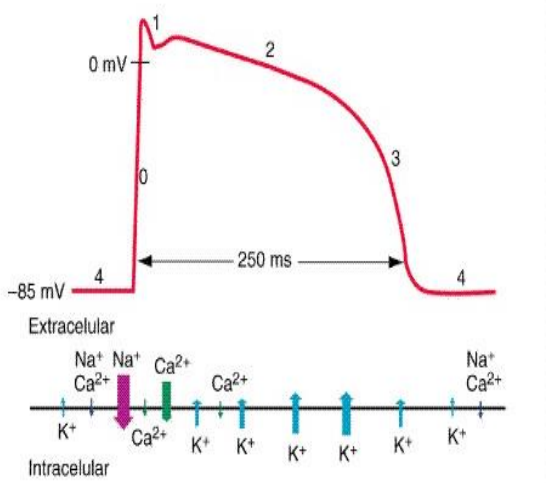

Figure 8: K_V7.1/KCNE1 channels and the ventricular myocyte action potential. A: K_V7.1 α -subunit and KCNE1 subunits suggested stoichiometry of KCNE-containing K_V channel complex. B: ventricular action potential waveform indicating the major ionic currents that contribute to its morphology and duration. Adapted from: Crump et al., (2014) **Front Genet** 24;5:3.

1.5.2.1 K_V7.1/KCNE1 channels in heart

K_V7.1/KCNE1 channels are the cloned counterpart of the I_{Ks} current, which plays a crucial role in the heart repolarization. Mutations in both components are related with several congenital diseases that can lead to dead (long QT syndrome: LQTS, short QT syndrome: SQTS, atrial fibrillation: AF or Brugada Syndrome: BS) (186). Thus, mutations in potassium channels that exhibit a loss-of-function can be responsible of a prolongation of the cardiac AP and thus, to a LQTS. This congenital syndrome may lead to a potential lethal tachycardia (*torsades des pointes*) (187). On the contrary, gain-of-function mutations in potassium channels involved in AP repolarization leads to a shortening of the AP duration, which can develop in a SQTS and also cardiac arrhythmias. These different channelopathies can finally develop sudden cardiac death. K_V7.1/KCNE1 channels are highly regulated channels. They are regulated by different compounds and are targets for antiarrhythmic drugs(152, 153, 157, 188, 189). PIP_2 modulation of K_V7.1 is coupled to cardiac physiology via α1-adrenergic receptors (190). In this manner, less activity of K_V7.1/KCNE1 channels are observed as a consequence of the decrease of α1-adrenergic stimulation, when the levels of PIP_2 are reduced. Therefore, in this situation, the cardiac action potential is prolonged (133).

In addition, activation of the β1-adrenergic receptor results in the activation of K_V7.1/KCNE1 channels via cAMP. β1-adrenergic stimulation is involved in the increase of cardiac rates, which leads to the shortening of cardiac action potentials. This process is especially important in stressed-mediated situations (191). The increase of cAMP levels involves the activation of PKA, which through the macromolecular complex of the AKAP Yotiao and C-terminus of K_V7.1 channels drives the phosphorylation of the N-terminus of the K_V7.1 α-subunit (132). The phosphorylation not only increases the magnitude of I_{Ks}, but also accelerates the activation process promoting the shortening of the cardiac action potential (132, 192).

1.5.3 Physological role of n-6 and n-3 PUFAs on K_V7 channels

Omega 3 (n-3) and omega 6 (n-6) polyunsaturated fatty acids (PUFAs) are essential nutrients. They are mainly obtained from diet in foods such as fish and vegetal oils (for n-3 PUFAs, EPA / DHA and ALA, respectively), and from vegetal oils or meats for n-6 PUFAs (AA) (193). Docosahexanoic acid (DHA) and Arachidonic acid (AA) are the most abundant fatty acids in mammalian membrane.

n-3 and n-6 PUFAs are integrated in plasma membrane as part of phospholipids. They not only playing a fundamental structural role and contribute to membrane fluidity, but also regulate several processes as free PUFAs (being released by the activity of different phospholipases, such as PLA2, PLC or PLD, PUFAs).

The dramatic increase in the n-6/n-3 ratio in the diet of the population of Western countries after the industrial revolution has, at least in part, contributed to the rise in cardiovascular disease (194, 195). An increased intake of omega 3 fatty acids (n-3 PUFAs) has been reported to have beneficial properties for cardiovascular health (196) and neurological disorders such as epilepsy and pain (197). Sinclair et al described in 1944 the rarity of cardiovascular disease CVD in Greenland Eskimos, who consumed a diet rich in n-3 PUFAs (whale, seal and fish) (198, 199). Since that moment, large evidence from cellular and animal studies (200) and from clinical trials outcomes (201-204) suggested that an increased intake of fish oil fatty acids has favorable effects on cardiovascular health. These beneficial effects mainly occur through the prevention of sudden cardiac death (SCD) that is often preceded by ventricular arrhythmias; suggesting that n-3 PUFAs are antiarrhythmic. However, not all studies have demonstrated cardioprotective effects in CVD with PUFA consumption. The recent randomized trials Alpha OMEGA and OMEGA involving patients who suffered a myocardial infarction did not showed any improvement in the clinical results following n-3 PUFA supplementation (205, 206). Moreover, pro-arrhythmic actions have been also described for n-3 PUFAs in animal models during acute regional myocardial ischemia (207) and a deleterious effect due to an increase risk of cardiac death was reported in men with stable angina (without myocardial infarction) advised to eat fish (208) and in patients with an implantable cardioverter defibrillator (ICD) (209). These differences could be explained by the fact that a diet rich in fish oil could be antiarrhythmic in some patients and proarrhythmic in others.

PUFAs affects in a different way the voltages gated channels. It has been described that PUFAs modulates cardiac ion currents, i.e. it inhibits I_{Kur}, I_{to}, I_{Ca}, and I_{Kr} and it increases I_{K1} and I_{Ks}. It is also described that PUFAs block Na_V channels (210-218).

The mechanism of action by which PUFAs modify ion channel activity has been debated for years. Several theories, ranging from: 1) nonspecific effects on the cell membrane (219) to: 2) specific binding to the ion channel (213, 220-223), have been proposed. The identification of residues in the ion channel protein involved in n-3 PUFAs sensitivity argues in favor of the second theory. Thus, for $hK_{Ca}1.1$ channels, PUFAs binding site is located in the pore domain segments (S5-S6). Moreover, Hoshi and colleagues, described that DHA increased $hK_{Ca}1.1$ currents, but it was greater in the presence of specific beta-regulatory subunits (290). For *shaker K*+ channels and $K_V7.1$ channels, it has been proposed that DHA binding site is localized in the S3-S4 of the VSD

Indirect mechanism has also been suggested, PUFAs can alter the lipid composition of the membrane, i.e. the reported effects on the cell membrane fluidity.

The effects of AA and DHA on HERG channels were tested in CHO cells. Both PUFAs block HERG channels in a time-, voltage- and state-manner, which is consistent with an open channels block mechanism. DHA showed more affinity for this state of the channel than AA. It seems that AA also interact with the inactivate state; this modulation by AA was also observed in other K^+ channels. Previously reports showed that AA introduced a rapid-voltage inactivation into non-inactivating K_V channels (allosterically closure mechanism) (210-218).

During ischemia and reperfusion, AA levels rise at the intracellular and extracellular levels (306). This increase is related to a protected role to prevent arrhythmias. Moreover, similar role has been proposed to DHA because it blocks Na_V and Ca_V channels and enhances I_{Ks} currents. In all these situations, there is a shortened of the cardiac AP. In addition, these compounds block I_{Kr}, I_{K1} and I_{to} which results in a lengthened cardiac AP. The sum of the results suggests an elongate refractory period and a shorter cardiac excitability (210-218).

Among other targets, the beneficial actions of n-3 PUFAs occur through the modulation of K_V7 channels. In the heart, n-3 PUFA decrease the expression of $K_V7.1$ channels reducing the risk of arrhythmia by shortening the action potential duration (216, 225, 226). In the neuronal system, the activation of $K_V7.2/K_V7.3$ channels (major components of the neuronal M-current) decreases neuronal excitability and therefore the risk of seizure (227).

On the contrary, the effects of n-6 PUFAs are associated with pro-inflammatory processes (228). For instance, the increase in the n-6/n-3 ratio, promoted by a disbalance diet, raises the risk of cardiovascular diseases (229).

1.5.3.1 n-6 and n-3 PUFAs derivatives are specific pro-resolving mediators

The inflammation process exhibits two active steps, the pro-inflammatory and the resolution phases. The last one was considered a passive one until few years ago. Both are orchestrating by different immune cells and compounds, whose composition and levels change through the development of the whole process. Resolution of acute inflammation involves a recruitment of active programs, which make possible return to pre-inflammatory states (230).

n-6 PUFAs metabolites: Lipoxins

AA is an essential fatty acid involved in a plethora of physiological process. Its metabolism generates several compounds (prostaglandins PGs, tromboxanes TXs, leukotriens LTs, and HETEs) that are involved in different processes such as inflammation, control of the vascular tone, platelet aggregation, etc. In general they are related with in pro-inflammatory effects (231). However, AA-derived metabolites, such as LXA_4 and e-LXA_4, have an active role in the resolution phases of the inflammatory processes (232). Briefly, AA is metabolized by two main enzymes; COX (COX1, constitutively active, and COX2, triggered by aspirin and inflammatory processes) and LOX enzymes. COX especially promotes the synthesis of PGs, whereas LOX activity leads the synthesis of 5-HETE, 5-HpETE and LT (series 4) both mainly in cells of the immune system (granulocytes, mastocytes, monocytes and macrophages) (228). LXA_4 and e-LXA_4 are products of the LOX-5 and COX-2 metabolism, respectively (see scheme below, Figure 9). The effects triggered by LXA_4 and e-LXA_4 are mediated, at least in part, by the ALX receptor (233, 234)

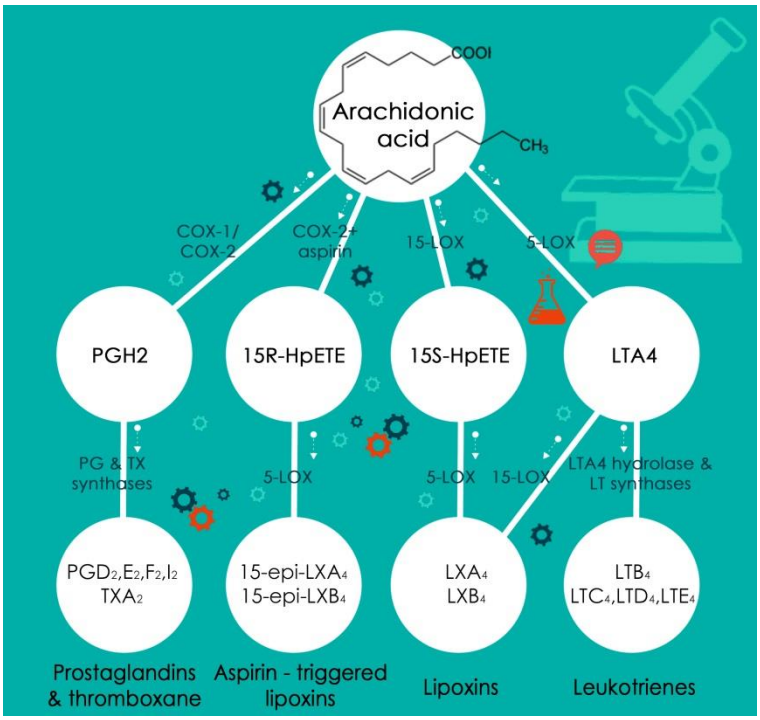

Figure 9: Schematic view of Arachidonic acid metabolism. Modified from: Yee-Ping et al., (2009) **Prostaglandins Leukot Essent Fatty Acids** 81(5-6):357-366.

n-3 PUFAs metabolites: Resolvins

Increased levels of EPA and DHA in the plasma membrane displace AA of the lipid environment. This increase in n-3 PUFAs also displace the enzymatic production balance to the production of n-3 PUFAs-derived metabolites (231, 235). The main n-3 PUFAs derivatives are maresins, protectins and resolvins. These derivatives, together with LXA_4 and e-LXA_4, act in the resolution of inflammation and are known as SPMs (specialized pro-resolving mediators).

There are two main groups of resolvins (Rv): i) metabolites from EPA (RvE), and ii) DHA metabolites (RvD). RvE group can also be subdivided in RvE1 and RvE2. RvD can be subdivided in those that appear in the absence of aspirin (17-S-hidroxi Rv, 17-S RvD1) and those triggered by the consumption of aspirin and that are metabolized through the activity of COX-2 (*17-R-hidroxi,*17-R RvD1 or ATRvD1).

It is important to mention that n-3- and n-6-derived metabolites (resolvins and lipoxins) share the same cellular receptor (230).

In inflammation there is an increase in the enzymatic synthesis of resolvins. RvD1 showed a potent anti-inflammatory and pro-resolution effectiveness. It has been observed in kidney ischemia an improving of the functional and morphological injury, reducing the interstitial fibrosis and blocked Toll-like receptor that mediates macrophages activation (236-238). Moreover, RvD1 blocked the neutrophil recruitment and also controls inflammation after oxidative stress. Several cardiovascular diseases, such as atrial fibrillation, myocardial infarction or heart failure, involve inflammation (104, 239-241). Therefore, the knowledge of the precise mechanisms that lead these mechanisms may help to find new molecular targets for the treatment and/or prevention of these diseases.

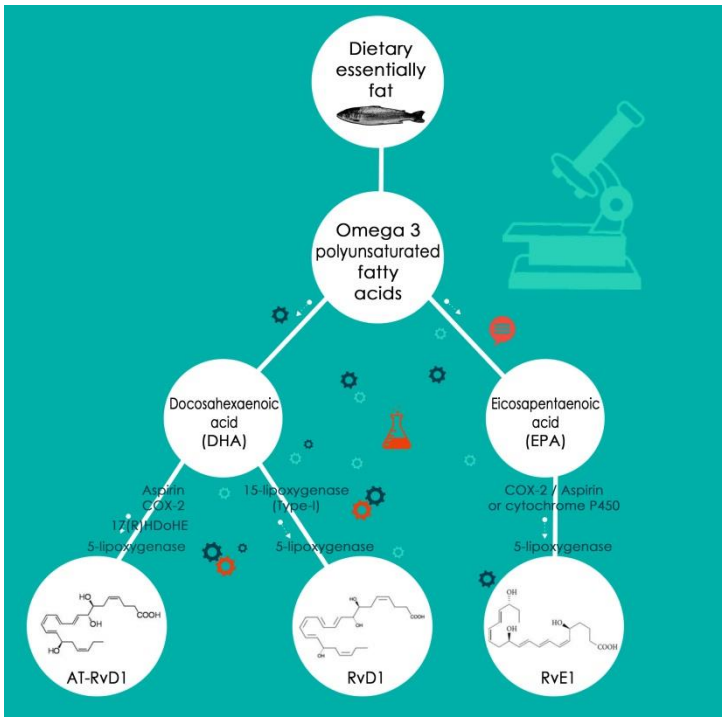

Figure 10: Schematic view of Resolvins Synthesis route. n-3 PUFAs are derived from dietary essentially fat (especially enriched in fish). RvD1 and AT-RvD1 are derived from DHA, whereas RvE1 is derived from EPA. COX-2, cytochrome P450, and 5- and 15-lipoxygenase enzymes are involved in these processes. Adapted from: Ji R et al., (2011) **Trends Neurosci.** 34:599-609.

2. OBJECTIVES

Voltage dependent potassium channels are membrane proteins highly modulated by several physiological, pharmacological and pathological events and are involved in a plethora of pathophysiological process, including immune response, cardiac arrhythmias and vascular function.

It has been demonstrated that K_V7 channels control vascular tone (182, 242). Indeed, K_V7 biophysical properties resemble K^+ currents recorded in arterial and venous musculature. However, a relationship between functional currents and specific genes has not been established (242). Heterotetramerization of K_V7 isoforms shapes K^+ currents, and this complexity is further increased by KCNE regulatory subunits (243, 244). Cardiovascular musculature mostly expresses $K_V7.1$, $K_V7.4$, and $K_V7.5$ channels (111, 181). Accordingly, K_V7 blockers produce contractions that may vary in magnitude depending on the vascular bed (245, 246). The existence of channel combinations makes difficult to decipher pharmacological implications. Therefore, determining the K_V7 isoforms that control smooth muscle tone is crucial.

It has been described that n-3 or n-6 PUFAs can exert anti- or proarrhythmic actions, maybe due to their interaction with cardiac ion channels. However, the effects of n-3 and n-6 PUFAs and their metabolites (LXA_4, 15-epi-LXA_4 and RvD1) on K_V7 channels and their different effects after acute or chronic administration are not completely understood (247). The scenario becomes more difficult because PUFAs active metabolites are involved in the resolution of inflammation (230, 248) (lipoxins and resolvins), and their effects on cardiac K_V channels have not been studied until now. They can exert their anti-inflammatory effects through their initial actions on K_V channels.

The **Hypothesis** of the present Doctoral Thesis is that K_V7 channels have crucial effects on the cardiovascular system, and that the effects of polyunsaturated fatty acids and their derivatives on these channels can trigger important effects on cardiac arrhythmias and vascular tone.

The **Main Objective** of the present Doctoral Thesis is to analyze the functional effects of K_V7 channels in vascular smooth muscle, and their modulation by polyunsaturated fatty acids and their metabolites (LXA_4, 15-epi-LXA_4 and RvD1) on $K_V7.1$/KCNE1 channels.

In order to achieve this Objective, our **specific objectives** are to determine:

- The role of $K_V7.1$/$K_V7.5$ channels in vascular smooth muscle.
- The electrophysiological effects of docosahexaenoic (n-3) and arachidonic acids (n-6) on $K_V7.1$/KCNE1 channels.
- The electrophysiological effects of 15-epi-LXA_4, LXA_4 and resolvin D1 on K_V channels in bone marrow derived macrophages and in $K_V7.1$/KCNE1 channels.

. MATERIALS AND METHODS

3.1 PRIMARY CELL CULTURE

3.1.1 Rat blood vessel myocytes

The procedures used conformed the NIH guidelines (Guide for the care and use of laboratory animals) (NIH publications number 23–80) revised in 2011; and from Directive 2010/63/EU of the European Parliament on the protection of animals used for scientific purposes were approved by the Ethics Committee of the University of Barcelona. Rat aorta, coronary artery and cava venous myocytes were isolated by enzymatic digestion as previously described (249) and they were used for confocal and electrophysiological studies (250). Briefly, coronary arteries (250-350 μm internal diameter) were isolated from male Wistar rats (250 to 300 g) in Krebs solution. For myocyte isolation, arteries were cut into small segments and placed into a nominally Ca^{2+}-free physiological salt solution (PSS, Table 2) containing (in mg/mL): papain 1, dithiothreitol 0.8, and albumin 0.7 for 20 min. Thereafter, artery segments were incubated for additional 15 min in Ca^{2+}-free PSS (Table 2) containing (in mg/mL) collagenase F 1, collagenase H 0.3, and albumin 0.7. Cells were stored in Ca^{2+}-free PSS (4 ºC) and used within 8 h of isolation (Table 2). These experiments were performed in Drs. Cogolludo and Felipe´s Laboratories. (250).

3.1.2 Guinea-pig cardiac ventricular myocytes

The procedures used conformed the NIH guidelines (Guide for the care and use of laboratory animals) (NIH publications number 23–80) revised in 2011; and from Directive 2010/63/EU of the European Parliament on the protection of animals used for scientific purposes and approved by the University of Milano-Bicocca ethics review board.

Adult Dunkin-Hartley guinea-pig were anesthetized by 100 mg/kg sodium thiopental (Sigma Aldrich) and euthanized by cervical dislocation and exsanguinated. Cardiac ventricular myocytes were isolated by using a retrograde coronary perfusion method previously published (251) with minor modifications. Briefly, hearts were quickly removed, and the ascending aorta was connected to the outlet of a Langendorff column, perfused with: 1st) normal Tyrode's solution (37°C), 2nd) Ca^{2+}-free Tyrode solution, 3rd) Ca^{2+}-free Tyrode solution with collagenase and trypsin and 4th) Ca^{2+}-free Tyrode solution. Cells were maintained at 4ºC until use (225). These experiments were performed in Dr. Zaza´s Laboratory.

3.1.3 Bone marrow-derived macrophages (BMDM)

The procedures used conformed the NIH guidelines (Guide for the care and use of laboratory animals) (NIH publications number 23–80) revised in 2011; and from Directive 2010/63/EU of the European Parliament on the protection of animals used for scientific purposes and approved by the Institutional committee on bioethics (authorization 28079-37A to the Instituto de Investigaciones Biomédicas "Alberto Sols", Madrid). BALB/c mice (aged 8 to 12-weeks) were sacrificed by CO_2 chamber euthanasia. Pelvises, femurs and tibiae were dissected removing adherent tissue. Total bone marrow was obtained by flushing pelvises, femurs and tibiae with Dulbecco´s Modified Eagle´s Medium (DMEM). Bone marrow mononuclear phagocytic precursor cell were propagated in suspension by

culturing in DMEM containing 10% fetal bovine serum (FBS), 100 UmL^{-1} penicillin, 100 μgmL^{-1} streptomycin (all from Gibco, ThermoFisher), and 0.2 nM recombinant murine M-CSF (Pepro-Tech) in tissue-culture plates. The precursor cells were becoming adherent within 7 days of culture. For priming of BMDM, cells were maintained in DMEM medium supplemented with 10% FBS for 14 h prior to use. Experiments were carried out in phenol-red free DMEM medium and 2% of heat-inactivated FBS plus antibiotics (234). The cellular extraction was performed in Dr. Boscá´s Laboratory.

3.2 CULTURE CELL

3.2.1 COS-7 cells

The fibroblast-like cell line from African green monkey COS-7 was obtained from the American Type Culture Collection (Rockville, MD, US). COS-7 cells were cultured in DMEM supplemented with 10% FBS, 100 U mL^{-1} of penicillin and 100 µg mL^{-1} streptomycin (all from Gibco). Cells were grown in a humidified atmosphere with 5% CO_2 at 37ºC. COS-7 cells have an endogenous acid-sensitive K^+ current (252) which did not interfere with the recordings obtained after transfecting the cells with K_V7 subfamily channels, which are the potassium channels of our interest. Moreover, these cells do not express any endogenously accessory subunits, which could interfere or modify the current of interest, being COS-7 a good cell model for this study.

For electrophysiological recordings, cells were incubated in 35 mm pretreated sterilized dishes, whereas for protein extraction and Western blot, cells were grown in 100 mm culture dishes (Falcon).

3.2.2 HEK293 cells

The HEK293 cell line (Human Embryonic Kidney derived cell line) was obtained from the American Type Culture Collection (Rockville). HEK293 cells were cultured in DMEM supplemented with 10% FBS, 100 UmL^{-1} of penicillin and 100 UmL^{-1} streptomycin (all from Gibco). HEK293 cells exhibit a very small endogenous K_V currents (~200 pA) (253), which do not interfere with the currents elicited by the over expression channels that were transfected in this study. It is also a good cellular model because, although the mRNA of regulatory subunits has been observed; there is no evidence of this type of proteins which could modulate the channels of interest (253). For patch-clamp experiments, cells were grown in 35 mm sterilized dishes (Falcon). For confocal studies, HEK293 cells were plated in poly-lysine coated coverslips (136, 254).

3.2.3 Transfection process

For patch-clamp experiments, KCNQ1 and KCNQ5 cDNA were transfected or co-transfected in COS-7 cells using 0.5 µg pEYFP-N1-KCNQ1 plasmid that codifies for $K_V7.1$ channels and 1 µg pEYFP-N1-KCNQ5 plasmid that codifies for $K_V7.5$ channels (both kindly provided by Dr. Felipe, University of Barcelona, Barcelona, Spain). For the electrophysiological studies on $K_V7.1/K_V7.5$ heterotetrameric channels, both plasmids were co-transfected. For electrophysiological experiments with omega-3 and omega-6 PUFAs, and their metabolites on the $K_V7.1$-KCNE1

currents, transfection of COS-7 cells was performed with 0.5 μg pEYFP-N1-KCNQ1 and 0.5 μg pECFP-C1-KCNE1 (which codifies for KCNE1 regulatory subunits).

In those experiments in which the electrophysiological effects of lipoxin A_4 (LXA_4) and 15-epi-lipoxin-A_4 (e-LXA_4) on $K_V1.5$ and $K_V1.3$ currents were analyzed, HEK293 cells were transfected with $K_V1.5$ (0.5 μg) and $K_V1.3$ (0.2 μg). $K_V1.5$ was cloned into a modified pBK plasmid (kindly provided by Dr. M.M. Tamkun, Colorado State University, Fort Collins, CO, USA) and $K_V1.3$ cloned into pEYFP-C1 (gift from Dr A. Felipe, University of Barcelona, Barcelona, Spain). In all cases, transfection was performed together with 0.5 μg of the reporter plasmid EBO-pcD-Leu2-CD8 (for selection transfected cells) per 35 mm culture dish (136).

Transient transfections were carried out in cells at 60-80% confluence following the FuGENE6 transfection method (Promega). The ratio μg DNA:μL Fugene was 1:3. Before experimental use, transfected HEK293 or COS-7 cells were incubated with polystyrene microbeads precoated with anti-CD8 antibody (Dynabeads M450, Dynal)

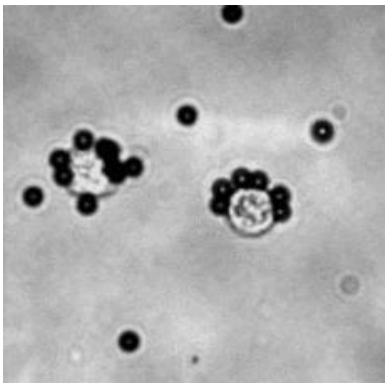

Figure 11: Polystyrene microbeads binding cells as selection process.

For confocal studies, coinmmunoprecipitation and Western blot (WB) analysis, HEK293 cells were transfected with Metafectene™ (Biontex) nearly at 80% confluence, following the manufactor's directions.

For protein extraction and posterior WB related to the effects of n-3 PUFAs, 100 mm culture dishes were transfected at 60 to 80% confluence with 4 μg of pEYFP-N1-KCNQ1 with or without 4 μg pECFP-C1-KCNE1 using Fugene 6 (see above). Afterwards, culture cells were incubated (48 h) with DHA (30 and 100 μM) or without it for control conditions.

3.3 DRUGS AND REAGENTS

The K_V7 specific activators and blockers used in the present Doctoral Thesis were: retigabine (RTG, also called ezogabine), chromanol 293B and linopirdine (Table 1). All of them were dissolved in DMSO to yield stock solutions of 3.10^{-2} M. RTG stock solution was diluted to 1-30 μM concentration, with external solution for its use in patch-clamp and in rat arterial reactivity experiments. Further dilutions of chromanol 293B and linopirdine stock solution were performed as previously described (250).

In the present Doctoral Thesis, we used DHA (n-3 PUFA) and Arachidonic acid (AA) (n-6 PUFA) (Table 1). Both PUFAs were diluted in absolute ethanol to yield stock solution of 10^{-2} M and 10^{-4} M. DHA and AA were ampoule

aliquoted and stored under an inert argon atmosphere (in order to prevent oxidation of the samples) at -20 ºC. DHA was used at the concentration range of 20-100 µM and AA was used at a concentration of 20 µM, after being diluted in external solution (see below) (212).

Table 1: Classification of products used. Left to right: common name, chemical name and reference.

Common name	Chemical name	Reference and origin
Retigabine	N-(2-Amino-4-(4-fluorobenzylamino) phenyl) carbamic acid ethyl ester	90221- Sigma-Aldrich
Chromanol 293B	trans-N-[6-Cyano-3,4-dihydro-3-hidroxy-2,2-dimethil-2H-1-benzopyran-4-yl]-N-methyl-ethanesulfonamide	C2615- Sigma-Aldrich
Linopirdine	1,3-Dihydro-1-phenyl-3,3-bis(4-pyridinylmethyl)-2H-indol-2-one	L134- Sigma-Aldrich
Docosahexanoic acid (DHA)	cis-4,7,10,13,16,19-Docosahexaenoic acid	53171- Sigma-Aldrich
Arachidonic acid (AA)	Eicosa-5Z,8Z,11Z,14Z-tetraenoic acid	10931- Sigma-Aldrich
17(S)-Resolvin D1 (RvD1)	7S,8R,17S-trihydoroxy-4Z,9E,11E,13Z,15E,19Z-docosahexaenoic acid	Sc-204877- Santa Cruz Biotechnology
Lipoxin A_4 (LXA_4)	5S,6R,15S-trihydroxy-7E,9E,11Z,13E-eicosatetraenoic acid or 5(S),6(R),15(S)-triHETE	90410- Cayman Chemical Company
15-Epi-lipoxin A_4 (e-LXA_4)	5(S),6(R),15(R)-trihydroxy-7E,9E,11Z,13E-eicosatetraenoic acid	90415- Cayman Chemical Company

The effects of DHA and AA metabolites, 17(S)-Resolvin D1 (RvD1), LXA_4 and 15-e-LXA_4 were also studied (Table 1). These compounds were dissolved in ethanol and stored protected from light at -80 ºC to prevent oxidation. They were used, for electrophysiological recordings, at a 5-500 nM concentration range.

3.4 ELECTROPHYSIOLOGICAL RECORDINGS

Electrical activity is part of animal physiology. In the XIX century, experiments performed by Galvani (1791), Volta (1792) and Matteuci (1840) detected bioelectricity. They showed that the muscular contraction could be induced after applying electrical stimulation. In the early 50´s, Cole and Marmont introduced the basis of the work which make possible that Hodgkin and Huxley investigate the time- and voltage- conductance for Na^+ and K^+ ions that form the basis of the time course of the action potential (3, 4). These studies led them to get the Nobel Prize in 1963. Later on,

Sackmann and Neher (1976) developed the *patch-clamp technique* that permits the recording of the activity of single ion channels after establish high resistance seals between microelectrodes and the cell membrane. They got the Nobel Prize of Physiology or Medicine on 1991.

The electrophysiological experiments used in the present Doctoral Thesis were performed by using the patch-clamp technique (255). The aim of this technique is the recording of ionic currents, generated either: 1) by a single ion channel (*i: unitary current*) or 2) by the activation of all the channels present in the cell membrane or in a membrane patch (*I: macroscopic current*). In the present Doctoral Thesis, we have recorded the current generated by the activation of all channels present in the cell membrane.This technique is a refinement of the voltage-clamp technique and uses a glass micropipette pulled to a fine tip of approximately 1-4 μm containing an electrode. The recording electrode or "patch pipette" is filled with a saline solution and sealed (with a high resistance, GΩ) onto a patch on the surface of the cell membrane, allowing the researcher to keep constant the voltage while measuring the current flowing across the membrane of a cell or even from a single channel localized in the membrane patch.

Several configurations of the patch-clamp technique were developed (cell-attached, whole-cell, inside-out and outside-out patch-clamp). The most commonly used when studying macroscopic ion currents across the cell is the whole-cell patch-clamp technique. In this approach, after the seal is formed between the electrode and the cell membrane, a gentle suction is applied, rupturing the cell membrane in the patch and gaining access to the cytoplasm. Consequently, the internal pipette solution enters in direct contact with the intracellular space. The cell membrane is voltage clamped, and the recorded currents are a composite of the activity of all ion channels present in the cell membrane (Figure 12).

A variation of the same procedure is the perforated-patch technique. In this configuration, the internal solution contains a small concentration of an antifungal agent (like amphotericin B or nystatin), which diffuses into the membrane patch forming small pores in the cell membrane, which provides electrical access into the intracellular space, without dialyze the cell cytoplasm; thus, retaining most intracellular signaling mechanisms.

In the present Doctoral Thesis, the whole-cell and the perforated patch-clamp configurations were used to record the ion currents. Before experimental use, transfected HEK293 or COS-7 cells were incubated with polystyrene microbeads precoated with anti-CD8 antibody (Dynabeads M450, Dynal). A suspension of guinea-pig ventricular myocytes, rat vascular myocytes, BMDM, HEK293 or COS-7 cells were plated in a 0.5 mL chamber which was over an inverted microscope (TMS, Nickon). After 15 min for settlement of the cells, they were perfused with external solution (which mimics extracellular media, Table 2) at a constant speed.

Micropipettes were made from borosilicate glass capillary tubes (GD-1 model, Narishige) on a horizontal puller (P-87 model, Sutter Instrument Co.) and heat-polished with a micro-forge (MF-83, Narishige). After heat-polishing, the resistance of the patch electrodes tip (filled with the internal solution) averaged 2-4 MΩ. The patch electrodes were filled with an internal solution whose composition mimics the cytosol media (see below, Table 2).

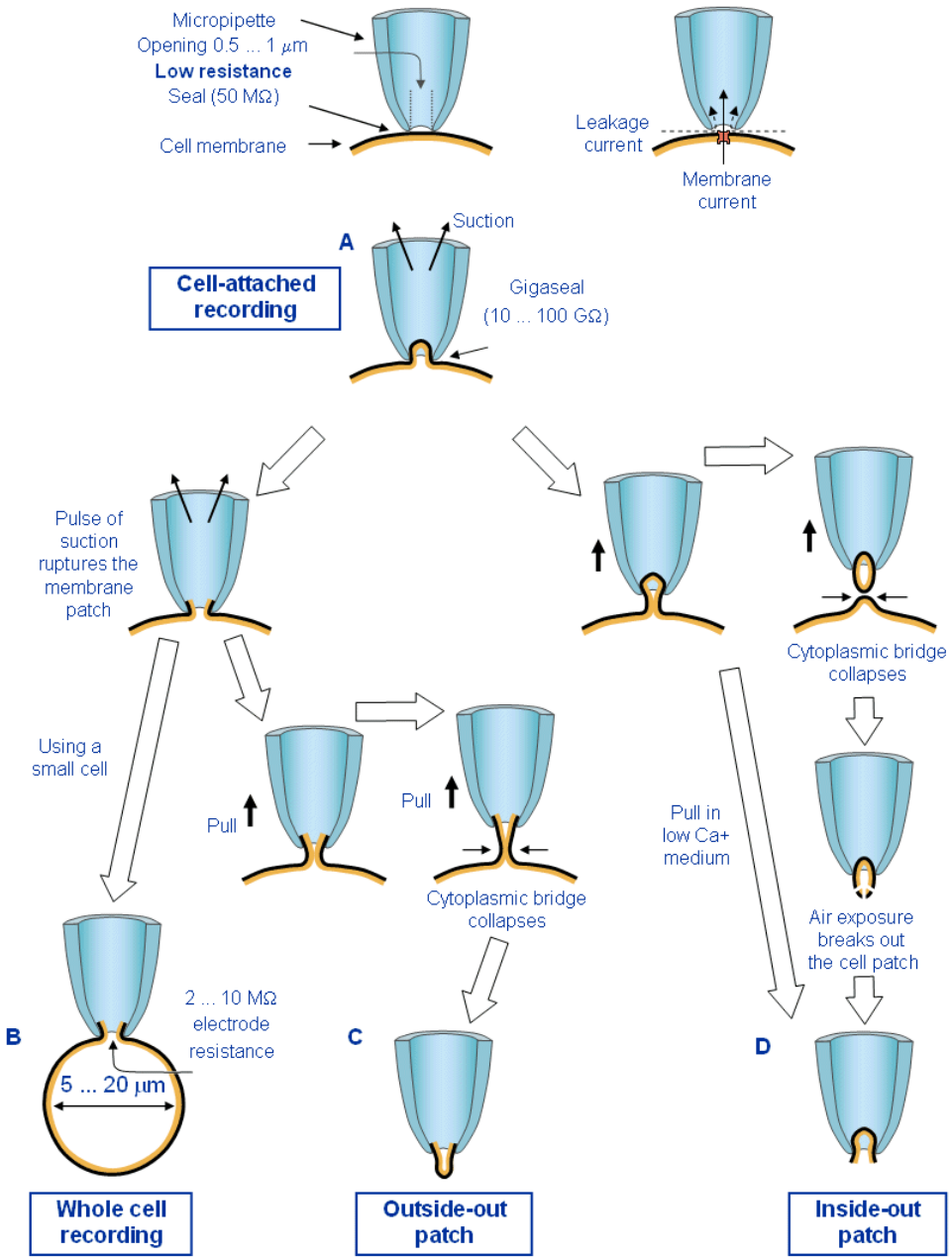

Figure 12: The patch clamp technique configurations. The started configuration *cell- atached* (**A**) from which it is possible to achieved the others. (**B**) *Whole cell* configuration, (**C**) *Outside-out* configuration and (**D**) *inside-out* configuration. Modified from: Hamill et al., (1981) **Pflügers Arch**. 391:85-100

In BMDM, transfected HEK293 cells, guinea-pig ventricular myocytes and rat coronary myocytes, the whole-cell configuration of the patch-clamp technique was used (234). Transfected HEK293 cells and rat coronary myocytes, currents were recorded at room temperature (23-25ºC) at a stimulation frequency of 0.03 Hz. In rat coronary myocytes, to reduce the contribution of other delayed rectifier potassium currents (such as K_V1), long (4 s) depolarizing pulses were applied (249). Current-voltage relationships (I-V relationships) were constructed by measuring the currents at the end of the pulse (250).

Table 2: Composition of the internal and the external solutions of different cell types.

	Internal solution (mM)				External solution (mM)		
	Cell lines	Guinea-pig myocytes	Vascular smooth muscle cells		Cell lines	Guinea-pig myocytes	Vascular smooth muscle cells
K-aspartate	80	110		**NaCl**	130	154	130
KCl	50	23	110	**KCl**	4	4	5
Phosphocreatine	3	5	-	**$CaCl_2$**	1.8	2	-
$CaCl_2$	-	-	-	**$MgCl_2$**	1	1.2	1.2
$MgCl_2$	-	3	1.2				
KH_2PO_4	10	-	-				
Mg-ATP	3	-	-	**HEPES-Na**	10	5	10
Na-GTP	-	0.4	-	**glucose**	10	5.5	10
Na-ATP	-	5	5				
HEPES-K	10	5	10				
EGTA-K	5	10	10				
Adjusted with KOH	pH 7.25	pH 7.3	pH 7.3	**Adjusted with NaOH**	pH 7.40	pH 7.40	pH 7.3

Isolated guinea-pig ventricular myocytes were re-suspended in external solution (Table 2). Only rod-shaped, Ca^{2+}-tolerant myocytes were used within 12 h from dissociation. Measurements were performed only in quiescent cardiomyocytes with clear-cut striation at physiological temperature. The solution temperature was monitored at the pipette tip with fast-response digital thermometer (BAT-12, Physitemp) and kept at 36 ± 0.5 °C. The composition of the internal solution used in the experiments performed in guinea-pig ventricular myocytes is shown in Table 2. I_{Ks} was elicited after applying a 5 s depolarizing step at +20 mV every 20 s. Holding potential was set at -40 mV to inactivate Na^+ channels. Nifedipine (10 μM) and E-4031 (5 μM) were added to the external solution (Table 2) to inhibit the L-type Ca current (I_{CaL}) and the rapidly activating delayed rectifier K^+ channel (I_{Kr}), respectively (225). Elicited currents from COS-7 transfected cells were registered using the perforated patch-clamp configuration of the patch-clamp technique. Amphotericin B (100 μg/mL) (PHR1662- Sigma-Aldrich) was added to the internal solution to make pores in the membrane seal (203, 207, 256, 257).

Electrophysiological recordings were performed using an Axopatch-200B amplifier (Molecular Devices, Sunnydale, CA, USA). Current recordings were low pass-filtered and sampled at 2 kHz with an analog-to-digital converter DigiData 1440A (Molecular Devices) (data acquisition system). Command voltages and data storage were controlled with pClamp10 software (Axon Instruments). Gigaohm seal formation was achieved by suction (2-5 GΩ). Thereafter,

capacitance and series resistance compensation were optimized and, usually, 80% compensation of the effective access resistance was obtained. Uncompensated series resistances were 4-8 MΩ and voltage errors from uncompensated series resistance were less than 2 mV.

The holding potential was set to -80 mV (unless other comments are stated), and the interpulse interval was set to a minimum of 10 s or 30 s, depending on the ion current that we are recording. The voltage pulse protocols were adjusted to determine the biophysical properties of each channel. Time constants of activation, inactivation and deactivation were determined by fitting the current recordings with a single or double exponential functions:

$$y = A_1 \exp(-t/\tau_1) + A_2 \exp(-t/\tau_2) + C$$

where τ_1 and τ_2 are the system time constants, A_1 and A_2 are the amplitudes of each component of the exponential, and C is the baseline value (207, 256, 258, 259). The voltage dependence of channel activation was fitted to a Boltzmann equation:

$$y = 1/[1 + \exp(-(E - V_h)/s)]$$

in which *s* represents the slope factor, *E* represents the applied voltage, and V_h the voltage at which 50% of the channels are activated (136, 258). Origin 8.5 (OriginLab Software, Northampton, MA) and CLAMPFIT software were used to analyze data, perform least-squares fitting and for data presentation.

3.5 RECORDING OF RAT ARTERIAL REACTIVITY

For contractile tension recording, rat endothelium-intact coronary arteries rings were mounted in a wire myograph as previously described (249). After an equilibration period of 30 min, vessels were stretched to a resting tension corresponding to a transmural pressure of 100 mmHg. Coronary artery rings were first stimulated by raising the K^+ concentration of the buffer (to 80 mM) in exchange for Na^+. Vessels were washed three times and allowed to recover before a new stimulation (185, 250).

Afterward, vessels were incubated with vehicle (DMSO, control), chromanol 293B (10 μM) or linorpiridine (10 μM) during 20 min before the stimulation with serotonin (5-HT, 1 μM). Finally, the relaxation induced by RTG (1-30 μM) was analyzed (185, 250).

3.6 INMUNOCYTOCHEMISTRY

Enzymatically isolated smooth muscle cells from rat coronary aorta or cava vessels were seeded into sterile 12 mm diameter gelatine coated glass coverslip for up to 48 hours. After fixation for 15 min with methanol (-20 ºC) at room temperature, cells were washed twice with phosphate buffered saline (PBS) during 5 min to rehydrate cells and block. Cells were permeabilized during 1 h with blocking buffer (PBS containing 0.4% Triton X-100 and 3% bovine serum albumin). After incubating with rabbit anti-K_V7.1 (1:100, APC-022 Alomone Labs) and rabbit anti-K_V7.5 (1:500, APC-155 Alomone Labs) antibodies at 4 ºC overnight, cells were incubated at 37 ºC for 15 min. Cells were washed

with wash buffer (PBS containing 3% bovine serum albumin) and exposed to a secondary antibody CY3 conjugated donkey anti-rabbit (1:200, Jackson inmunoresearch) for 2 h. Then, cells were stained with 4,6-diamidino-2-phenilindole (DAPI) for 5 min at 37ºC. Glass coverslips were mounted with Aqua Poly/Mount (from Polysciences, Inc). These preparations were examined with a Leica TCS SL laser scanning confocal spectral microscope (Leica Microsystems). A 63× oil immersion objective lens (NA 1.32) and a double dichroic filter (458/514 nm) was used to acquire images (250).

3.7 PROTEIN EXTRACTION, CO-INMUNOPRECIPITATION AND WESTERN BLOT

Rat heart, brain, aorta and cava were frozen in liquid nitrogen. Samples were softly processed with a polytron homogenizer in MBS (0.15M NaCl, 25 mM MES) at 4 ºC. Nuclei and debris were pelleted by centrifugation at 12,000 × *g* for 10 min. The resulting supernatant was centrifuged at 100,000 × *g* for 1 h. The pellet of crude membranes was resuspended in the same buffer (0.5 mL/g tissue).

In the case of HEK293 cells, they were lysed (24 h after transfection) in 1% Triton X-100, 50 mM Tris, pH 7.2, 150 mM NaCl, 1 mM EDTA supplemented with 1 µg/mL aprotinin, 1 µg/mL leupeptin, 1 µg/mL pepstatin and 1 mM phenylmethylsulfonyl fluoride. Homogenates were centrifuged at 12,000 × *g* for 10 min, and the supernatant was aliquoted and stored at -20ºC.

For co-immunoprecipitation experiments, samples were pre-cleared with protein G/A-Sepharose beads (Santa Cruz Biotechnology) in order to eliminate not specific binding between the reagents used and the proteins. Then, A/G protein was precipitated and discarded. The samples were incubated overnight with monoclonal anti-GFP, which also reacts with YFP, and polyclonal anti-K_V7.1, -K_V7.5 and -KCNE1 antibodies (4 ng/µg protein, Roche) at 4 °C. Protein sepharose (30 µl) was added to each sample for 4 h at 4 °C. Antibody-bound sepharose beads (and therefore, protein-bound antibody) were centrifuged at 5,000 × g for 45 s at room temperature and then washed to remove all the antibody and channel unbound or non-specifically bounded. The beads were removed, washed four times in NGH buffer (50 mM HEPES, 150 mM 5 NaCl, 1% Triton X-100, 10% Glycerol, pH 7.2) and resuspended in 70 µl of Laemmli SDS loading buffer. Protein samples (50 µg) and immunoprecipitates were boiled in Laemmli SDS loading buffer and were separated on 10% SDS-PAGE gels. Samples were transferred to nitrocellulose membranes (Immobilon-P, Millipore) and were blocked in 5% dry milk with 0.05% Tween-20 in PBS before immunoreactions. Membranes were immunoblotted with antibodies against K_V7.1 (1:200, APC-022 Alomone Labs) or K_V7.5 (in house, 1:500) (136, 148, 250). These experiments were performed in Dr. Felipe´s Laboratory.

Transiently transfected COS-7 cells (see above) were incubated in the absence and in the presence 30 and 100 µM of DHA and EPA. For total protein extraction, cells were washed and then centrifuged. The pellet was lysed and homogenate as previously described in (225). Samples were separated into aliquots and stored at -80ºC. The amount of protein (20-40 µg/lane) was resuspended in SDS loading buffer and boiled first at 55ºC during 12 min, in order to detect K_V7.1, and then heated at 95ºC for 5 min, to analyze KCNE1. Samples were run in 7-10% SDS-

PAGE, and transferred to a PVDF membrane (GE Healthcare). Membranes were blocked and incubated with anti-GFP antibodies (1:1000, cat. nº 11814460001 Roche) and anti-β- actin (1:40000, Sc-1615 Santa Cruz Biotechnology). Horseradish peroxidase linked goat anti-mouse (1:10000, Calbiochem) as secondary antibody was used. Immunoblot signals were visualized by chemiluminescence using ECL-plus reagent (Amersham, GE Healthcare). Quantification of band intensity was performed with the Image J software.

3.8 LIPIDS RAFTS EXTRACTION

Lipid rafts are specific membrane domains rich in cholesterol and sphingolipids. They are resistant to detergent solubilisation at 4°C and are destabilized by cholesterol- and sphingolipid-depleting agents. The methods used to isolate the lipid rafts are based on the insolubility of these structures in the non-ionic detergent Triton X-100. Following ultracentrifugation on sucrose density gradients, lipid rafts will float away from the soluble proteins, forming a cloudy band at the top of the centrifugation tube.

Lipid raft isolation was performed from HEK293 cells transiently transfected with pECFP-N1-KCNQ1, pEYFP-N1-KCNQ5 and co-transfected with pECFP-N1-KCNQ1/pEYFP-N1-KCNQ5, and also from COS-7 cells transiently transfected with pECFP-N1-KCNQ1 and pECFP-N1-KCNE1. In the last case, cells were previously incubated in the absence and in the presence of 100 μM of DHA, and crude membrane preparations from rat tissues were used as samples in lipids rafts isolation assay, as previously described (260, 261).

Briefly, transfected cells were washed twice in cold PBS, scrapped and centrifuged for 8 min. The pellet was resuspended in 0.5 mL of MES-buffered saline containing 1% (v/v) Triton X-100, MES 25 mM, NaCl 150 mM, pH 6.5 and supplemented protease inhibitors and homogenized by repeated passing (10 times) through a 25G (0.4 × 1.6 mm) needle. The addition of 1.5 mL of 53.28 % sucrose prepared in MES buffer yielded to the homogenate a final concentration of 40 % sucrose and it was placed at the bottom of an ultracentrifuge tube. Then, a 5-30 % linear sucrose gradient was formed above the homogenate and centrifuged at 39,000 rpm at 4 ºC for 20-22 h in a SW41 rotor (Beckman Instruments). A light scattering band confined to the 15-20 % sucrose region was observed that contained endogenous caveolin used as a positive control, but excluded most of other cellular proteins. Gradient fractions (1 mL) were collected from the top, separated by SDS-PAGE and analyzed by western blotting. Filters were inmunoblotted with antibodies against K_V7.1 (1:200, APC-022 Alomone Labs) and KCNE1 (1:1000, APC-163 Alomone Labs) or K_V7.5 (in house, 1:500). Caveolin, a marker of lipids rafts fractions, was detected with anti-pan-caveolin antibody (1:2500, BD Transduction Laboratories), and an anti-clathrin antibody was used to characterize non-floating fractions (1:1000, Chemicon) (225, 250).

3.9 STATISTICAL ANALYSIS

Data are expressed as mean ± SEM of n experiments. Comparisons were performed by a paired (between means values in control conditions versus mean values in the presence of drug for a single variable) or unpaired (between two different groups of conditions) Student's t- test. ANOVA was used to compare more than two groups. Differences were considered significant if $P < 0.05$.

. RESULTS

4.1 PART I. ROLE OF $K_V7.1/K_V7.5$ IN VASCULAR SMOOTH MUSCLE

4.1.1 Expression of $K_V7.1$ and $K_V7.5$ in different tissues

K_V7 channels are widely distributed in the different tissues and even within different regions of a same tissue. In order to know the expression pattern of $K_V7.1$ and $K_V7.5$, several approaches were made.

Figure 13A shows the levels of expression of these proteins in five different tissues (from rat). On the one hand, $K_V7.1$ channel is expressed in brain, skeletal muscle and heart, and, to a lesser extent, in aorta and cava. On the other hand, the highest $K_V7.5$ channel expression was observed in brain and aorta, lower in skeletal muscle and cava, and it was not present in the heart. The expression pattern of $K_V7.1$ and $K_V7.5$ channels was also analyzed in isolated rat coronary myocytes by immunocytochemistry and we observed that both channels are present in these cells (Figure 13B). In order to elucidate the presence of homo- and/or heterotetramers of these channels in rat coronary myocytes, we analyzed the pharmacology of the K^+ currents in these cells (Figure 13C).

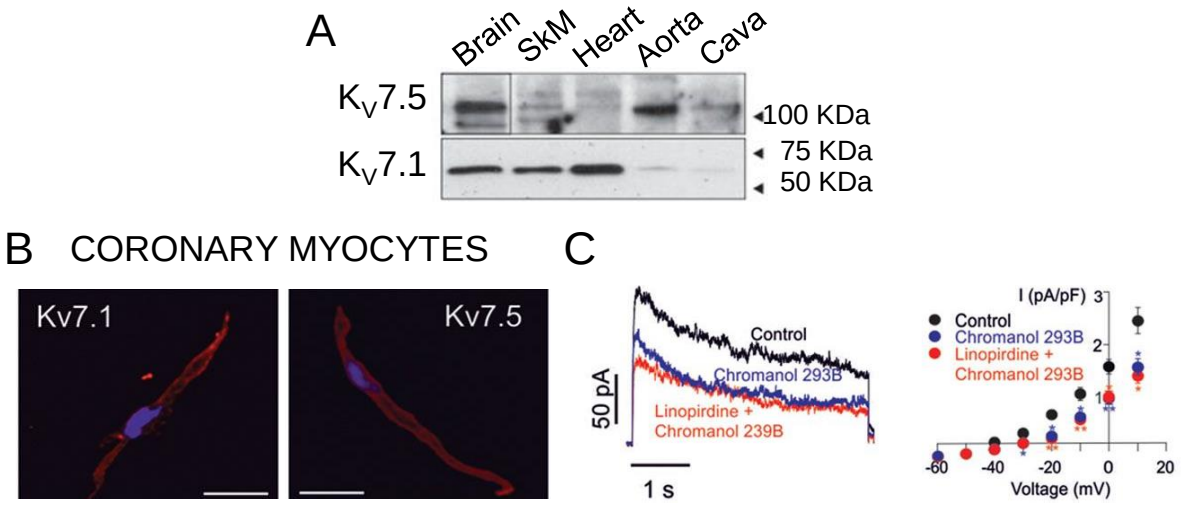

Figure 13: Expression pattern and function of $K_V7.1$ and $K_V7.5$ channels. **A**: $K_V7.1$ and $K_V7.5$ abundances in plasma membrane preparations of rat brain, quadriceps (skeletal muscle, SkM), heart, aorta artery and cava vein. **B**: Immunocytochemistry of $K_V7.1$ and $K_V7.5$ channels in isolated coronary myocytes from rat. Myocytes were stained with anti-$K_V7.1$ (left) or anti-$K_V7.5$ (right). Bars represent 20 µm. **C**: K_V currents in isolated rat coronary myocytes. Left panel shows representative K_V current recordings after applying 4-s depolarization pulses from a holding potential of -60 mV to +10 mV, in the absence (black traces) or in the presence of chromanol 293B (10 µM, blue traces) or chromanol 293B plus linopirdine (10 µM, red traces). Right panel shows I-V relationships in the absence (control condition, black circles), in the presence of chromanol 293B (10 µM, blue circles) or in the presence of linopirdine plus chromanol 293B (red circles). Data show the mean ± SEM of 6 experiments per group. *: $P < 0.05$, **: $P < 0.01$ *vs.*control

Chromanol 293B (selective blocker of $K_V7.1$) and linopirdine (blocker of all members of K_V7, (173) were used to demonstrate that these currents are, at least in part, the consequence of the activation of K_V7 subfamily channels (184, 262). Figure 13C shows representative current traces obtained after applying 4 s depolarizing pulses from -60 to +10 mV recorded in isolated coronary myocytes. Current recordings were studied in the absence (control), in the presence of 10 µM chromanol 293B and in the presence of 10 µM linopirdine plus 10 µM chromanol 293B. Block

produced by chromanol 293B and chromanol 293B+linopirdine was similar (39.48 ± 4.5 %, n = 6, and 39.35 ± 3.0 %, n = 5, P > 0.05, respectively), suggesting that the K_V7 subfamily channels are involved in the K^+ currents elicited by isolated coronary myocytes. Concomitantly to the expression pattern of $K_V7.1$ and $K_V7.5$ channels (Figure 13B), K^+ currents were similarly blocked by linopirdine and chromanol 293B (Figure 13C).

K_V7 channels are present in several cardiovascular tissues and it is known that they can form heterotetramer channels (263, 264). To assess if $K_V7.1$ and $K_V7.5$ channels interact, we first performed co-immunoprecipitation experiments in rat aorta myocytes and HEK293 cells (Figure 14).

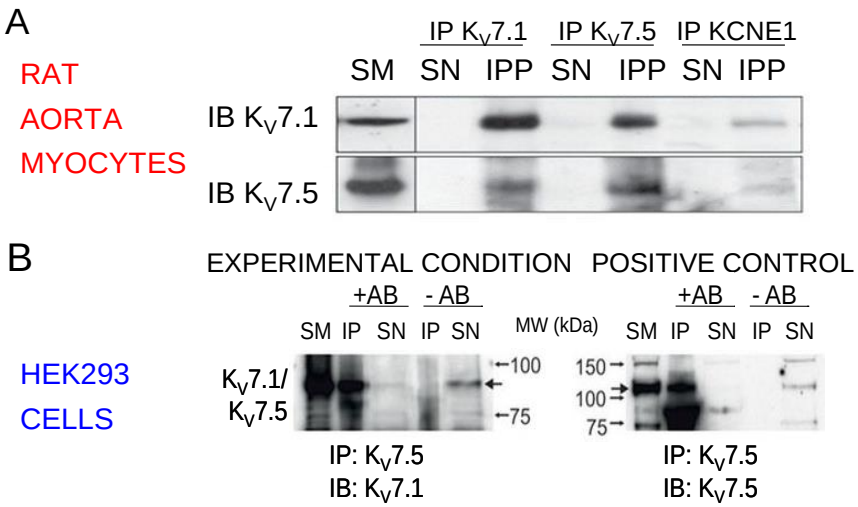

Figure 14: Co-inmunoprecipitation assay of $K_V7.1$ and $K_V7.5$ channels. A: Anti-$K_V7.1$ and anti-$K_V7.5$ were used for immunoprecipitation (IP) and immunoblotting (IB) in rat aorta myocytes. The presence of KCNE1 in the co-inmunoprecipitation complex was also analyzed, immunoprecipitating KCNE1. **B:** $K_V7.1$ inmunoprecipitates with $K_V7.5$ channels in transfected HEK293 cells with $K_V7.1$ and $K_V7.5$ channels. Anti-$K_V7.5$ in IP, in experimental condition (left) and in positive control condition (right). The resulting IPs were IB with anti-$K_V7.1$ and anti-$K_V7.5$ in experimental condition (left) and in positive control condition (right) respectively. SM: starting material, SN: immunoprecipitated supernatant and IPP: immunoprecipitated.

Figure 14A shows co-immunoprecipitation assays performed in rat aorta myocytes. Both approaches: i) immunoprecipitation (IP) with anti-$K_V7.1$ and immunoblotting (IB) with anti-$K_V7.5$ and ii) IP with anti-$K_V7.5$ and IB with anti-$K_V7.1$ antibody were done. We obtained positive results in both conditions (IPP detected signal). Because smooth muscle cells also express KCNE subunits, an IP with anti-KCNE was performed and it was blotted by using both, anti-$K_V7.1$ and anti-$K_V7.5$. In both cases, there was a positive result, although the intensity when IB with anti-$K_V7.5$ was lower. The results obtained when a co-immunoprecipitation assay was performed in transient transfected HEK293 cells with $K_V7.1$-YFP and $K_V7.5$-YFP were similar to those performed in rat aorta myocytes. All these results suggest that $K_V7.1$ subunits interact with $K_V7.5$ subunits and that this complex might be interacting with KCNE1 regulatory subunits.

4.1.2 $K_V7.1$ but not $K_V7.5$ channels target lipids rafts

The spatial location of cardiovascular ion channels in lipid raft microdomains is physiologically relevant (265-267). In fact, it has been demonstrated that vascular smooth muscle caveolar rafts are important for muscular reactivity (268). Previous studies demonstrated that $K_V7.1$ and $K_V7.5$ differentially target to lipid rafts (225, 269, 270). Lipid rafts

fractions were detected using caveolin protein, whereas clathrin fractions indicate areas of plasma membrane out of lipid-enriched microdomains. We first, transfected HEK293 cells with KCNQ1-YFP or KCNQ5-YFP in order to analyze the targeting of each channel. The results confirmed that $K_V7.1$ channels target caveolin-rich membrane fraction. In contrast, $K_V7.5$ channels did not fractionate with caveolin.

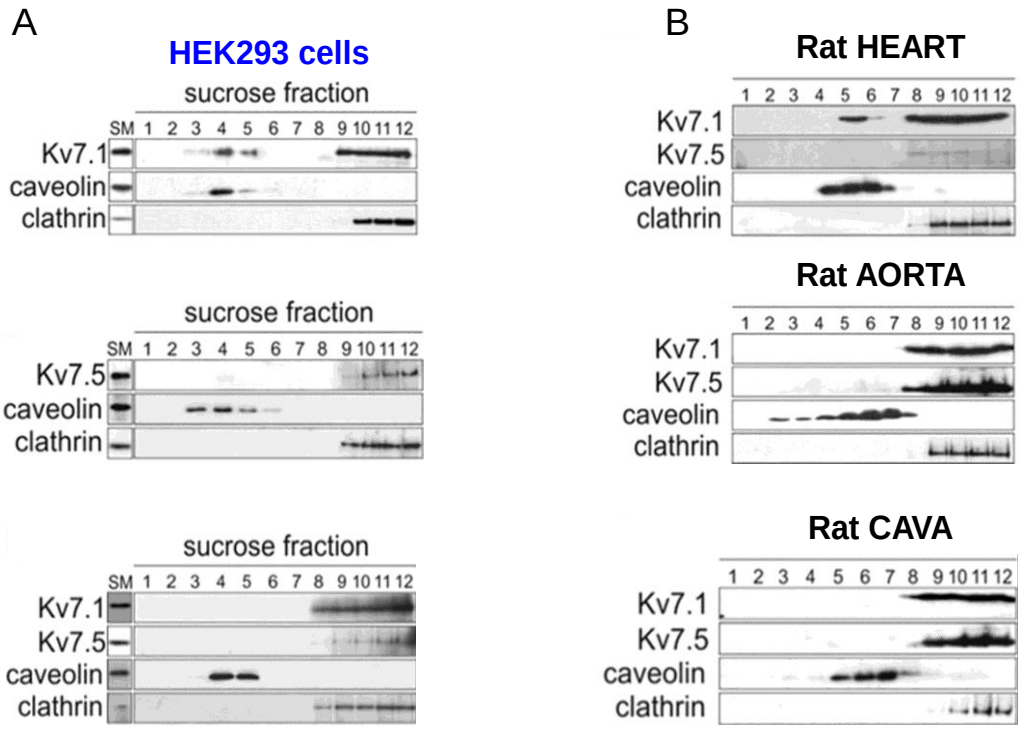

Figure 15: $K_V7.1$ and $K_V7.5$ channels differentially target to lipids rafts. Caveolin indicates low-buoyancy rafts and clathrin distributes in nonfloating fractions, numbers denote different fractions from the top (1) to the bottom (12) of the sucrose density gradient. **A:** $K_V7.1$ channels target to lipids rafts (top) whereas $K_V7.5$ channels not (middle) in previously transfected HEK293 cells. Both channels were co-transfected in HEK293 cells and they were not detected in lipids rafts (bottom). **B:** Representative sucrose gradient fractions of the heart (top), aorta artery (middle) and cava vein (bottom).

Thus, $K_V7.1$ was enriched in rafts (44 ± 8 %; Figure 15 A-top), whereas $K_V7.5$ was almost completely confined to clathrin fractions (90 ± 3%; n = 3, $P < 0.05$, Figure 15A-middle). We next analyzed whether or not $K_V7.1/K_V7.5$ heterotetrameric channels target lipid rafts. When HEK293 cells were cotransfected with $K_V7.1$ and $K_V7.5$, $K_V7.1$ shifted out from raft domains (96 ± 7%; Figure 15A).

Secondly, we analyzed lipid rafts approaches in different tissues (Figure 15B). As we can observe, $K_V7.1$ channels were located in caveolin-enriched microdomains in those tissues in which $K_V7.5$ channels were not expressed, as heart. However, in the tissues in which both channels were expressed, aorta artery and cava vein, neither of the channels targeted lipids rafts. These results confirm that when $K_V7.5$ channels are present, $K_V7.1$ channels location change along the plasma membrane.

4.1.3 $K_V7.5$ and $K_V7.1$ α-subunits form functional heterotetrameric channels.

The co-IP and lipid raft targeting experiments indicate that both $K_V7.1$ and $K_V7.5$ α-subunits physically interact. In order to know if these heterotetramers are able to generate a functional channel, patch-clamp experiments in COS-7 cells transfected with $K_V7.1$, $K_V7.5$ and $K_V7.1$+$K_V7.5$ were performed. To that end, COS-7 cells were transiently transfected or co-transfected with KCNQ1-YFP and KCNQ5-YFP plasmids. Figure 16A shows current records generated after the activation of $K_V7.1$ or $K_V7.5$ homotetramers and $K_V7.1/K_V7.5$ heterotetrameric channels. Currents were evoked by a series of 5.5-s pulses from a holding potential of -80 mV to +100 mV in 20 mV steps and returned to -40 mV. Figure 16B shows the I-V relationships obtained after measuring the current at the end of the 5.5 s test pulse versus the membrane potential. Figure 16C shows the voltage-dependence of activation of the currents analyzed after measuring the initial magnitude tail currents at -40 mV.

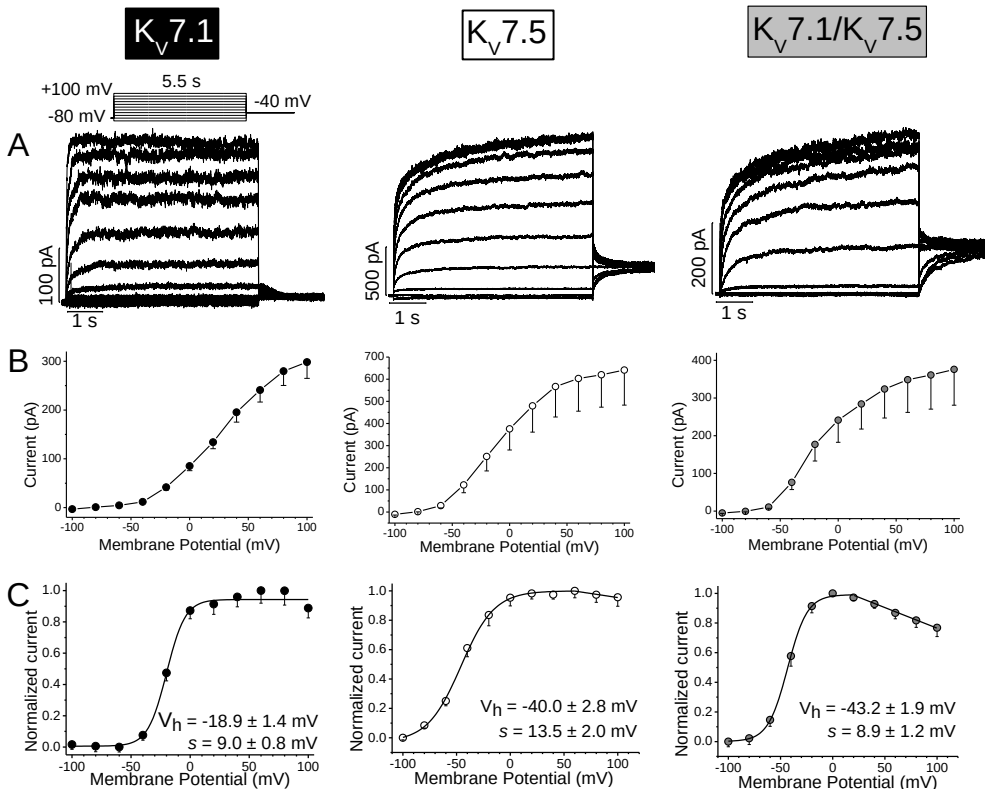

Figure 16: Electrophysiological properties of $K_V7.1$, $K_V7.5$ and $K_V7.1/K_V7.5$ currents. A: Current traces recorded after applying depolarizing 5.5-s pulses from a holding potential of -80 mV to +100 mV in +20 mV steps. **B:** I-V relationships obtained after measuring the ion current at the end of the test pulse. **C:** Activation curves of $K_V7.1$, $K_V7.5$ and $K_V7.1/K_V7.5$ current obtained after representing the initial tail current amplitude *vs.* the previous step potential. V_h and s were obtained after fitting the activation curves to a Boltzmann equation. Data are presented as mean values ± SEM of n = 7-13 experiments.

The obtained values were fitted to a Boltzmann equation from which we obtained the midpoint of activation (V_h) and the slope of the curve (s) (see Materials and Methods section). Thus, we obtained values of V_h = -18.9 ± 1.4 mV and s = 9.0 ± 0.8 mV (n = 17) for $K_V7.1$ channels; V_h = -40.0 ± 2.8 mV and s = 13.5 ± 2.0 mV (n = 13) for $K_V7.5$ channels; and V_h = -43.2 ± 1.9 mV and s = 8.9 ± 1.2 mV (n = 8) for $K_V7.1$/ $K_V7.5$ channels.

Therefore, the phenotype of the $K_V7.1/K_V7.5$ current was intermediate between $K_V7.1$ and $K_V7.5$ channels. They had a V_h similar to that of $K_V7.5$ (-43.2 ± 1.9 mV *vs.* -40.0 ± 2.8 mV, P > 0.05), but more negative than $K_V7.1$ (-43.2 ± 1.9

mV *vs.* -18.9 ± 1.4 mV, P < 0.05). However, the $K_V7.1/K_V7.5$ slope factor was similar to that of $K_V7.1$ (8.9 ± 1.2 mV *vs.* 9.0 ± 0.8 mV, P > 0.05), but steeper than that of $K_V7.5$ (8.9 ± 1.2 mV *vs.* 13.5 ± 2.0 mV, P < 0.05).

To further investigate the electrophysiological properties of $K_V7.1/K_V7.5$ channels, activation and deactivation kinetics of the current elicited by a 5.5-s pulse to +60 mV, from -80 mV, followed by a -40 mV pulse, were analyzed in these three types of channels. The activation kinetics was analyzed by fitting the current recorded at + 60 mV to a mono- or a bi-exponential equation. The deactivation kinetics was analyzed by fitting the tail currents (recorded on returning to -40 mV from +60 mV), which represent the closing process of the channels, to a mono-exponential equation.

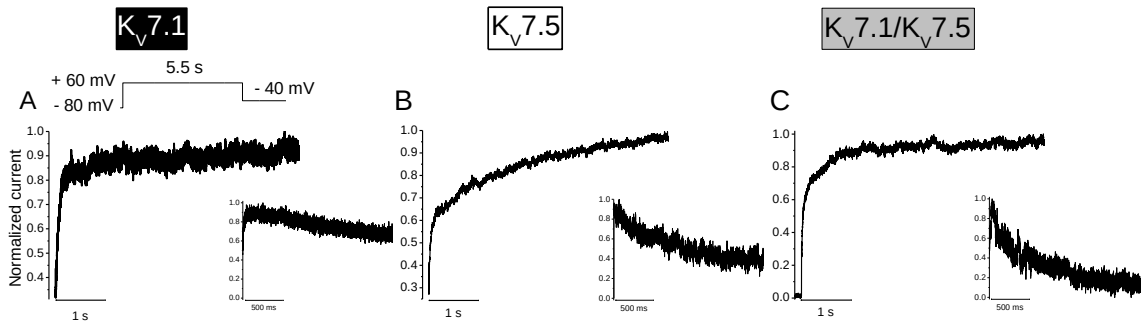

Figure 17: Activation and deactivation processes of $K_V7.1$, $K_V7.5$ and $K_V7.1/K_V7.5$ channels. Representative traces of activation process (obtained using the protocol shown in the left-top of the figure) of $K_V7.1$ (**A**), $K_V7.5$ (**B**) and $K_V7.1/K_V7.5$ channels (**C**). The inset of each panel shows the deactivation traces for each channel. Activation and deactivation kinetics were obtained after fitting traces to a mono- or bi- exponential equation (see Material and Methods).

In the case of $K_V7.1$ channels, both, activation and deactivation processes, were fitted to a monoexponential function (Figure 17, Table 3). Activation kinetics for $K_V7.1$ current was faster than that reported for other K_V7 channels, whereas the deactivation kinetics was slower than that displayed by the other K_V7 members (154, 155). $K_V7.2$-5 display slowly activating and deactivating K^+ currents with distinct electrophysiological and pharmacological properties (109). $K_V7.5$ currents were fitted to a bi-exponential and to a mono-exponential equation for activation and deactivation process, respectively. $K_V7.5$ channels have a slow activation kinetics (n = 14, P < 0.01 *vs.* $K_V7.1$) and fast deactivation kinetics (n = 14, P < 0.01 *vs.* $K_V7.1$, Table 3), which are more common for the K_V7 subfamily. Albeit $K_V7.1/K_V7.5$ activation process were fitted to a bi-exponential equation, the slow time constant of activation was faster than the slow time constant of activation of $K_V7.5$ currents (n = 9, P < 0.01 *vs.* $K_V7.5$, Table 3), being the activation process faster in $K_V7.1/K_V7.5$ channels than in $K_V7.5$ channels, but slower than in $K_V7.1$ (n = 9, P > 0.05 *vs.* $K_V7.1$ channels, Table 3). However, the deactivation kinetics of $K_V7.1/K_V7.5$ channels was similar to that observed for $K_V7.1$ channels (n = 9, P < 0.01 *vs.* $K_V7.5$, P > 0.05 *vs.* $K_V7.1$, Table 3)

Table 3. Activation and deactivation kinetics of $K_V7.1$, $K_V7.5$ and $K_V7.1/K_V7.5$ channels.

	Activation			Deactivation
Channel	τ_s	τ_f	$A_f/(A_f+A_s)$	τ
$K_V7.1$		36.1± 6.1**##		887.4 ± 172##
$K_V7.5$	1178.7 ± 131.8**	89.1 ± 15.1**	0.43 ± 0.03	300.1 ± 21.5**
$K_V7.1/K_V7.5$	512.1 ± 88.7##	37.5 ± 6.8##	0.50 ± 0.08	605.4 ± 73.6##

Data are shown as the mean ± SEM of n = 9-25. **: P < 0.01 *vs.* $K_V7.1$/ $K_V7.5$ channels, #: P < 0.05 and # #: P < 0.01 *vs.* $K_V7.5$ channels.

4.1.4 Modulation of $K_V7.1$/ $K_V7.5$ channels by KCNE subunits

K_V7 channels are highly regulated by KCNE regulatory subunits, providing the channels additional electrophysiological properties. $K_V7.1$ channels interact with all members of the KCNE family (KCNE1-5). In the heart, $K_V7.1$ channels interact with the KCNE1 subunit generating the I_{Ks}, which is one of the most important currents contributing to the cardiac AP repolarization. In other tissues, such as intestinal or mammary airway epitheliums, KCNE3 interacts with $K_V7.1$ channels forming a constitutively active K_V channel (146, 271, 272). KCNE1-5 assemble with $K_V7.5$ channels, but $K_V7.5$ electrophysiological characteristics are only modifyed by KCNE1 and KCNE3. Indeed, while KCNE1 slows the activation and suppresses the inward rectification of the channel, KCNE3 drastically decreases the $K_V7.5$ currents (137).

In order to know if $K_V7.1/K_V7.5$ channels were susceptible of regulation by KCNEs regulatory subunits, the effects of KCNE1 and KCNE3 on $K_V7.1/K_V7.5$ currents were studied in COS-7 cells co-transfected with KCNQ1-YFP and KCNQ5-YFP.

Figure 18 shows the effects produced by the KCNE1 and KCNE3 regulatory subunits in $K_V7.1/K_V7.5$ channels. At first sight, $K_V7.1/K_V7.5$/KCNE1 currents look very similar to the $K_V7.1$/KCNE1 current because of the extremely slow activation induced by KCNE1. However, after analyzing the electrophysiological properties, we can observe that $K_V7.1/K_V7.5$/KCNE1 currents have specific biophysical and pharmacological features, different from those of $K_V7.1$/KCNE1. KCNE1 slows the activation kinetics of the $K_V7.1/K_V7.5$ current (n = 16, Table 4) and dramatically right-shifts its voltage-dependence by ~ +80 mV (n = 16, Table 5, Figure 18).

KCNE3 regulatory subunit effects on $K_V7.1/K_V7.5$ channels were also analyzed. KCNE3 accelerated the activation process (Table 4). KCNE3 slightly shifted the activation curve towards negative potentials (by 10 mV, n = 7, P > 0.05) (Table 5, Figure 18B) and it significantly shifted the activation curve if we compare it with the V_h values obtained for $K_V7.1$ channels alone (Table 5).

Table 4. Activation and deactivation kinetics of $K_V7.1/K_V7.5$, $K_V7.1$/KCNE1, $K_V7.1/K_V7.5$/KCNE1 and $K_V7.1/K_V7.5$/KCNE3 channels measured at +60 mV.

	Activation			Deactivation
Channels	**τ_s**	**τ_f**	**$A_f/(A_f+A_s)$**	**τ**
$K_V7.1/K_V7.5$	512.1 ± 88.7**	37.5 ± 6.8**	0.50 ± 0.08	605.4 ± 73.6*
$K_V7.1$/KCNE1	3757.8 ± 440.8##	837.5 ± 407.8##	0.72 ± 0.06	439.1 ± 30.5#
$K_V7.1/K_V7.5$/ KCNE1	2490.9 ± 42.0##	634.9 ± 75.0##	0.49 ± 0.08*	306.6 ± 28.8##**
$K_V7.1/K_V7.5$/ KCNE3	522.1 ±106.1¶¶	45.6 ± 6.5¶¶	0.84 ± 0.07#&¶	368.2 ± 30.5

Data are shown as the mean ± SEM of n = 7-29. #: P < 0.05 *vs.* $K_V7.1$/ $K_V7.5$ channels, ##: P < 0.01 *vs.* $K_V7.1/K_V7.5$ channels *: P < 0.05 *vs.* $K_V7.1$/KCNE1, **: P < 0.01 *vs.* $K_V7.1$/KCNE1. ¶: P < 0.05 *vs.* $K_V7.1/K_V7.5$/KCNE1 channels, ¶¶: P < 0.01 *vs.* $K_V7.1/K_V7.5$/KCNE1.

$K_V7.1/K_V7.5$/KCNE1 deactivation kinetics was faster than $K_V7.1/K_V7.5$ and $K_V7.1$/KCNE1 channels. However $K_V7.1/K_V7.5$/KCNE3 deactivation kinetics was similar to that observed for $K_V7.1/K_V7.5$ channels (Table 4). These results suggest that $K_V7.1/K_V7.5$ channels are highly regulated by KCNEs regulatory subunits. They are able to modify the biophysical $K_V7.1/K_V7.5$ channels properties.

Table 5. Half-activation (V_h) and slope (s) of the steady-state activation of $K_V7.1$, $K_V7.5$ and $K_V7.1/K_V7.5$ currents in the absence and in the presence of KCNE1 and KCNE3.

		$K_V7.1$	$K_V7.5$	$K_V7.1/K_V7.5$
	V_h (mV)	-18.9 ± 1.4	-40.0 ± 2.8##	-43.2 ± 1.9##
	s (mV)	9.0 ± 0.8	13.5 ± 2.0*#	8.9 ± 1.2
KCNE1	V_h (mV)	+29.4 ± 2.4##	-42.2 ± 0.9	+49.0 ± 2.9**¶¶
	s (mV)	18.9 ± 0.8##	11.3 ± 2.0	23.0 ± 1.5**¶
KCNE3	V_h (mV)	+59.4 ± 3.2	-45.9 ± 0.9	-50.0 ± 2.9
	s (mV)	22.7 ± 1.8	11.5 ± 2.0	7.2 ± 0.3

Data are shown as the mean ± SEM of n = 7-29. *: P < 0.05 and **: P < 0.01 *vs.* $K_V7.1/K_V7.5$ channels. #: P < 0.05 and ##: P < 0.01 *vs.* $K_V7.1$ channels. ¶: P < 0.05 and ¶¶: P < 0.01 *vs.* $K_V7.1$/KCNE1 channels. Parameters of $K_V7.5$/KCNE1 and $K_V7.5$/KCNE3 currents were obtained from *Xenopus* oocytes.

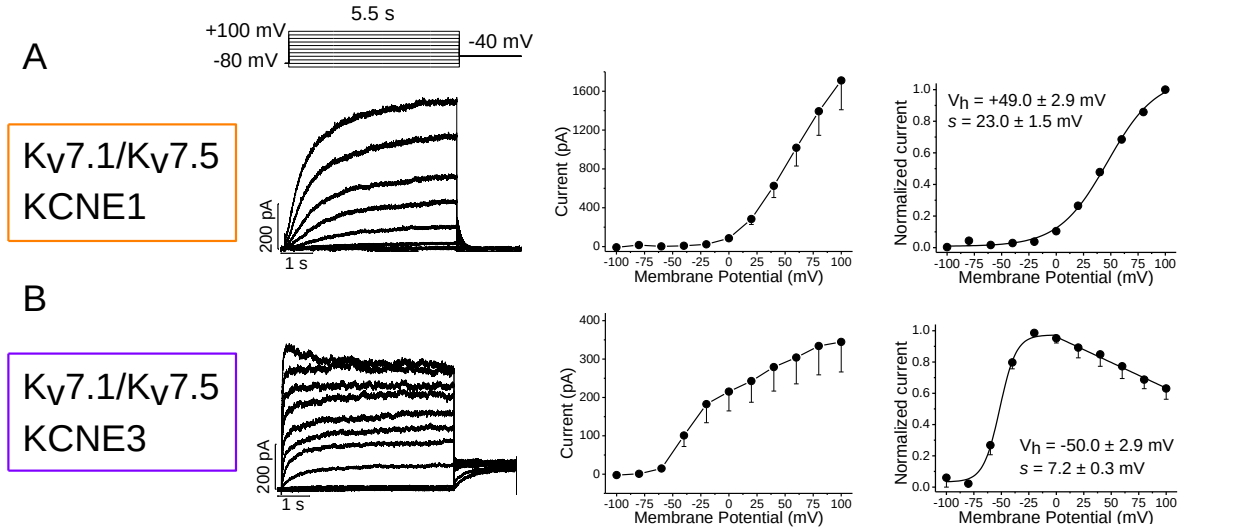

Figure 18: Voltage-dependent K^+ currents recorded in COS-7 cells expressing K_V7.1/K_V7.5/KCNE1 and K_V7.1/K_V7.5/KCNE3 channels. Currents were evoked by a series of 5.5-s pulses from -100 to +100 mV in 20 mV steps from a holding potential of -80 mV and returned to -40 mV. Representative current records from COS-7 cells transfected with K_V7.1/K_V7.5/KCNE1 (**A**, left) and K_V7.1/K_V7.5/KCNE3 (**B**, left). I-V relationships measured at the end of the pulses of K_V7.1/K_V7.5/KCNE1 currents (**A**, middle) and of K_V7.1/K_V7.5/KCNE3 currents (**B**, middle). Voltage dependence of activation. Activation curves were obtained by plotting the normalized initial magnitude tail current *vs.* the test membrane potential. Data were fitted to a Boltzmann equation that is shown with a solid line for K_V7.1/K_V7.5/KCNE1 channels (**A**, right) and K_V7.1/K_V7.5/KCNE3 channels (**B**, right). Data show the mean ± SEM of 7-16 cells per group.

Since the current elicited by K_V7.1/K_V7.5/KCNE1 channels was similar to K_V7.1/KCNE1 channels, we wanted to investigate the pharmacological consequences of the presence of K_V7.5 in this heterotetramer channel. Thus, to assess this approach, a selective K_V7.1/KCNE1 channel blocker, chromanol 293B, was used to compare the blocking effects of this drug on K_V7.1/KCNE1 and on K_V7.1/K_V7.5/KCNE1 channels.

Figure 19 shows chromanol 293B effects on K_V7.1/K_V7.5/KCNE1 channels. Chromanol 293B (5 µM) blocks K_V7.1/KCNE1 channels by 12.3 ± 3.0 % (n = 3, P < 0.05, Figure S1) and K_V7.1/K_V7.5/KCNE1 channels by 53.0 ± 3.0 % (chromanol 293B conditions *vs.* control conditions, n = 9, P < 0.05, Figure 19) Therefore, block induced by chromanol 293B block was greater in the presence of K_V7.5 subunits. Chromanol 293B did not changed the gating properties of K_V7.1/K_V7.5/KCNE1 channels. Moreover, block was not time- or voltage-dependent. All these results suggest that K_V7.1, K_V7.5 and KCNE1 subunits are able to assemble and form functional channels, with specific electrophysiological and pharmacological properties.

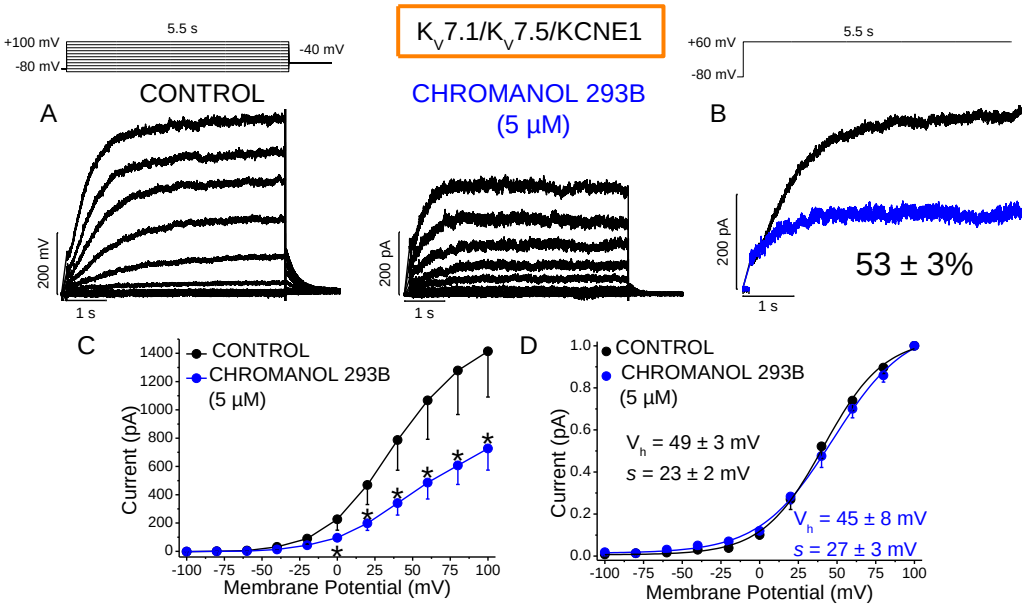

Figure 19: **Chromanol 293B effects on $K_V7.1/K_V7.5$/KCNE1 currents**. **A:** Representative current records from COS-7 cells co-transfected with $K_V7.1/K_V7.5$/KCNE1. Currents were evoked applying the protocol shown on the top of the figure in the absence or in the presence of 5 µM chromanol 293B. **B:** Representative traces obtained after applying 5.5 s pulses of +60 mV from a holding potential of -80 mV, in the absence (black trace) and in the presence of 5 µM chromanol 293B (blue trace), the percentage of block is shown. **C:** I–V relationship measured at the end of the pulses for $K_V7.1/K_V7.5$/KCNE1 currents in the absence (black circles) and in the presence of 5 µM chromanol 293B (blue circles). **D:** Activation curves were obtained by plotting the normalized tail currents *vs* the membrane potential. Data were fitted to a Boltzmann equation that is shown with a solid line (black circles represent control conditions while blue circles represent 5 µM chromanol 293B conditions). Data show the mean ± SEM of 9 cells.

4.1.5. Pharmacological properties of $K_V7.1$/ $K_V7.5$ channels

To further study the pharmacological characteristics of $K_V7.1/K_V7.5$ heterotetrameric channels, experiments with a $K_V7.2$-5 activator were performed. To that end, the effects of the antiepileptic drug retigabine (RTG) were analyzed. RTG is an activator of $K_V7.2$-5 channels that have no activator effect on $K_V7.1$ channels. RTG (10 µM) increased $K_V7.5$ currents at all membrane potential tested (Figure 20B, middle). Thus, at +60 mV RTG (10 µM) increased the $K_V7.5$ current by 198.5 ± 57.3 % (n = 6, P < 0.05). However, this drug blocks $K_V7.1$ currents at all membrane potential tested, arising a mean value, at +60 mV, of 14.9 ± 3.4% (n = 8, P < 0.05 Figure 20B, left) as previously reported (174). $K_V7.1/K_V7.5$ currents were registered after applying 5.5-s pulses from a holding potential of -80 mV to +100 mV in 20 mV steps. Potassium currents were analyzed in the absence and in the presence of the drug. RTG (10 µM) increased the current by 130.6 ± 16.5 % at +60 mV (n = 6 P < 0.01). RTG did not modify the voltage dependence of activation of $K_V7.1$ channels, but shifted the activation curves of $K_V7.1/K_V7.5$ channels towards negative potentials (-43.7 ± 2.0 mV *vs.* -51.4 ± 2.5 mV, n = 7, P < 0.05), without modifying the slope factor (9.22 ± 1.4 mV *vs.* 12.0 ± 1.8 mV, n = 7, P > 0.05), in the same manner as it was observed in $K_V7.5$ channels (n = 4, -40.1 ± 7.3 mV *vs.* -55.0 ± 7.9 mV, P < 0.05, and 15.7 mV ± 5.1 *vs.* 26.2 ± 7.8 mV, P > 0.05) (Figure 20C, right)

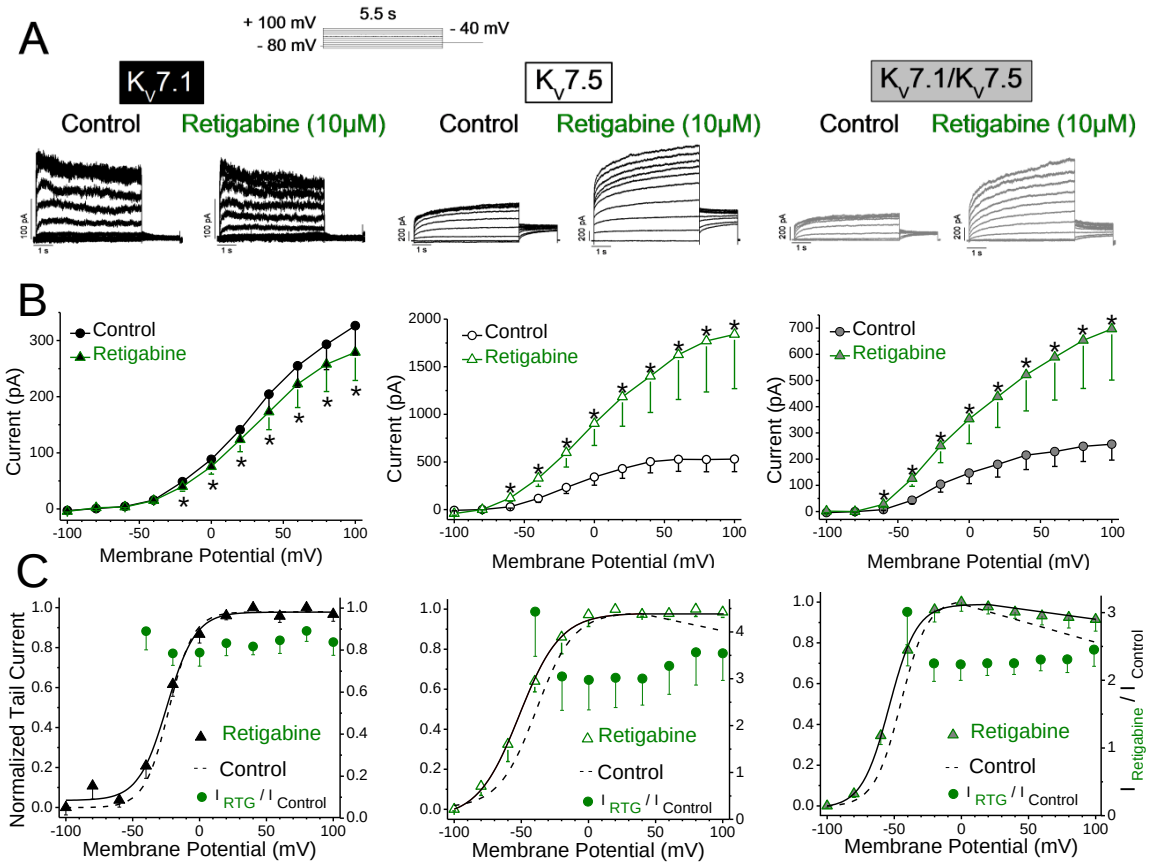

Figure 20: RTG effects on $K_V7.1$, $K_V7.5$, and $K_V7.1/K_V7.5$ channels. Currents were evoked by a series of 5.5-s pulses from -100 to +100 mV in 20 mV steps from a holding potential of -80 mV and returned to -40 mV. **A:** Representative current records from COS-7 cells transfected with $K_V7.1$ (left), $K_V7.5$ (middle), and $K_V7.1/K_V7.5$ (right) in the absence and in the presence of RTG (10 µM). **B:** Voltage-dependent effects of RTG. I-V relationship measured at the end of the pulse for $K_V7.1$, $K_V7.5$, and $K_V7.1/K_V7.5$ channels in the presence of RTG (10 µM). **C:** Voltage dependence of activation. Activation curves were obtained by plotting the normalized peak tail currents *vs.* the membrane potential of $K_V7.1$, $K_V7.5$, and $K_V7.1/K_V7.5$ channels in the absence (dashed line) and in the presence of RTG (10 µM) (solid line). Data were fitted to a Boltzmann equation that is shown with a solid line. Green dots represent the relative current showed as $I_{Retigabine}/I_{Control}$ *vs.* membrane potential. Results are shown as the mean ± SEM of 6 to 8 cells per group, *: $P < 0.05$.

RTG increased $K_V7.5$ and $K_V7.1/K_V7.5$ currents by shifting the voltage dependence of the activation of these channels towards more negative membrane potentials, thus facilitating activation and stabilizing the ion channel in the open conformation. Indeed, the maximum increase produced by RTG was observed at -40 mV both, in $K_V7.5$ and $K_V7.1/K_V7.5$ channels However, the increase and the slight block induced by RTG was not voltage dependent for $K_V7.5$, $K_V7.1/K_V7.5$ and $K_V7.1$ channels (green circles, Figure 20C).

We did not see any effect on the time constants of the activation or deactivation process on $K_V7.1$ channels were observed (Figure 21A, Table 6). However, RTG slowed the activation of $K_V7.5$ and $K_V7.1/K_V7.5$ channels (Table 6, n = 5-8, $P < 0.05$, Figure 21BC). No effect on the time constants of the deactivation processes of $K_V7.5$ and $K_V7.1/K_V7.5$ channels, were observed (Table 6, n = 5-8, $P > 0.05$, Figure 21BC inset).

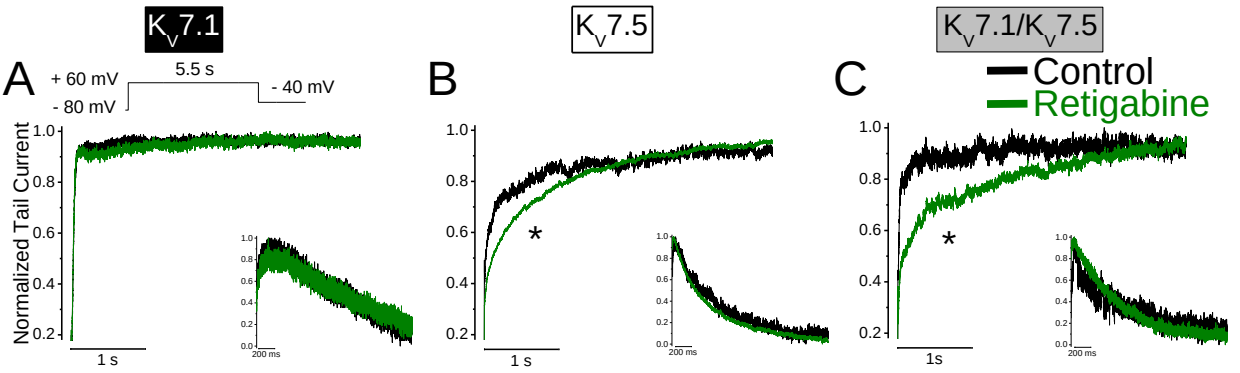

Figure 21: Activation and deactivation process of $K_V7.1$, $K_V7.5$ and $K_V7.1/K_V7.5$ channels in the absence and in the presence of RTG (10 µM). Representative current traces of $K_V7.1$ channels (**A**), $K_V7.5$ channels (**B**) and $K_V7.1/K_V7.5$ channels (**C**) in the absence (black trace) and in the presence of 10 µM RTG (green trace), obtained using the protocol shown in the left-top. The inset of each panel shows the deactivation current for each channel in the absence (black trace) and in the presence of 10 µM RTG (green trace). Activation and deactivation kinetics were obtained after fitting traces to a mono- or bi- standard equation. *: $P < 0.05$, n = 6-9 cells per group.

Table 6: Activation and deactivation Kinetics of $K_V7.1$, $K_V7.5$ and $K_V7.1/K_V7.5$ channels in the absence (Control) and the presence of RTG (10 µM).

	Activation				Deactivation	
Channels	**Control**		**RTG**		**Control**	**RTG**
	τ_s	τ_f	τ_s	τ_f	τ	τ
$K_V7.1$		46 ± 12		50 ± 11	858 ± 300	1187 ± 384
$K_V7.5$	1178 ± 132	89 ± 15	2409 ± 400*	222 ± 53*	300 ± 2	640 ± 126
$K_V7.1/K_V7.5$	520 ± 100	33 ± 6	2371 ± 609**	137 ± 34*	605 ± 73	490 ± 67

Data are shown as the mean ± SEM of 5-12 experiments per group, **: $P < 0.01$ *vs.* Control, *: $P < 0.05$ *vs.* control.

4.1.6. Role of $K_V7.1$/ $K_V7.5$ channels on the vascular tone

All the events that we have analyzed suggest that $K_V7.5/K_V7.1$ heterotetrameric channels are functional channels present in cardiovascular system. Our last aim was to analyzed if these heterotetrameric channels play a specific role in the regulation of the vascular tone. Vessels were incubated with vehicle (DMSO, control), chromanol 293B (10 µM) or linopirdine (10 µM) for 20 min before the stimulation with serotonin (5-HT, 1 µM). Finally, the relaxation induced by RTG (1-30 µM) was analyzed. RTG induced a relaxant response that was differentially inhibited by the presence of

chromanol 293B (10 µM) and linopirdine (10 µM). In control conditions, RTG (10 µM) was able to achieve the relaxation of the coronary arteries, whereas 30 µM of RTG was needed to complete the relaxation process in the presence of chromanol 293B.

Finally, higher RTG concentrations (>30 µM) were needed to complete the relaxation process in the presence of linopirdine, an inhibitor of the K_V7 channels subfamily (Figure 22). All these results suggest that $K_V7.1/K_V7.5$ heterotetramers are present in rat coronary arteries and they might play a specific role in the vascular tone.

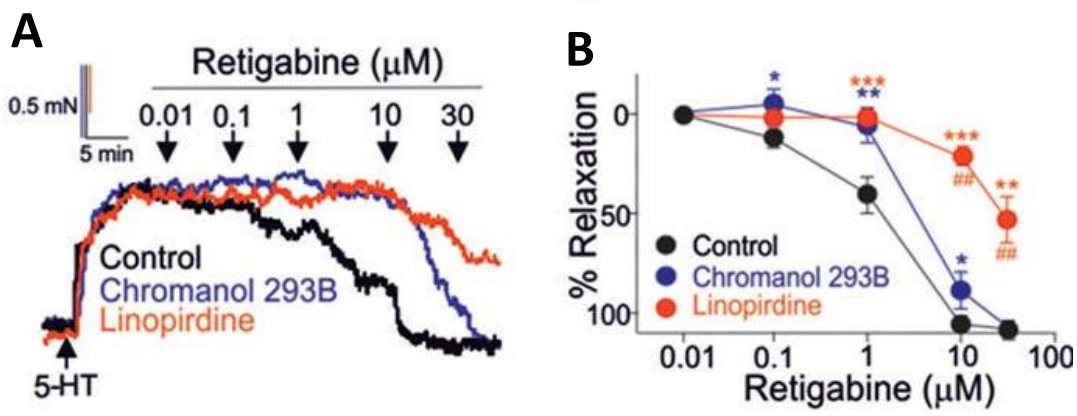

Figure 22: Recordings of rat coronary arteries reactivity. Representative traces (**A**) and average values (**B**) showing the vasodilation induced by RTG in coronary arteries incubated with chromanol 293B and linopirdine as compared with those incubated with vehicle (control) for 20 min before the addition of the vasoconstrictor 1 µM serotonin (5-HT). Results are means ± SEM. *: P < 0.05; **: P < 0.01; ***: P < 0.001 *vs.* control and ##: P <0.01 linopirdine *vs.* chromanol 293B (1-way ANOVA) of n= 4-5. Black traces indicate control; blue traces, chromanol 293B; and red traces, linopirdine.

4.2 PART II. n-3 and n-6 PUFAs AND THEIR DERIVATIVES, RESOLVIN D1 AND LIPOXIN A4, MODULATE K_V7.1/KCNE1 CURRENT

4.2.1 DHA and AA modulate KV7.1/KCNE1 gating

PUFAs antiarrhythmic properties have been related to their ability to modulate Na, Ca and K channels (210, 273). K_V7.1 and KCNE1 are the two major pore-forming and ancillary subunits, respectively, responsible for the biophysical properties of I_{Ks} channels (152, 210). It has been reported that eicosapentaenoic acid (EPA) and docosahexaenoic acid (DHA) do not increase K_V7.1 current, although DHA, but not EPA, increases the magnitude of the K_V7.1/KCNE1 current in *Xenopus* oocytes (210). In cardiac myocytes from pigs fed with a PUFAs enriched-diet, I_{Ks} magnitude was greater than that recorded in myocytes from control animals (216). Therefore, the aim of this part of the present Doctoral Thesis was to study how n-3 and n-6 PUFAs modulate K_V7.1/ KCNE1 channels, the counterpart of the I_{Ks}

4.2.1.1 DHA and AA increase K_V7.1/KCNE1 current

First, we analyzed the effects of AA (20 µM) on the K_V7.1/KCNE1 channel. AA strongly increased the amplitude of the current (Figure 23). During the perfusion of COS-7 cells transfected with K_V7.1/KCNE1 channels, a time-curse of the AA effect was analyzed. The maximum increase of the current was achieved after ~12 min. Figure 23 shows how the maximum increased produced by AA was achieved in the pulse #20 followed by a slight decrease of the current. We also analyzed the effects of DHA on K_V7.1/KCNE1 channels, obtaining similar qualitative results.

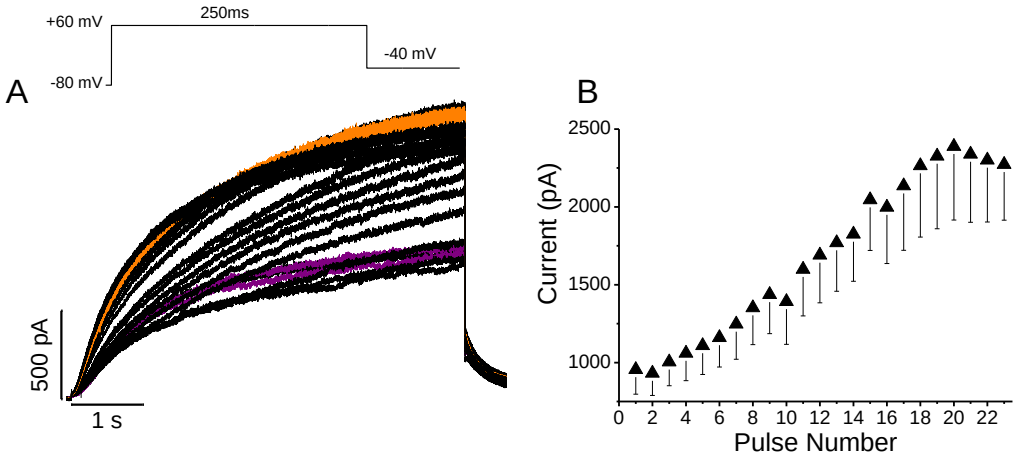

Figure 23: Time-course of acute AA (20 µM) effect. A: K_V7.1/KCNE1 original traces recorded from a holding potential of -80 mV to +60 mV during 5.5-s pulses. Control condition is shown in violet traces, K_V7.1/KCNE1 traces in the presence of 20 µM AA reached their maximum increase at pulse 20 (orange traces). **B:** Representative increase of K_V7.1/KCNE1 current in the presence of 20 µM AA. Current magnitude at the end of the pulses *vs.* the number of pulses needed to achieve the maximum increase, is represented (Results are shown as the mean ± SEM. n = 9).

These experiments were performed using 20 µM of each compound (DHA and AA). The choice of DHA concentration is based on the SOFA Trial and on the reported EC_{50} for the effects of PUFAs on ion channels, that ranges between 5.0 and 16.4 µM (214, 274). For better comparisons between n-3 and n-6 PUFAs effects on K_V7.1/KCNE1 current, the same AA concentration was used.

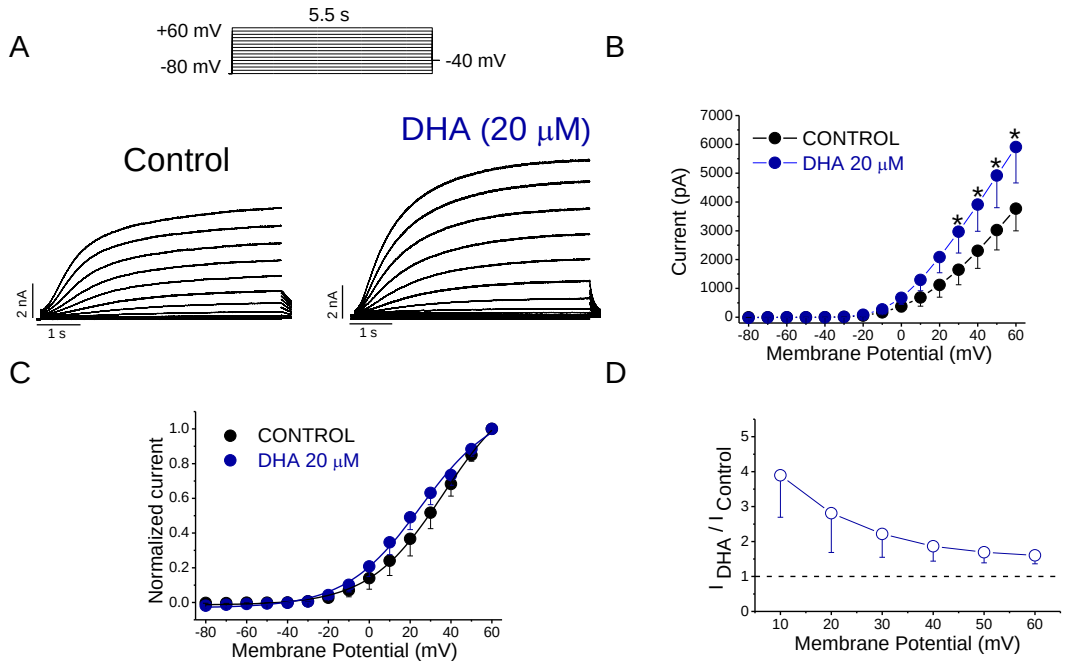

Figure 24: Voltage-dependent effects of DHA. A: Current traces obtained after applying the pulse protocol shown in the top, in the absence and in the presence of DHA (20 μM). **B:** I-V relationships obtained under control conditions and after perfusion with DHA (20 μM). **C:** Activation curves of K_V7.1/KCNE1 current obtained after representing the maximum tail current amplitude *vs.* the previous step potential. **D**: Ratio between the current in the presence of DHA and the current in control conditions. Data are shown as the mean ± SEM. *: P < 0.05, n= 5.

We analyzed the effects of DHA and AA on K_V7.1 channels in transfected COS-7 cells. No significant changes on the current elicited by these channels were observed (Figure S2, (225)). However, when we analyzed the effects of DHA and AA in the presence of the KCNE1 regulatory subunit, a great increase in the K_V7.1/KCNE1 current was observed (Figures 24 and 25). Figure 24A shows K_V7.1/KCNE1 traces obtained after applying 5.5-s depolarizing pulses from a holding potential of -80 mV to +60 mV in 10 mV steps, in the absence and in the presence of DHA (20 μM). Figure 24B shows the I-V relationships under control conditions and in the presence of DHA. As it can be observed, DHA increased the K_V7.1/ KCNE1 current at all membrane potentials tested positive to +30 mV (n = 8, P < 0.05,). DHA did not modified the V_h of the activation curve (+29.9 ± 6.4 *vs.* +26.4 ± 6.9 mV, in control conditions and after perfusion with DHA, P > 0.05, n = 5) or the slope factor of the activation curves (14.2 ± 1.1 mV *vs.* 16.7 ± 0.7 mV, in control condition and after perfusion with DHA, P > 0.05, n = 5) (Figure 24C). We analyzed the voltage-dependence of the increasing of the current induced by the compound by plotting the ratio between the current in the presence and in the absence of DHA ($I_{DHA}/I_{Control}$, Figure 24D).Although not significant, the increase in the current induced by DHA showed a tendency to decrease after +10 mV (P > 0.05 n = 8). This effect might be due to the slight negative shift produced by DHA on the activation curve. Similar qualitative effects to DHA were produced by EPA (225).

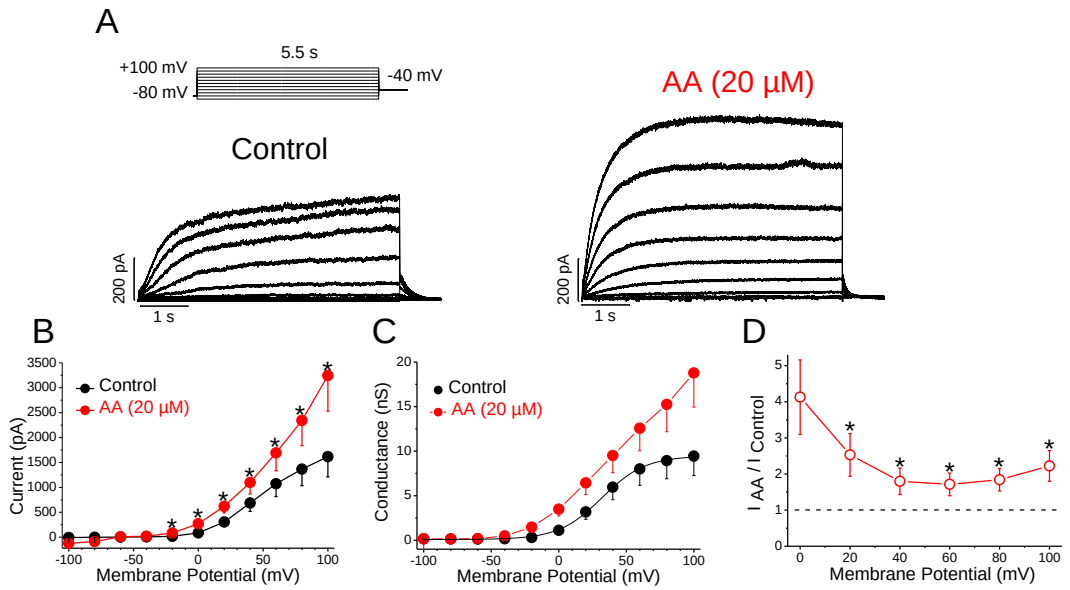

Figure 25: Voltage-dependent effects produced by AA on K_V7.1/KCNE1 current. A: Current traces obtained after applying the pulse protocol shown in the top in the absence and in the presence of AA (20 µM). **B:** I-V relationships obtained under control conditions and after perfusion with AA. **C:** Activation curves of K_V7.1/KCNE1 current obtained after representing the conductance *vs.* the previous step potential recorded in the absence (V_h = +39.1 ± 5.0 mV, *s* = 12.0 ± 2.0 mV) and in the presence of AA. **D:** Ratio between the K_V7.1/KCNE1 current in the presence and in the absence of AA. Data are shown as the mean ± SEM. *: P < 0.05, n= 8.

Figure 25 shows the same approach for AA (20 µM). K_V7.1/KCNE1 currents were evoked after applying 5.5-s depolarizing pulses from a holding potential of -80 mV to +100 mV in 20 mV steps. Figure 25A shows K_V7.1/KCNE1 currents in the absence and in the presence of AA. As it can be observed, AA, similarly to DHA, increased the magnitude of the K_V7.1/KCNE1 current. Figure 25B shows the I-V relationships in control and after perfusion of the cells with AA. This PUFA increased the current at all membrane potentials tested positive to -20 mV (n = 8, P < 0.05, Figure 25B). Because the activation curves in the presence of AA did not reach the steady-state level, it was not possible to fit the data to a Boltzmann equation (Figure 25C), but it can be observed that AA shifted the threshold activation of the current towards more negative membrane potentials. In contrast to DHA and EPA (225), the AA-induced increase of K_V7.1/KCNE1 current was voltage-dependent, decreasing at membrane potentials positive to +20 mV (P < 0.05, n= 8, Figure 25D).

The increase of the current produced by DHA and AA was also measured at shorter depolarization times (1.5 s). The increase induced by DHA was not time-dependent, this effect being similar either after long or short depolarizing pulses (91.8 ± 19.3 % and 92.7 ± 23.8 %, after 1.5 s and 5.5 s, respectively, n = 13, P > 0.05). Similarly, increase produced by AA was not time-dependent, the increase being equal after short or long depolarizations (119.3 ± 45.8% and 120.2 ± 37.8%, measured after 1.5 and 5.5 s depolarizing pulses, n = 8, P > 0.05).

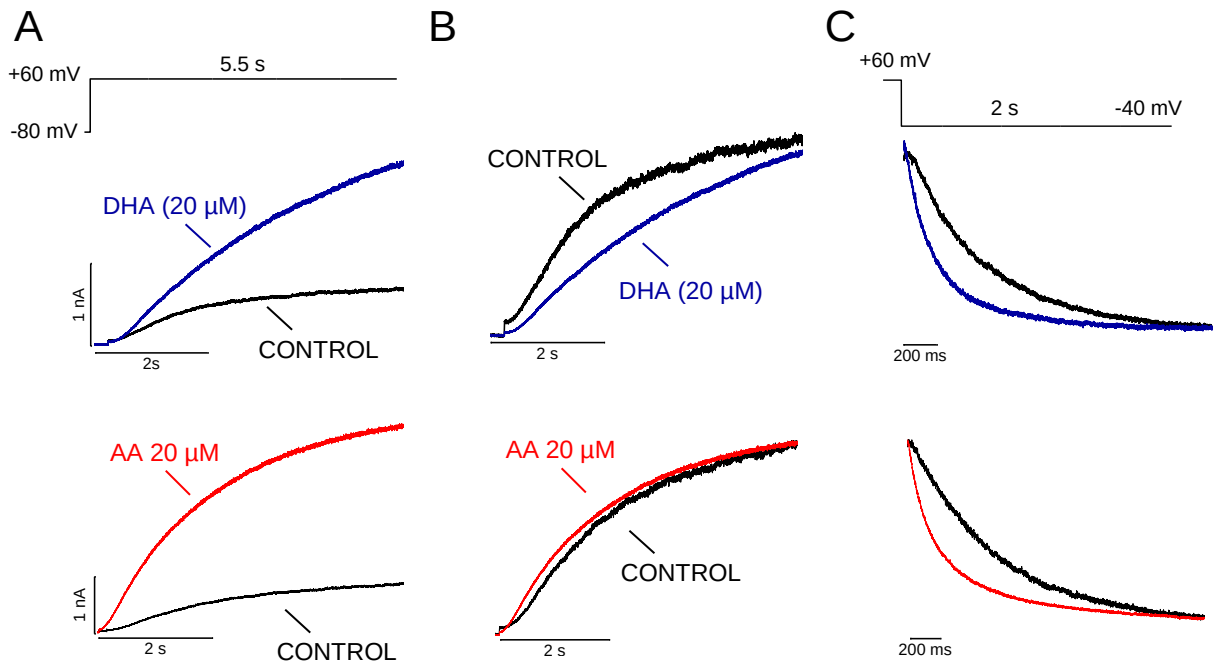

Figure 26: Effects of DHA and AA (20 µM) on K_V7.1/KCNE1 activation and deactivation kinetics. A: K_V7.1/KCNE1 current traces obtained in the absence and in the presence of DHA and AA (left panels). **B:** Normalized traces of K_V7.1/KCNE1 current obtained in the absence and in the presence of DHA and AA. **C:** Normalized tail currents of K_V7.1/KCNE1 obtained in the absence and in the presence of DHA and AA. Data are mean ± SEM, n= 5-8 per group.

In order to analyze the activation kinetics, K_V7.1/KCNE1 current at +60 mV were fitted to a biexponential equation. In control conditions, the activation time constants arose mean values of τ_s = 3757.8 ± 440.8 ms and τ_f = 837.5 ± 75.7 ms (Figure 26, n = 29). Although DHA accelerated the fast time constant of activation (737 ± 53 ms *vs.* 592 ± 52 ms, in control and in the presence of DHA, respectively. P < 0.05, n = 8), the contribution of the slow component of activation to the total process increased (0.19 ± 0.04 *vs.* 0.46 ± 0.07, n = 8, P < 0.0,5 in control and in the presence of DHA, respectively), resulting in a slower activation kinetics (Figure 26B). AA also accelerated the fast time constant of activation (979 ± 85 ms *vs.* 455 ± 42 ms, in control and in the presence of AA, n = 13, P < 0.05) and increased the contribution of the slow component of activation process (0.10 ± 0.05 *vs.* 0.77 ± 0.07, n = 8, P < 0.01 in control and in the presence of AA, respectively). Thus, AA did not modify the activation kinetics of the current (Figure 26AB). Therefore, DHA slowed activation kinetics of K_V7.1/KCNE1, while AA did not modify the activation kinetics.

Regarding the deactivation kinetics, both DHA and AA accelerated this process, which changed from monoexponential to biexponential processes. In the case of DHA, the control deactivation time constant was 502.7 ± 65.2 ms (n = 18), whereas in the presence of the drug, the τ_s value was 497.2 ± 45.7 ms (n = 18, P > 0.05 compared to the control time constant) and the τ_f value was 109.5 ± 9.5 ms. The contribution of the fast component of the deactivation process reached a mean value of 0.62 ± 0.08, thus accelerating the total process. Similarly, the deactivation process became biexponential in the presence of AA (20 µM). Thus, the control time constant was 341.1 ± 43.5 ms and, in the presence of AA, exhibited a similar slow time constant than the control one (369.1 ± 66.8

ms, n = 6, P > 0.05) and a fast time constant of 95.7 ± 13.8 ms (n = 6). The contribution of the fast component to the total process was 0.593 ± 0.089 (n = 6), thus accelerating the deactivation. As the slow time constants obtained in the presence of DHA or AA resulted to be similar to the time constant obtained under control conditions, DHA and AA accelerated the deactivation by adding a fast component to it.

Effects of DHA in native I_{Ks} currents from guinea pig ventricular myocytes

The effects of DHA were also tested in native I_{Ks} currents from guinea pig ventricular myocytes. I_{Ks} was recorded at 36 ºC after applying depolarizing pulses from -40 mV to +20 mV in the presence of nifedipine (10 µM) and E-4031 (5 µM), to block I_{CaL} and I_{Kr} currents, respectively. A total of 14 myocytes were analyzed. In 11 myocytes, DHA (10 µM) increased I_{Ks} amplitude (37.7 ± 6.0 %, P < 0.05) (Figure 27A) and accelerated its deactivation recorded at -40 mV ($t_{1/2}$ -19.1 ± 8 % *vs.* control, P < 0.05) (Figure 27B). However, in 5 of 11 myocytes, during long-time recordings, the initial increase of I_{Ks} was followed by a progressive decrease in the current. Finally, in 3 of them, exposure to 10 µM DHA was directly followed by a decline in I_{Ks} amplitude (data not shown).

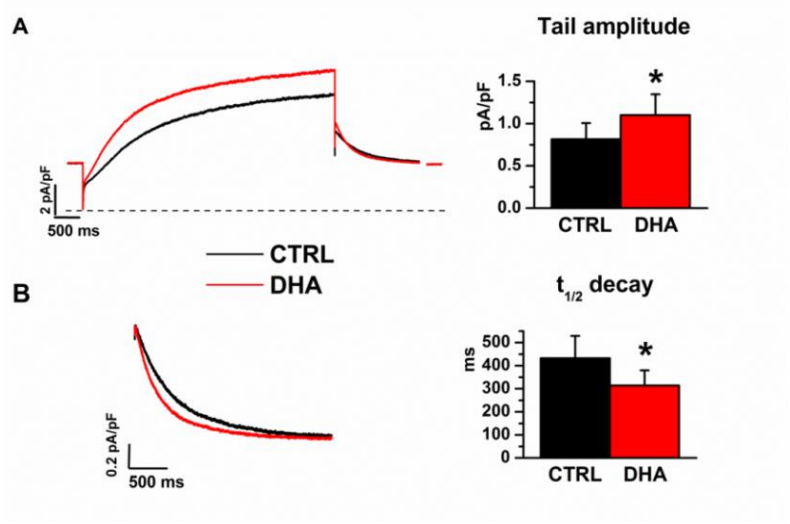

Figure 27: DHA effects on I_{Ks} from guinea-pig ventricular myocytes. I_{Ks} was elicited a by 5-s voltage step to +20 mV from -40 mV every 20 s. **A**: Representative I_{Ks} traces, elicited in control and in the presence of DHA (10 µM); statistics of I_{Ks} tail amplitude on the right. **B**: Normalized tail currents at -40mV; statistics of I_{Ks} deactivation (t½ decay) on the right. n = 11. * P < 0.05 *vs.* control.

4.2.1.2 DHA and AA chronic effect on K_V7.1/KCNE1 current

An increased consumption of PUFAs leads to increased blood and tissue levels of PUFAs (274). However, the relative contribution of short- and long-term administration on the electrophysiological effects on ion currents has not been determined. We wanted to analyze and correlate the electrophysiological effects produced by DHA with the levels of expression of channel protein and also with the channel targeting to lipid rafts. The same conditions were used in all these experiments: COS-7 cells were co-transfected with KCNQ1-YFP and KCNE1-CFP and incubated for 48 h with DHA and AA (20 µM) in serum-free medium. Controls of these experiments were COS-7 cells co-transfected with KCNQ1-YFP and KCNE1-CFP incubated for 48 h in serum-free medium without DHA neither AA. Three different

approaches were performed to elucidate the effects of these compounds on K_V7.1/KCNE1 channels related with their effects on the plasma membrane. COS-7 cells were transfected with K_V7.1/KCNE1 channels and incubated with DHA or AA (only for electrophysiological experiments) during 48 h in serum-free medium. Control conditions in serum-free medium of K_V7.1/KCNE1 currents were studied (Figure S3). In the absence of compound, no differences between the currents with or without serum in the medium were observed.

First, we analyzed the electrophysiological effects after chronic exposure to DHA/AA (Figure28 and 29). Long-term conditions of DHA or AA did not modify the magnitude of K_V7.1/KCNE1 currents. Long-term conditions for 20 µM DHA accelerated the activation process of K_V7.1/KCNE1 current recorded in COS-7 cells. The contribution of the fast and slow components of the activation kinetics were similar in the absence and in the presence of 20 µM DHA [$(A_f / (A_s+A_f)) = 0.47 \pm 0.08$ and $(A_f / (A_s +A_f)) = 0.54 \pm 0.08$, for control conditions and chronic DHA, $P > 0.05$, n = 12-18, respectively]. However, incubation with DHA during 48 h accelerated the slow activation constant of the activation process (5151 ± 788 ms *vs.* 3100 ± 429 ms for control conditions and chronic DHA, respectively, n = 9-18, $P < 0.05$) without modifying the fast activation time constant (649 ± 42 ms *vs.* 587 ± 74 ms, $P > 0.05$, n = 9-18 for control conditions and chronic DHA, respectively).

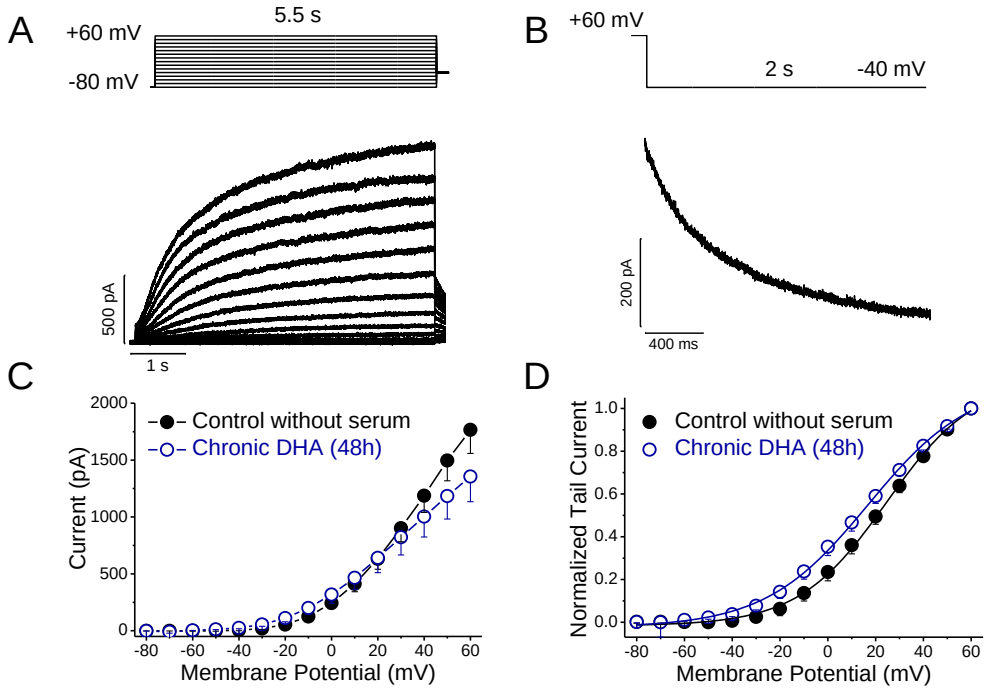

Figure 28: Effects of chronic DHA exposure on K_V7.1/KCNE1 currents. A: K_V7.1/KCNE1 original traces recorded after applying depolarizing 5.5-s pulses from a holding potential of -80 mV to +60 mV in 10 mV steps. **B:** Original tail current recorded at -40 mV after 5.5-s depolarization to +60 mV **C:**. I-V relationships obtained measuring the current after 5.5s. **D:** Activation curves obtained after representing the maximum tail current amplitude versus the previous step potential. Data are shown as the mean ± SEM, n= 12.

For AA (20 µM), the contribution of each component of activation kinetics was similar in control and after incubation with AA [$(A_f / (A_s+A_f)) = 0.42 \pm 0.04$ and $(A_f / (A_s +A_f)) = 0.55 \pm 0.09$, for control conditions and chronic exposure to AA during 48h, $P > 0.05$, n = 6-18, respectively]. However, the fast time constant of activation was slower after chronic exposure to AA than under control conditions (649 ± 42 ms *vs.* 1233 ± 117 ms, for control and

chronic AA, respectively, n = 6-18, P < 0.05) without changes in the slow activation time constant (5298 ± 821 ms *vs.* 7348 ± 709 ms, for control and chronic AA, respectively, n = 6-18, P > 0.05, Figure 29). In summary, chronic DHA accelerated the activation kinetics whereas chronic AA slowed it.

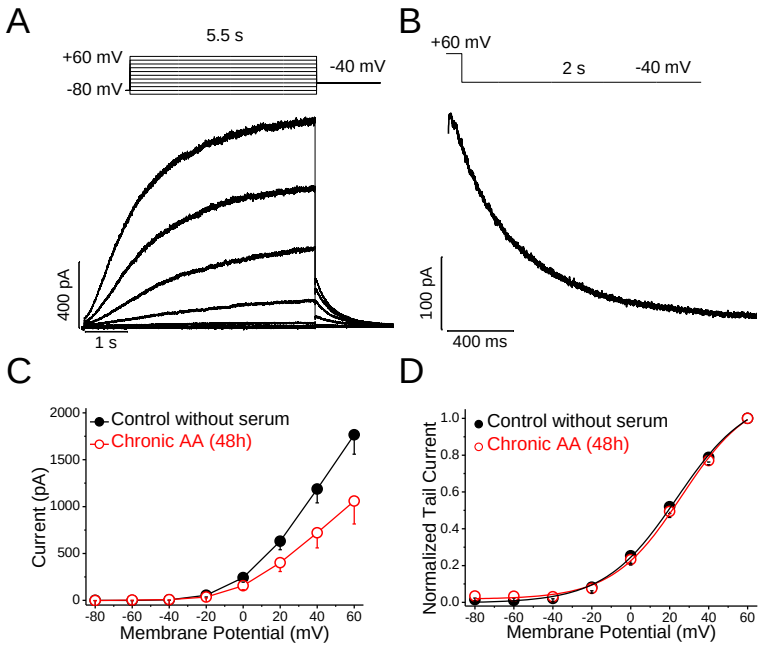

Figure 29: AA chronic effects on K_V7.1/KCNE1 channels. A: Original traces K_V7.1/KCNE1 recorded after applying depolarizing 5.5 s pulses from a holding potential of -80 mV to +60 mV in 10 mV steps. **B:** Original tail current recorded at -40 mV after 5.5 s depolarization to +60 mV. **C:** I-V relationships obtained after measure the current after 5.5 s. **D:** Activation curves of K_V7.1/KCNE1 channels obtained after representing the maximum tail current amplitude *vs.* the previous step potential recorded in cells incubated for 48 h with 20 µM AA. Results are represented as the mean±SEM, n= 6, P > 0.05.

Figures 28C and 29C show the I-V relationship after chronic treatment of K_V7.1/KCNE1 channels with DHA and AA, without differences in the mean values. The activation curves under these conditions were also studied (Figures 28D and 29D). In control conditions, the V_h = 29.4 ± 2.5 and *s* = 16.6 ± 1.4 (n = 9) were obtained. DHA induced a negative shift of the activation curve (V_h = 13.1 ± 3.7 mV, n = 12, P < 0.05 and *s* = 14.7 ± 4.0, n = 12, P > 0.05, n = 12, for DHA). On the contrary, AA did not produce changes in the activation curve (V_h = 29.9 ± 4.2 mV and *s* = 19.1 ± 1.8 mV, P > 0.05, n = 6, for AA). Thus, DHA, but not AA, after 48 h incubation, shifted to more negative potentials the activation curve of the channel. Thus, both DHA and AA exhibited different effects after acute and chronic exposure, suggesting that the time of exposure and the differences between n-3 and n-6 PUFAs, promote specific effects on K_V7.1/KCNE1 channels.

As it has been shown, DHA and AA modulate K_V7.1/KCNE1 channels. Since the effects of DHA were different after acute and chronically exposure to this PUFA, our second approach was to examine if the total amount of K_V7.1/KCNE1 channels, in cells, was susceptible to be regulated by DHA. To that end, western blot analyses were performed. Figure 30A shows that DHA reduced the expression of K_V7.1 and K_V7.1/KCNE1 proteins in a concentration-dependent manner (EPA promotes similar results (225)). Indeed, the channels sensitivity to these compounds increased in the presence of KCNE1. It has been described for K_V1.5 channels, that DHA and EPA are

able to regulate their degradation via proteasome, and thus, regulate the amount of protein in the cells. In order to know if the decrease of K_V7.1/KCNE1 channels depends on the increase of degradation via proteasome, experiments with MG132 proteasome inhibitor were performed. Figure 30B shows an increase of K_V7.1/KCNE1 channels in the presence of MG132 inhibitor. Moreover, a significant increase in protein levels was observed, in increasing concentrations of DHA, in the presence of KCNE1 regulatory subunit. Because of the significant increased observed in the presence of KCNE1, experiments with COS-7 cells previously transfected with KCNE1-YFP alone, were performed. As we can observe in Figure 30C, the amount of total KCNE1 protein was not altered in the presence of DHA (similarly than that observed in the presence of EPA (225)).

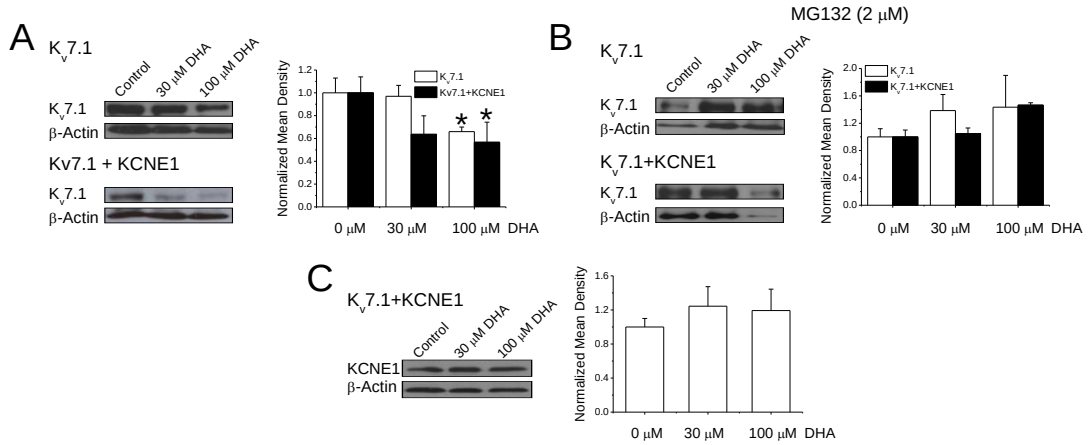

Figure 30: DHA decreases the K_V7.1 protein abundance in COS-7 cells. A: Left: shown are representative western blots that illustrate treatments with DHA. Note that DHA induces dose-dependent reductions of K_V7.1 protein. Cellular lysates were prepared from COS-7 cells transiently transfected with K_V7.1/KCNE1 channels and incubated for 48 h with 30 and 100 μM DHA. Samples were subjected to SDS-PAGE, transferred to PVDF membrane and probed with anti-K_V7.1. Right: Bar graph summarizing densitometry measurements used to compare proteins levels for the treatments of DHA for 48h. β-actin levels were used as a loading control (n = 3; *: P < 0.05). **B:** Representative western blots and graph showing the effects of DHA (0, 30 and 100 μM) on K_V7.1 in cells transfected with K_V7.1 or K_V7.1/KCNE1 in the presence of MG132 10 μM (proteasome inhibitor). **C:** Representative western blots and graph showing the effects of DHA (0, 30 and 100 μM) on K_V7.1 in cells transfected with KCNE1, anti-KCNE1 was used.

These results suggest that n-3 PUFAs reduce the amount of K_V7.1 channels via proteasome, without altering the concentration KCNE1 regulatory subunit. Previous reports showed that PUFAs may insert within the plasma membrane and modify the microdomains (216). It seems that PUFAs are able to modify the lipid composition and, therefore, protein location. For this reason, our third aim was to analyze the effects of DHA on K_V7.1/KCNE1 channels and their microenvironment. To that end, lipid rafts extraction assay was performed (analysis of the distribution of K_V7.1 and K_V7.1/KCNE1 channels in a sucrose gradient in chronic administration manner DHA, was made). Figure 31 shows that DHA partially disrupts lipids rafts. Indeed, in the presence of DHA the fraction pattern observed for caveolin, which indicates these enriched-domains of cholesterol and sphingolipids, were disturbed in the presence of this n-3 PUFA (Figure 31). In those lines we analyzed the distribution of K_V7.1/KCNE1 channels, in the presence of n-3 PUFAs. We observed that the location

of K_V7.1/KCNE1 channels was different compared with control conditions. These results indicate that these compounds modulate the location of these channels in the plasma membrane. All these results suggest that n-3 PUFAs produced an indirect effect on K_V7.1/KCNE1 channels regulating their electrophysiological features, their degradation via proteasome and also their location, in lipid-enriched microdomains, in the plasma membrane.

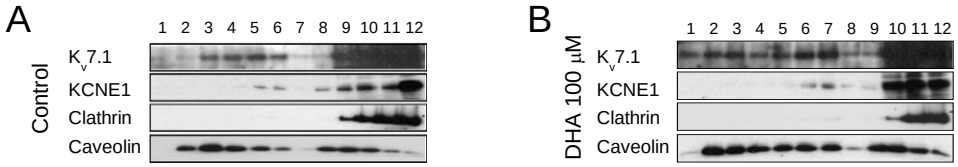

Figure 31: Sucrose density gradient fractions of cells expressing K_V7.1 and KCNE1 in the absence (A) and in the presence (B) of DHA. While caveolin indicated floating lipids rafts with low density, clathrin labeled non-raft fractions. K_V7.1 and KCNE1 colocalized with caveolin in low-buoyant density fractions (fraction 2-6) in control experiments whereas DHA triggered a wider distribution of proteins (fractions 1-12) and rafts. Pictures are representative images of at least 3 independent lipids rafts extractions analyzed by western blot.

4.2.2 Lipids-derived mediators effects, lipoxins (e-LXA4 and LXA4) and resolvin D1, on K_V channels

As it has been shown, the K_V7.1/KCNE1 effects produced by acute and chronic DHA/AA are different. Both are metabolized to resolvins and lipoxins, eicosanoids with potent anti-inflammatory effects. Therefore, we studied: 1) the effects of 15-epi-lipoxin A_4 (e-LXA_4) (aspirin-triggered 15-epi-lipoxins), lipoxin A_4 (LXA_4) and resolvin D1 (RvD1) in inflammation-related cells directly modulated by K_V channels, bone marrow derived macrophages (BMDM). 2) The effects of RvD1 and LXA_4 in K_V7.1/KCNE1 channels expressed in COS-7 cells.

4.2.2.1 Lipoxins (e-LXA4 and LXA4) and resolvins D1 effects on bone marrow derived macrophages

The electrophysiological properties of macrophages depend on their state of functional activation (91, 94). Changes in the ion channels along plasma membrane that promote changes in membrane potential are one of the previous events to activation process on macrophages (275). In this process, ion channels are widely involved and K_V channels play a pivotal role in the regulation of macrophage immunomodulatory responses (94, 275). Therefore, our purpose was to analyze the electrophysiological effects of e-LXA_4, LXA_4 and RvD1 on K_V currents elicited in BMDM.

Long-term experiments with e-LXA_4 (500 nM) were carried out in resting (control) and with e-LXA_4 and LXA_4 (500 nM) in LPS (100 ng/ml)-activated BMDM. Under control conditions, no significant effects were observed after incubate BMDM with e-LXA_4 (Figure 32A) at any membrane potential tested. Both e-LXA_4 and LXA_4 reversed the LPS effects while RvD1 (50 nM) did not (Figure 32B). e-LXA_4 significantly decreased K_V currents at membrane potentials positive to +10 mV, the magnitude being similar to that observed in resting BMDM (546 ± 152 *vs.* 178 ± 48 pA, in LPS-activated and LPS+e-LXA_4 BMDM, respectively, n = 7-9, $P < 0.05$, Figure 32D). Interestingly, e-LXA_4 did not modify the inactivation kinetics on resting BMDM, whereas it slowed this process in LPS-activated BMDM (τ = 456 ± 43 ms *vs.* 1123 ± 335 ms, for LPS and LPS+e-LXA_4 BMDM, respectively, n = 6-11, $P < 0.05$ Figure 32D). It has been described that LPS-activation up-regulate the expression of K_V1.3 channels (91, 94). Also, the K_V recorded from macrophages is the results of the activation of K_V1.3:K_V1.5 heteromultimers.

Because the level of K_V1.5 is not modified in LPS-activated macrophages, the ratio K_V1.3:K_V1.5 increases under LPS activation (91, 276). These results suggest that e-LXA$_4$ prevents the LPS-induced changes in the stoichiometry of K_V, leading the formation of heterotetramers with a lower K_V1.3:K_V1.5 ratio (91). Thus, the resulting K_V phenotype closely resembles that of resting BMDM. LXA$_4$ produced similar effects, but to a lesser extent than those induced by e-LXA$_4$ (323.6 ± 49.2 pA *vs.* 177.5 ± 47.9 pA, n=5-7, P < 0.05, in e-LXA$_4$ *vs.* LXA$_4$).

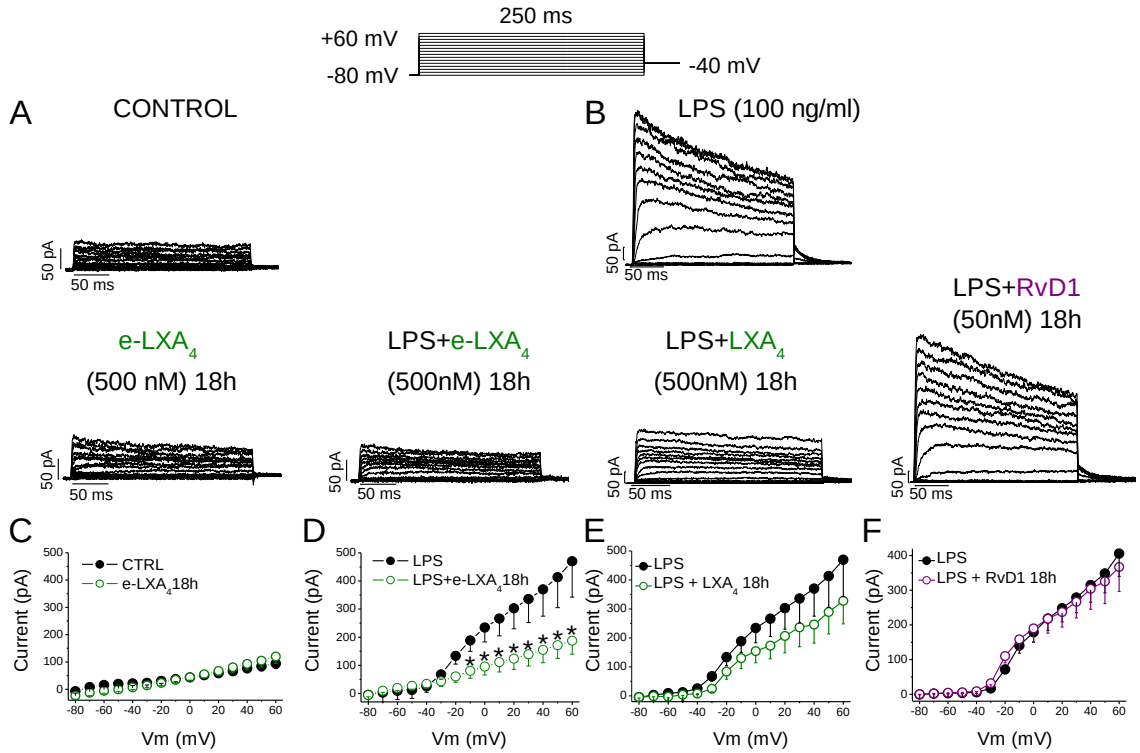

Figure 32: Effects of long-term treatment with e-LXA$_4$, LXA$_4$ and RvD1 on K_V currents in control and LPS-activated BMDM. **A:** Representative currents traces of K_V currents recorded from control (resting) BMDM and with e-LXA$_4$ (500 nM) treatment for 18 h BMDM, **B:** Traces obtained in control LPS-activated BMDM (top-middle) and LPS-activated BMDM after incubation for 18 h with e-LXA$_4$ (left), LXA$_4$ (middle) and RvD1(right). **C:** I-V relationships of resting BMDM + e-LXA$_4$ BMDM **D:** I-V relationships of LPS-BMDM + e-LXA$_4$ LPS-BMDM. **E:** I-V relationships of LPS-BMDM + LXA$_4$ LPS-BMDM and **F**: I-V relationships of LPS-BMDM + RvD1 LPS-BMDM. Data are shown as the means ± SEM. *: P < 0.05, n = 3-10 per group.

Previous reports showed that RvD1 (50 nM) inhibit the macrophages TNF-α release, which are associated with LPS-activation of macrophages (236). Long-term RvD1 (50 nM for 18h) experiments did not reverse the LPS-induced effect (406 ± 66 pA *vs.* 367 ± 70 pA, measured at the end of 250 ms pulses applied from -80 to +60 mV, in LPS-activated and LPS+RvD1-BMDM, respectively, n = 7-18, P > 0.05, Figure 32F). To assess whether the effect observed with 500 nM e-LXA$_4$ was due to a direct effect on K_V channels or if they act through some cell signaling pathway, two different approaches were performed.

First, K_V currents of resting and LPS-activated BMDM were analyzed before and after perfusion with e-LXA$_4$ (1-1000 nM, only data with 500 nM e-LXA$_4$ are shown). e-LXA$_4$ significantly decreased K_V currents, at positive potentials to 0 mV, elicited by LPS-activated macrophages (20.1 ± 3 % at +60 mV, n = 12, P < 0.05), without producing any effect on K_V currents elicited by resting macrophages (94.0 ± 18.0 pA *vs.* 105.2 ± 19.1 pA, n = 12, P > 0.05, Figure 33A).

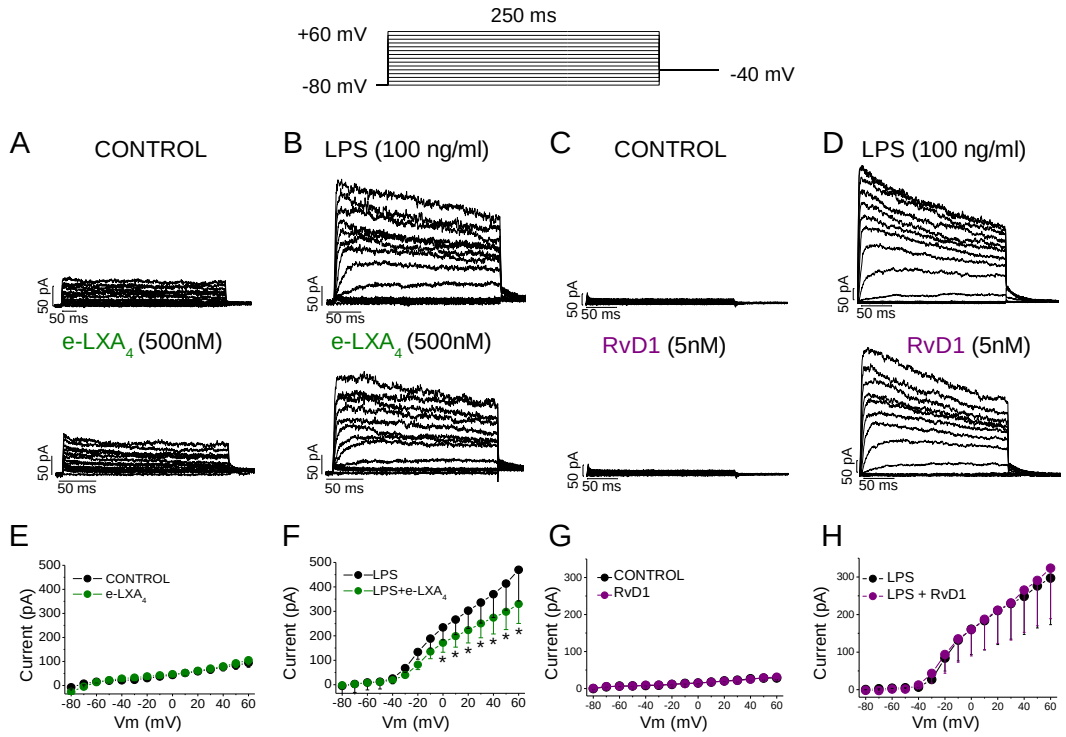

Figure 33: Early effects of e-LXA$_4$ and RvD1 on K_V currents. Representative traces of K_V currents recorded in control or LPS-activated BMDM (top panel). Cells were untreated (**A, C**) or treated with LPS (100 ng/ml) (**B, D**) for 18h. Current traces were recorded in the absence and after perfusion with e-LXA$_4$ (500 nM) and RvD1 (5 nM) (**A-D**). I-V relationships in the absence and in the presence of e-LXA$_4$ (500 nM) and RvD1 (5 nM) in non-stimulated BMDM (**E**, **G**), and in LPS-activated BMDM **(F**, **H**). Data are mean±SEM. *P < 0.05, n = 3-10 per group.

Acute RvD1 (5 nM and 50 nM) was tested in resting and LPS-activated BMDM. No significant effects were observed at any membrane potential tested in the presence of RvD1 (5 nM) neither resting nor LPS-activated BMDM (Figure 33GH). Also, no significant effects were observed in the presence of 50 nM RvD1 measured at +60 mV (34.3 ± 3 pA *vs.* 29.0 ± 4 pA, measured at the end of 250 ms pulses applied from -80 to +60 mV, in resting-BMDM and resting + RvD1-BMDM, respectively, n = 5-7, P > 0.05 and 207 ± 90 pA *vs.* 191 ± 89 pA, measured at the end of 250 ms pulses applied from -80 to +60 mV, in LPS-activated and LPS+ RvD1-BMDM, respectively, n = 5, P > 0.05, Figure S4).

The second approach performed to elucidate if the effects of lipoxins are due to a direct effect on K_V channels was to study the effects of e-LXA$_4$ in a heterologous system previously transfected with the K_V channels of interest. HEK293 cells were transfected with K_V1.3 and K_V1.5 channels, whose activation generates the BMDM K_V current. Figure 34 shows the currents obtained from transfected HEK293 cells after applying a 250-ms depolarizing pulses from -80 mV to + 60 mV in 10 mV steps, in the absence and in the presence of 1-1000 nM e-LXA$_4$. The results show that neither K_V1.3 nor K_V1.5 channels were modulated by e-LXA$_4$ (Figure 34). Moreover, the slight effects observed was concentration-independent

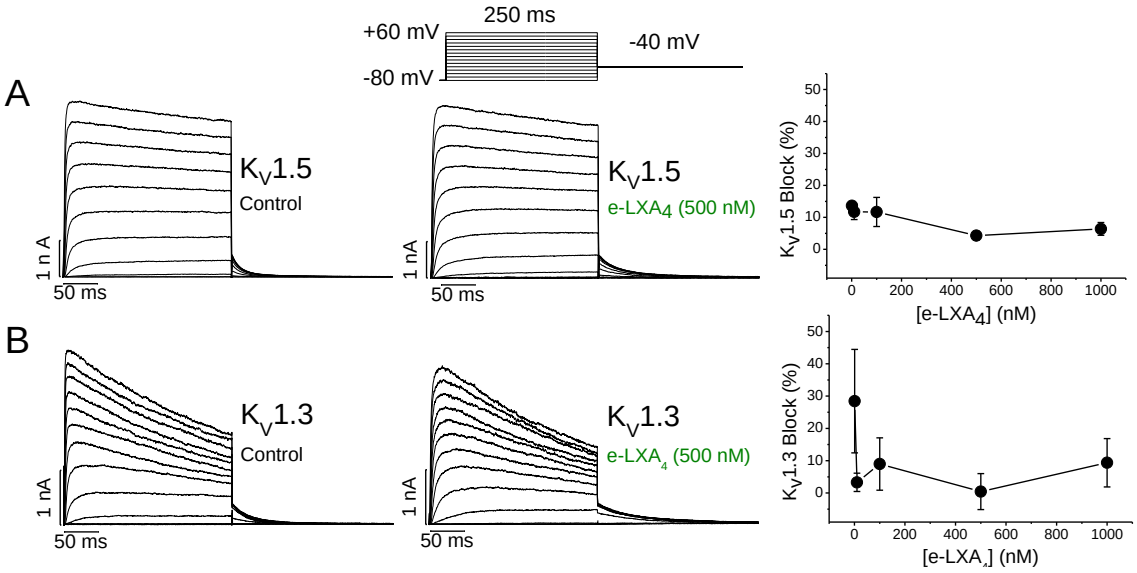

Figure 34: Effects of e-LXA$_4$ on K_V1.5 and K_V1.3 currents in transfected HEK293 cells. Currents were elicited after applying depolarizing pulses from a holding potential of -80 mV to different depolarizing voltages from -80 to +60 mV in 10 mV steps (250-ms in duration). Representative traces of K_V1.5 (**A**) and K_V1.3 (**B**) currents in HEK293 cells recorded in the absence (control) and in the presence of 100 nM e-LXA$_4$. Concentration-response curve (right panel, **A** and **B**) from 1 to 1000 nM e-LXA$_4$ on K_V1.5 and K_V1.3 channels. Plots show the degree of block *vs.* different e-LXA$_4$ concentrations. Data are shown as the mean ± SEM. P > 0.05, n = 3-5 per group.

Taken together, all these results suggest that e-LXA$_4$ and LXA$_4$, but not RvD1, are able to reverse, at least in part, the LPS-effect on BMDM. Also, the effects observed with e-LXA$_4$ are not mediated by a direct interaction with K_V1.3 or K_V1.5 channels, which are the main K_V channels expressed in these cells.

4.2.2.2 Lipoxin (LXA$_4$) inhibits K_V7.1/KCNE1 current

Figure 35 shows the effects of 500 nM LXA$_4$ on K_V7.1/KCNE1 channels. Current recordings were obtained after applying the pulse protocol shown in the top of the Figure, both in the absence and in the presence 500 nM of LXA$_4$. LXA$_4$ (500 nM) inhibited the K_V7.1/KCNE1 current by 33.0 ± 12.1% (n= 5, P < 0.05) measured at the end of 5.5 s from -80 to +60 mV. LXA$_4$ decreased the magnitude of the current measured at the end of 5.5-s depolarizing pulses at membrane potentials positive to 0 mV (Figure 35B). Figure 35B and 35C show the I-V relationships and the activation curves in the absence and in the presence of LXA$_4$. LXA$_4$ did not modify the midpoint of the activation curve of K_V7.1/KCNE1 current (+43.1 ± 4.6 mV *vs.* +38 ±.4.5 mV, n = 6, P > 0.05, in control and in the presence of LXA$_4$ conditions, respectively) or the slope values (22.1 ± 1.5 mV *vs.* 21.3 ± 1.2 mV, n = 6, P > 0.05, for control and LXA$_4$ conditions, respectively). Block produced by 500 nM LXA$_4$ was not voltage-dependent, being similar at -20 mV and at +100 mV (Figure 35D). No changes in the activation kinetics in the presence 500 nM LXA$_4$ were observed (τ_s = 3339.9 ± 851.7 ms and τ_f = 726.2 ± 160.4 ms *vs.* τ_s = 2506.7 ± 369.8 ms and τ_f = 674.5 ± 194.4 ms, n = 7, P > 0.05, in control and after perfusion with LXA$_4$ conditions, respectively). However, LXA$_4$ slowed the deactivation process (357.9 ± 50.1 ms, *vs.* 429.6 ± 41.7 ms, n = 7, P < 0.05, in control and after perfusion with LXA$_4$ conditions, respectively).

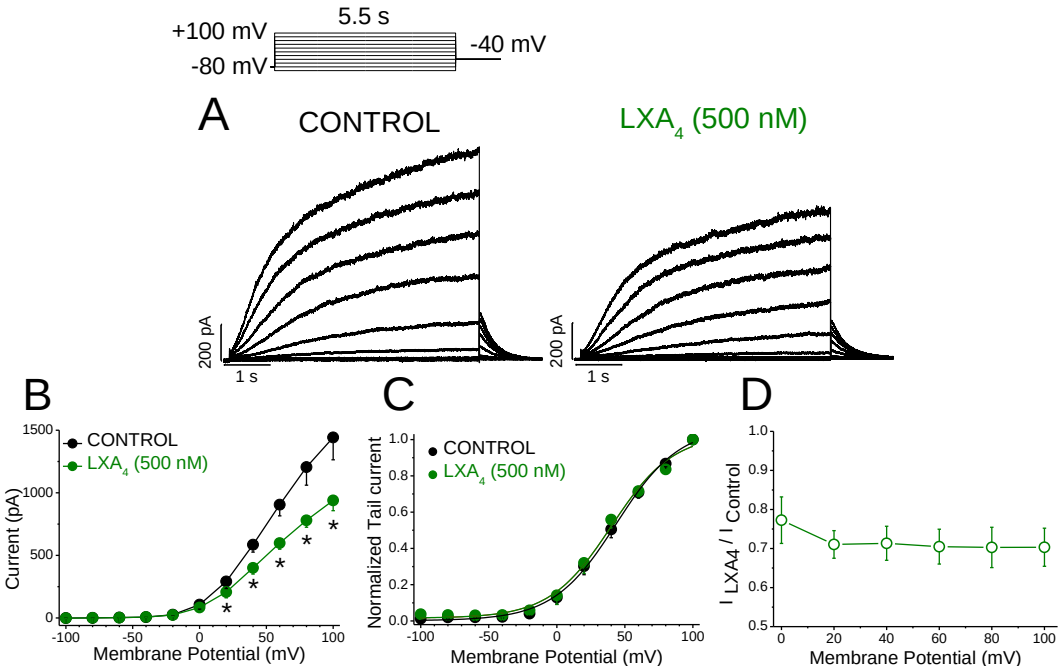

Figure 35: Voltage-dependent effects of LXA_4 on K_V7.1/KCNE1 current. **A:** Current traces were obtained after applying the pulse protocol shown in the top, both in the absence and in the presence of LXA_4 (500 nM). **B:** I-V relationships obtained under control conditions and after perfusion with LXA_4. **C:** Activation curves of K_V7.1/KCNE1 current obtained after plotting the maximum tail current amplitude *vs.* the previous step potential in the absence and in the presence of LXA_4. **D:** Ratio between the current in the presence and in the absence of LXA_4. Data are shown as the mean ± SEM. *: P < 0.05, n= 5.

After recording the K_V7.1/KCNE1 currents in the presence of LXA_4 (500 nM), cells were perfused with drug-free external solution. Under these conditions, the LXA_4 effects were almost completely washed-out (81.3 ± 7.6%, n = 6, P > 0.05 *vs.* control conditions, Figure S5).

4.2.2.3 Resolvins D1 (RvD1) inhibits K_V7.1/KCNE1 current

Figure 36 shows current traces of K_V7.1/KCNE1 channels generated after applying the pulse protocol shown in the Figure, both in the absence and in the presence of 5 and 50 nM of RvD1. RvD1 (5 nM and 50 nM) inhibited the K_V7.1/KCNE1 current by 48.6 ± 5.7 % (n= 5, P < 0.01) and 86 ± 5 % (n = 6, P < 0.01) measured at the end of 5.5 s from -80 to +60 mV. Figure 36B shows the I-V relationships obtained, in the absence and in the presence of RvD1 (5 nM and 50 nM), after plotting the current measured after 5.5 s depolarizing pulses from -80 to +100 mV versus membrane potential. RvD1 (5 nM and 50 nM) inhibits K_V7.1/KCNE1 current at membrane potentials positive to 0 mV. The activation curve and the slope factor were not modified in the presence of 5 nM of RvD1 (V_h = +31.5 ± 6.5 mV, *s* = 17.1 ± 2.3 mV and V_h = +35.6 ± 11.1 mV, *s* = 17.9 ± 1.6 mV, n = 4, P > 0.05, for control and 5 nM RvD1 conditions, respectively). Block produced by RvD1 was not voltage-dependent, being similar at all membrane potential tested (Figure 36D). RvD1 did not modify the activation (τ_s = 3608.3 ± 981.4 ms and τ_f = 908.5 ± 197.1 ms *vs.* τ_s = 3577.5 ± 784.1 ms and τ_f = 920.2 ± 181.4, n = 6, P > 0.05, for control and 5 nM RvD1 conditions, respectively) or deactivation kinetics (τ = 426.1 ± 95.3 ms, and τ = 464.6 ± 90.6 n = 5, P > 0.05 for control and 5 nM

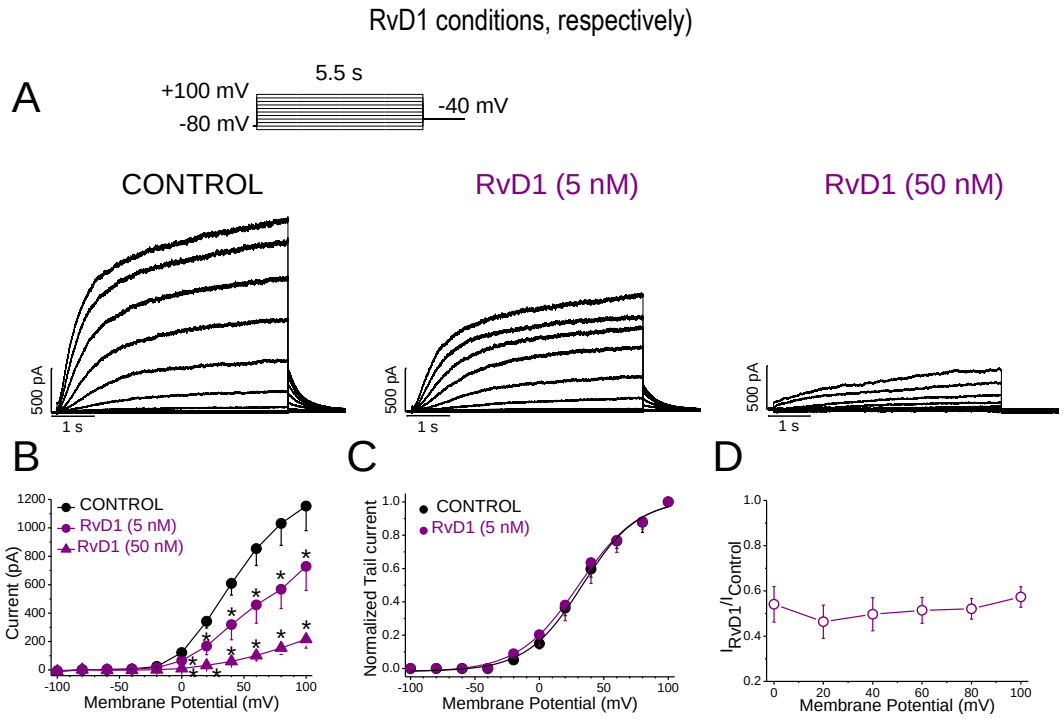

Figure 36: Voltage-dependent effects of RvD1 on K_V7.1/KCNE1 channels. **A:** Current traces obtained after applying the pulse protocol shown in the top, in the absence and in the presence of 5 and 50 nM RvD1. **B:** I-V relationships obtained after plotting the current at the end of 5.5-s *vs.* membrane potential, in the absence and in the presence of RvD1 (5 and 50 nM). **C:** Activation curves of K_V7.1/KCNE1 current obtained after representing the maximum tail current amplitude *vs.* the previous step potential, recorded in the absence and in the presence of 5 nM RvD1. **D:** Ratio between the current in the presence of 5 nM RvD1 and under control conditions. Data are shown as the mean ± SEM. *P < 0.05, n = 5-8.

As it was observed with LXA_4, the effects produced by RvD1 were washed-out after perfusion of the cells with drug-free external solution (73.5 ± 17.8 %, n = 4 *vs.* control conditions, P > 0.05, Figure S5). Therefore, the effects produced by RvD1 on the K_V7.1/KCNE1 current were much more potent than those observed with LXA_4.

Moreover, we studied the RvD1 (5 and 50 nM) effects on K_V7.1 channels alone (Figure S6). At 5 nM, RvD1-induced block was lower than that observed for K_V7.1/KCNE1 channels (28.9 ± 5.8 % n = 5, P < 0.05, *vs.* 48.6 ± 5.7% ,n= 5, P < 0.01, measured at the end of 5.5-ms pulses applied from -80 to +60 mV, in K_V7.1 and K_V7.1/KCNE1 channels, respectively), However, RvD1 (5 nM) right-shifted the midpoint of the activation curve of K_V7.1 channels (-16.5 ± 2.3 *vs.* -11.6 ± 1.8 mV, n= 4, P < 0.05, in the absence and in the presence of RvD1, respectively) without modifying the slope factor (7.1 ± 0.8 *vs.* 8.9 ± 0.7 mV, n= 4, P > 0.05). RvD1 did not modify the activation (τ_s = 18.9 ± 4.3 ms *vs.* τ_s = 30.3 ± 7.8 ms and τ_f = 920.2 ± 181.4, n = 6, P > 0.05, for control and 5 nM RvD1 conditions, respectively) or deactivation kinetics (τ = 816 ± 275 ms *vs.* τ = 827 ± 288 n = 5, P > 0.05 for control and 5 nM RvD1 conditions, respectively).

These results suggest that the presence of KCNE1 tunes the sensitivity of K_V7.1 channels to RvD1 of K_V7.1 channels, being RvD1 much more potent in the presence of the KCNE1 regulatory subunit.

All these results suggest that both LXA_4 and RvD1 block K_V7.1/KCNE1 channels, without modifying the voltage dependence or the activation kinetics of the channels. Moreover, and in contrast to that observed in the presence of and DHA, the K_V7.1/KCNE1 current magnitude was almost recovered when LXA_4 or RvD1 were removed for the external solution (Figure S5).

.

5. DISCUSSION

In the present Doctoral Thesis, we have studied: 1) the presence of $K_V7.1/K_V7.5$ functional channels in vascular smooth muscle, and in their role in the control of the vascular tone. 2) The regulation of $K_V7.1$/KCNE1 channels by n-3 and n-6 PUFAs and their metabolites (lipoxins and resolvins). Also, we have studied 3) the effects of lipoxins and resolvins on K_V currents from bone marrow derived macrophages.

5.1 $K_V7.1/K_V7.5$ HETEROTETRAMERIC CHANNELS

In this study, we have demonstrated that $K_V7.1$ and $K_V7.5$ form functional heteromeric channels that seem to be involved in the maintaining of the vascular smooth muscle tone. These heterotetramers exhibit intermediate electrophysiological and pharmacological properties between $K_V7.1$ and $K_V7.5$ channels. $K_V7.1/K_V7.5$ channels differently target lipid rafts than $K_V7.1$ channels alone. Indeed, on assembly with $K_V7.5$, $K_V7.1$ subunits are excluded from lipid rafts. In addition, the interaction with $K_V7.1$ results in intracellular retention of the $K_V7.1/K_V7.5$ heterotetramer (250). Assembly of $K_V7.1/K_V7.5$ channels triggers emerging properties on vascular muscle physiology. These results led us to propose that the formation of $K_V7.1/K_V7.5$ heteromeric channels provides efficient spatial and temporal regulation of smooth muscle cell function. Our results shed light on to new possible interactions and also to a highly specialized regulation of different processes in which K_V7 are involved.

Among others K_V channels, K_V7 channels are crucial in cardiovascular muscle contraction. $K_V7.1$, $K_V7.5$ and $K_V7.4$ channels are mostly expressed in vascular smooth muscle. Yeung and colleagues challenged the dogma that states that $K_V7.2$-7.5 channels are only expressed in neurons and in a few other tissues. These authors described that murine arteries like the aorta, carotid, femoral and mesenteric and portal vein express equal or higher levels of $K_V7.5$ and $K_V7.4$ than $K_V7.1$ channels, and that K_V7 channels play a pivotal role on vascular reactivity (111). Furthermore, other studies suggest that renal, coronary, aorta and cerebral arteries also express K_V7 channels (184). We have demonstrated that $K_V7.1$ and $K_V7.5$ channels are expressed in the coronary and aorta arteries, and also in cava vein (250). In addition, with immunoprecipitation assays performed in rat aorta arteries, we observed not only that both channels are present in the same tissue, but that they also form part of the same protein complex. Previous reports have also shown that $K_V7.4$ and $K_V7.5$ channels can form functional heterotetramers (277). $K_V7.1$, $K_V7.5$ and $K_V7.4$ channels are expressed in cerebral arteries, however, $K_V7.1$ channels do not seem to have relevance in the regulation of the vascular tone within this vessel (151, 277). Although $K_V7.5$ and $K_V7.4$ form homotetrameric channels, Chadha and colleagues suggest that the main control of the vascular reactivity is due to heterotetrameric $K_V7.4/K_V7.5$ channels (277).

Our immunoprecipitation assays revealed that $K_V7.1$ and $K_V7.5$ channels are present in the same protein complex in aorta artery isolated myocytes. These results are in contrast with other reports suggesting that $K_V7.1$ channels are unable to form heteromeric channels with other K_V7 members (Schwake and colleagues). This hypothesis is based in the fact that morphological elements of the A-domain from $K_V7.1$ are different to those from other K_V7 members. However, the reasons why these channels cannot form heterotetramers are still not clear. These authors state that $K_V7.2$ and $K_V7.1$ α-subunits cannot interact, whereas $K_V7.2$ and $K_V7.3$ can. This research group made chimeric channels between $K_V7.1$ and $K_V7.3$ α-subunits. They performed experiments in which “sid” or “si-domain” (which

encompasses A-domain) of $K_V7.3$ was inserted in $K_V7.1$ channels and *vice versa*. These experiments demonstrated that when the "$K_V7.1$ sid" was present, they were unable to detect any interaction with other K_V7 channel. However, these authors did not perform the experiments needed to show interactions between $K_V7.1$-$K_V7.4$ or $K_V7.1$-$K_V7.5$ channels (244, 278, 279). The presence of functional $K_V7.5$/$K_V7.4$ channels was demonstrated in middle cerebral arteries by Chadha and colleagues (277). In this study, pharmacological and proximity ligation assay (PLA) analysis were performed; without analyzing the possible existence of $K_V7.5$/$K_V7.1$ channels. Indeed, they studied the interactions between $K_V7.5$/$K_V7.5$, $K_V7.4$/$K_V7.1$ channels but not of $K_V7.5$/$K_V7.1$ channels. In summary, in all these reports the possible $K_V7.1$/$K_V7.5$ channel was not explored; and thus, the possibility that $K_V7.1$ and $K_V7.5$ channels form heterotetramers cannot be ruled out (244, 277, 279).

Our results confirmed that $K_V7.1$ and $K_V7.5$ channels interact both in HEK293 cells and also in and aorta arteries. Moreover, cells transfected with KCNE1 and both K_V7 subunits, demonstrated that all protein tested immunoprecipitated, indicating that they form part of the same protein complex. Traffic and FRET experiments confirmed physical interactions between both α-subunits (250).

Lipid rafts are lipid-enriched (cholesterol and sphingolipids) plasma membrane regions. These regions act as organizing centers along the membrane, concentrating molecular signaling and/or modulating molecular traffic or membrane fluidity. Our results demonstrate that $K_V7.1$ channels target lipids-rafts; however, $K_V7.5$ channels do not. Interestingly, when $K_V7.1$ channels and $K_V7.5$ channels were co-expressed together in HEK293 cells, the heterotetrameric channels do not target lipid-enriched domains. More importantly, the lipid raft targeting was studied in the heart, which only expresses $K_V7.1$ channels, and in aorta artery and cava vein, which express both K_V7 isoforms. Our experiments demonstrated that when both channels are present in the same tissue, $K_V7.1$ channels do not target lipid rafts. All these results suggest that there is a physiological relevant change in the targeting in plasma membranes when both channels are expressed together. The fact that $K_V7.1$/$K_V7.5$ channels target differentially than $K_V7.1$ channels alone may be crucial for its cellular modulation and, thus, for its contribution to the vascular tone.

The current elicited by $K_V7.1$/$K_V7.5$ channels expressed in COS-7 cells exhibited an intermediate phenotype between those observed for $K_V7.1$ and $K_V7.5$ channels. The $K_V7.1$/$K_V7.5$ current activation was slow, similar to other K_V7 members, but faster than those of $K_V7.5$ channels. Also, they exhibited a cummulative current at membrane potentials positive to +20 mV, indicative of fast inactivation typical of K_V7 channels (145, 146, 152, 153). The electrophysiological characteristics observed in $K_V7.1$, $K_V7.5$ and $K_V7.1$/$K_V7.5$ channels suggest that all of them exhibit fast inactivation process. However, additional voltage pulse protocols are needed to ensure it in $K_V7.1$/$K_V7.5$ heteromeric channels (145, 155). The voltage dependency of the activation of $K_V7.1$/$K_V7.5$ channels was very close to that exhibited by $K_V7.5$ channels, although the slope factor was closer to that observed in $K_V7.1$ channels. It was reported that the current magnitude of $K_V7.2$/$K_V7.3$ and $K_V7.3$/$K_V7.4$ heteromeric channels was greater than those elicited by the corresponding homotetramer channels (178). Similar results were reported for $K_V7.5$/$K_V7.3$ channels; suggesting that the increased in the current amplitude is promoted by the assembly with $K_V7.3$ α-subunits (280). In contrast to that observed in $K_V7.5$/$K_V7.3$ channels, in our experiments, the magnitude of the current generated by the activation of $K_V7.1$/$K_V7.5$ channels was similar to those elicited by $K_V7.1$ and $K_V7.5$ homomeric channels.

These results suggest that $K_V7.1$ and $K_V7.5$ α-subunits can interact to form functional channels with their own electrophysiological properties.

In addition to the ability to form heteromeric K_V7 channels, and because these channels are highly regulated by KCNE regulatory subunits that are also present in vascular smooth muscle (183, 184), the interactions between α- and β-subunits will lead to a larger and diverse group of K_V7 currents.

KCNEs subunits modify both $K_V7.1$ and $K_V7.5$ channels. All KCNE proteins have been detected in vascular smooth muscle (111, 137, 184), but their role in this tissue is not well understood. KCNE1 and KCNE3 modulation of $K_V7.1$ channels has been widely studied. $K_V7.1$/KCNE1 current is involved in the repolarization of the cardiac action potential, whereas $K_V7.1$/KCNE3 channels are constitutively active channels that are essential, at least, in colonic crypt cells. In this tissue, $K_V7.1$/KCNE3 channels, though releasing of K^+, generate the driving force needed for chloride secretion (146, 152, 153, 281). It is considered that the modulation of $K_V7.5$ channels by KCNE3 can be important in muscle and brain, where KCNE3 also regulates other K_V channels, such as $K_V2.1$, $K_V3.1$ and $K_V3.4$ channels (270). KCNE3 shifts to more positive membrane potentials the voltage dependence of the activation the $K_V7.5$ current. Also, KCNE3 significantly decrease $K_V7.5$ current (137). In addition, KCNE1 modulates $K_V7.5$ channels, in this case, increasing $K_V7.5$ currents at +60 mV by 2-fold, slowing the activation kinetics process and suppressing the inward rectification of the $K_V7.5$ current. The effects produced by KCNE1 on $K_V7.1$/$K_V7.5$ channels remind us the regulation by KCNE1 on both, $K_V7.1$ and $K_V7.5$ channels. However, this interaction produced a much greater depolarizing shift of the activation curve of $K_V7.1$/$K_V7.5$ channels (~ +80 mV). So, KCNE1 slowed the activation kinetics, shifted to positive membrane potentials the voltage-dependent of activation, increased the magnitude of the current and slowed the deactivation kinetics. These results suggest that KCNE1 effects are potentiated in the heterotetrameric channel. We also analyzed $K_V7.1$/$K_V7.5$/ KCNE3 channels. On the contrary, KCNE3 produced opposite effects on the $K_V7.1$/$K_V7.5$ tetrameric channel. KCNE3 did not decrease $K_V7.1$/$K_V7.5$ current, accelerated the activation kinetics, and shifted to more negative membrane potentials the voltage-dependence of the activation. Indeed, if we compare $K_V7.1$/$K_V7.5$/KCNE3 channels with $K_V7.1$/$K_V7.5$/KCNE1, we can observe that the first ones exhibit a threshold membrane potential of -60 mV (similar to that observed for $K_V7.1$ channels), whereas for $K_V7.1$/$K_V7.5$/KCNE1 channels is 0 mV. At physiological membrane potentials $K_V7.1$/$K_V7.5$/KCNE3 exhibit greater magnitude current than $K_V7.1$/$K_V7.5$/KCNE1 channels. Thus, KCNEs subunits modulate $K_V7.1$/$K_V7.5$ channels generating K^+ currents with their own electrophysiological properties.

The fact that the presence of different α- and β-subunits vary in different vascular smooth muscle cells is crucial to better understand the functional role and pharmacology of these channels in this tissue. As a result, the pharmacological tools have to be adjusted for each scenario expressing distinct K_V7 and KCNEs subunits. In fact, we demonstrated that chromanol 293B (5 μM) produced a 13% of block of $K_V7.1$/KCNE1 channels, whereas it blocked $K_V7.1$/$K_V7.5$/KCNE1 channels by 53%. Therefore, the presence of the heteromeric complex, as well as the presence of KCNE subunits, modifies the pharmacology of the channel, as previously shown for other ion channels (136, 254). Since the pharmacology of the channels is modified depending on the different subunits, we analyzed the effects of the well-known opener of $K_V7$channels, retigabine (282, 283). Retigabine activates all members of the K_V7 subfamily

with the exception of $K_V7.1$ channels. Our results showed that retigabine increased similarly the current in both $K_V7.1$/Kv7.5 and $K_V7.5$ channels and shifted the activation curve towards more negative membrane potentials as it was previously described for $K_V7.3$/$K_V7.5$ and $K_V7.3$/$K_V7.2$ channels (109, 280). Retigabine activates $K_V7.2$-5 channels by interfering with the normal voltage dependent of the channels, i.e. it shifts the voltage-dependence of activation to hyperpolarized potentials (284, 285). As a consequence, K_V7-mediated currents activate at more negative membrane potentials, effectively hyperpolarizing the resting membrane potentials (109, 280). In addition, retigabine accelerates the activation and slows the deactivation kinetics of $K_V7.2$, $K_V7.3$, $K_V7.2$/$K_V7.3$ and $K_V7.4$ and $K_V7.5$/$K_V7.3$ channels (109, 174). However, retigabine slows the activation kinetics in both $K_V7.5$ and $K_V7.1$/$K_V7.5$ channels, without modify the deactivation kinetics.

We observed that $K_V7.1$/$K_V7.5$ channels form functional heteromeric channels, with their own electrophysiological and pharmacological properties. Since different α- and β-subunits are expressed widely and their different assembly lead different currents, further investigation is necessary to elucidate the role of these channels in different tissues. In order to know if $K_V7.1$/$K_V7.5$ channels can regulate vascular tone, a series of experiments were performed. It was analyzed the K_V current elicited, after depolarization, by coronary myocytes. Using different pharmacological tools (chromanol 293B, linopirdine and retigabine), we show that these currents were, in part, elicited by K_V7 channels. Chromanol 293B inhibits K_V currents in these native cells by ~40% and linopirdine produced the same extent of inhibition. Interestingly, the simultaneous addition of linopirdine plus chromanol 293B did not trigger any further blockade, thus suggesting that K_V7 channels are involved in the K_V currents elicited by coronary myocytes. Because chromanol 293B had significant effects blocking these currents, it is possible suggest that $K_V7.1$ channels are involved in these currents. Moreover, these results suggest that these currents are not generated by the activation of $K_V7.2$-5 homotetrameric channels. Yeung and colleagues, suggested that in aorta, carotid and mesenteric arteries, where $K_V7.1$ channels are present, they do not have any relevance in control vascular reactivity. Chromanol 293B blocked K_V currents recorded from portal vein cardiomyocytes but not in aorta artery (286). In fact, $K_V7.1$ mRNA was detected in aorta, although the pharmacological tools used, failed to detect $K_V7.1$ channels. They suggested that $K_V7.1$ channels are not involved in the maintaining of the vascular tone. Therefore, further investigation in the role of $K_V7.1$ channels in vascular smooth muscle, is needed (111). Moreover, because KCNE expression is widely distributed in different vessels, this may change the pharmacological properties and thus, the study of the regulation of the vascular tone becomes more complex.

Other studies reported that R-L3, a specific $K_V7.1$ channel activator, did not produce any relaxant effect on cerebral arteries. Based on these results, they ruled out the possibility of $K_V7.1$ channels were involved in control of cerebral arteries vascular tone, even when $K_V7.1$ was detected by other techniques. However, the role of $K_V7.4$/$K_V7.5$ heterotetramer channels as main regulators of vascular tone seems to be greater than the role of $K_V7.4$ and $K_V7.5$ homotetramer channels (277). These authors pointed out the possibility that $K_V7.1$ and $K_V7.4$ channels may form heterotetramers (but they failed proving their presence). However, they did not perform the same approach for $K_V7.1$ and $K_V7.5$ channels. Khanamiri and colleagues observed that R-L3 relaxed mesenteric and pulmonary arteries whereas it did not relax coronary arteries. On the other hand, the mRNA levels of $K_V7.1$ channels, on coronary

arteries, were equal or even higher that those observed for $K_V7.4$ and $K_V7.5$ channels (184). According to these data, we cannot rule out the possibility that $K_V7.1$ and $K_V7.5$ channels may form heterotetrameric channels in coronary arteries. In our experiments, serotonin pre-constricted coronary arteries were incubated with both, chromanol 293B and linopirdine and the retigabine relaxation effects were analyzed. After constricted with chromanol 293B, 30 μM of retigabine completely relaxed the artery; while in the presence of linopirdine higher concentrations of retigabine were needed. These results suggest that $K_V7.1$ homotetrameric channels do not seem to be responsible of the regulation of the vascular tone in coronary arteries. All these results suggest that the vasorelaxant effects of retigabine on contracted vessels by chromanol 293B are due to the existence of $K_V7.1/K_V7.5$ channels. These data are consistent with the expression pattern of these K_V channels and with the functional pharmacological effects suggesting that neither $K_V7.5$ nor $K_V7.4$ are forming homotetramers. In addition, as we have been observed, the pharmacological results could differ from homotetramers to heterotetramers and even more if KCNEs subunits are present.

Retigabine does not affect cardiac $K_V7.1$ channels, and this pharmacological property has been related with its lack of toxicity. However, it has a significant impact on $K_V7.2$-7.5 channels. At higher concentrations than those required for anticonvulsant activity, it induces muscle relaxation and motor incoordination (283). A previous report showed that retigabine has low ability to cross the blood-brain barrier, being the concentration in plasma 5-fold more than in brain tissue. These findings suggest a reduction in antiepileptic efficacy and the increased risk in other tissues (287).
The study of K_V7 channels as pharmacological targets can be used in new drug design. This approach will also improve the great variety of drugs that are already in use, such as drugs used to treat epilepsy or cardiovascular disorders.

In summary, the results of this part of the present Doctoral Thesis suggest that $K_V7.1$ and $K_V7.5$ channels, expressed in vascular coronary myocytes, form functional heterotetrameric channels that seem to play a relevant role in the control of the vascular tone. The confirmation of the presence of $K_V7.1/K_V7.5$ heteromers paves the way for novel interactions that could shed light on pharmacological results in vascular musculature. The complexity is further increased by the KCNE expression pattern, with which they interact, and that has not been currently investigated.

5.2 n-3, n-6 PUFAs AND THEIR DERIVATIVES: LXA_4 AND RvD1, MODULATE $K_V7.1$/KCNE1 AND K_V1 CHANNELS

5.2.1 n-3 and n-6 PUFAs on $K_V7.1$/KCNE1 channels

In this part of the present Doctoral Thesis we investigated the effects of the most abundant n-6 and n-3 PUFAs (AA and DHA) on $K_V7.1$/KCNE1 channels. We demonstrated that: (i) At physiological concentrations, DHA and AA increased the current magnitude in acute, but not after chronic exposition, both in COS-7 cells and in guinea pig ventricular myocytes. (ii) DHA chronic application decreased the expression of $K_V7.1$ channels, but not that of KCNE1, due to an enhanced degradation via proteasome. Finally, (iii) chronic exposure of DHA modified the $K_V7.1$ location in membrane microdomains.

DHA and AA modulate K_V7.1/KCNE1 channels by modifying the magnitude of the current and the gating of the channels. Acute perfusion with DHA increased the K_V7.1/KCNE1 current magnitude, slowed its activation kinetics and accelerated the deactivation kinetics. However, although AA also increased the K_V7.1/KCNE1 current magnitude, it did not modify the activation kinetics, but, similarly to DHA, accelerated the deactivation kinetics. All these effects were only observed in the presence of KCNE1, suggesting an essential role for KCNE1 in the modulation exerted by acute DHA and AA. These results are in agreement with those previously reported by Doolan and colleagues, in which DHA increased K_V7.1/KCNE1 currents due to the presence of KCNE1 (210). However, Liin and colleagues state that KCNE1 impairs the effects produced by DHA on K_V7.1 channels, being greater the effects produced by DHA in K_V7.1 than in K_V7.1/ KCNE1 channels (226). They propose that a negative charge in the PUFA carboxyl head group is needed to shift the activation curve towards negative membrane potentials and, thus, increasing the magnitude of the current. Moreover, they suggest that the lack of effects observed in the presence of KCNE1 is due to a change in the environment of the channel induced by this subunit that neutralizes the charge of the head group of the DHA molecule (226). Our data and Liin and colleagues results are in agreement with those reported by Hoshi et al., who suggest that DHA can bind both the α and to the β-subunits of K_{Ca}1.1 channels. In fact, some β-regulatory subunits, but not all, highly potentiate the effect of DHA on K_{Ca}1.1 channels (288).

Dietary administration of PUFAs produces their incorporation on plasma membranes as part of phospholipids. Free PUFAs can modulate different processes or can be metabolized to several eicosanoids. It has been described that the acute and chronic effects of PUFAs can be different (207). Therefore, we analyzed both, acute and chronic effects of DHA and AA, as well of those of their metabolites (lipoxins and resolvins). Acute exposure of COS-7 cells transfected with K_V7.1/KCNE1 channels to DHA led to an increased current magnitude at positive membrane potentials, a slower activation and faster deactivation kinetics. Similar results were obtained when guinea-pig ventricular myocytes were exposed to the same DHA concentration. These results suggest that the primary mechanism of the increased magnitude of the K_V7.1/KCNE1 current may be due to a modification of the channel gating. On the other hand, chronic DHA administration did not increase the current magnitude at any potential tested. Interestingly, the effects of this PUFA on the activation were different than those observed for acute perfusion, in this case being faster than under control conditions. However, the deactivation kinetics was accelerated. Surprisingly, a shift towards more negative membrane potentials was observed in K_V7.1/KCNE1 channels after cells were incubated 48 h with DHA.

AA effects were slightly different. This n-6 PUFA increased the magnitude of the K_V7.1/KCNE1 current at membrane potentials positive to -25 mV (close to the threshold of activation of the channel). Similar results were previously observed with EPA (225). The effects of AA on K_V7.1/KCNE1 resemble those produced by KCNE1 on the K_V7.1 current and, thus, we could explain the increase produced by this PUFA by an increase of the channel conductance. However, single channel analysis is needed to assess this hypothesis. Another possibility is that AA promotes the transition to the open state of the channel and stabilizes the channel in this state. Interestingly, activation curve could not be fitted, because it did not achieve steady-state. On the other hand, long-term administration of AA did not

increase the magnitude of K_V7.1/KCNE1 currents; however, it slowed the activation and accelerated the deactivation kinetics. These results suggest that both, the time of exposure and the differences between n-3 and n-6 PUFAs, promote specific effects on K_V7.1/KCNE1 channels (224, 225). PUFAs can modify the gating of ion channels by simultaneously stablishing a direct interaction and also by modifying the properties of the lipid bilayer. It has been observed that PUFAs can alter voltage gated channels both, in acute and after long-term conditions. Some results can be attributable to direct interactions, whereas others seem to be indirect. There are several evidences that PUFAs interact directly with ion channels. It has been described that specific single mutations in Na_V1.5 and K_{Ca}1.1 channels modify PUFAs effects after acute administration (289, 290). Moreover, it has been reported that several voltage gated channels, such as *Shaker* K^+ channels or other K_V channels like K_V7.1, directly interact with PUFAs through a specific region located between the S3 and S4 of the VSD (226), whereas in other channels, like K_{Ca}1.1, PUFAs bind to the ion pore (290).

It has been also reported that PUFAs modify microenvironments of the plasma membrane in which certain ion channels are located. These studies suggest that their effects on the ion channels are a consequence of a disorder induced in those regions. Also, there is a correlation between the potency to block the cardiac I_{Na} and the ability of PUFAs to increase membrane fluidity (219). Moreover, PUFAs might indirectly modulate ion channels by changing the cellular redox status, the metabolism of phospholipids or the gene expression (195).

We wanted investigate further the mechanism by which acute and chronic n-3 PUFAs exert their actions on K_V7.1/KCNE1 channels. To that end, two other procedures were performed: 1) Because it was described that PUFAs decreased the expression of K_V1.5 channels (213) and since current magnitude was not increased after long-term PUFAs exposure, the K_V7.1/KCNE1 channels expression levels were analyzed after 48 h of incubation with DHA. After long-term conditions, K_V7.1, but not KCNE1, expression levels decreased in a concentration-dependent manner. It is stablished that Nedd4-2 ubiquitin-ligase regulates K_V7.1 internalization and degradation via proteasome. The decreased of expression levels of K_V7.1 channels was prevented by a proteasome inhibitor (MG-132), suggesting that DHA promotes K_V7.1 degradation via proteasome. 2) To investigate if DHA modulates the plasma membrane location of K_V7.1 channels during long-term incubation, targeting lipid-rafts was analyzed in the absence and in the presence of DHA. K_V7.1 channels partially target lipid rafts in ventricular myocytes (291), whereas KCNE1 localizes in low-buoyant density fractions only in association with K_V7.1 (269). Our results demonstrate that long term exposure to DHA delocalized K_V7.1 from lipid rafts (similar results were previously observed with EPA (225)). In addition, we previously performed electrophysiological experiments with metil-β-ciclodextrin (MβCD), which triggers lipid-rafts disruption (via cholesterol depletion) (225). When cells expressing K_V7.1/KCNE1 channels were treated with MβCD, the current generated increased and the activation curve was shifted towards positive potentials. Under these conditions, EPA effects were similar to those observed in non-cholesterol-depleted cells, suggesting a direct effect after acute application of EPA on K_V7.1/KCNE1 channels. Based on all these EPA results, and in those produced by DHA and AA in acute and after chronic exposure, we suggest that these PUFAs both directly and indirectly interact with K_V7.1/KCNE1 channels, although further investigations are needed to confirm this hypothesis.

Our results observed in K_V7.1/KCNE1 channels treated with AA are in agreement with the reported ability of the N-arachidonoyl-taurine to reverse chromanol 293B effects on action potential duration in rat embryonic cardiomyocytes, which do not generates I_{Kr}. This negatively-charged AA analogue acts as an antiarrhythmic agent decreasing the firing frequency produced by chromanol 293B (226). Given the fact that AA inhibits I_{Kr} (212) and increases I_{Ks}, our results may explain, at least in part, the antiarrhythmic effects observed in this study. These authors propose that the antiarrhythmic effects of n-3 PUFAs are due to their inhibitory effects on I_{Na} and I_{CaL}, because they do not observe any increase in K_V7.1/KCNE1 (226). However, in our expression system and in agreement to Doolan and colleagues (210), we observed the opposite, being necessary the presence of KCNE1 to observe an increase of K_V7.1/KCNE1 current.

Action potential simulations incorporating the effects of DHA and EPA showed that these PUFAs have a key role shortening the action potential as a consequence of their availability to increase I_{Ks}, when other repolarizing current are compromised, for instance when I_{Kr} or I_{Kur} are inhibited (213, 292). Likewise, the AA induced increase of I_{Ks} may lead similar effects.

5.2.2 Effects of e-LXA_4, LXA_4 and RvD1 on K_V currents from BMDM

In this part of the present Doctoral Thesis, we investigated the effects of PUFAs metabolites (e-LXA_4, LXA_4 and RvD1) on K_V currents recorded in BMDM. We demonstrate that: (i) e-LXA_4 and LXA_4, but not RvD1, reverse LPS-induced phenotype in BMDM in long-term conditions and (ii) e-LXA_4, but not RvD1, block K_V currents from immune native macrophages (BMDM) activated with LPS after acute perfusion.

e-LXA_4, LXA_4 and RvD1 are lipid-derived mediators which are products of the metabolism of AA and DHA, respectively. e-LXA_4, LXA_4 and RvD1 are able to mount resolution and anti-inflammation (293, 294).

RvE1, RvD1/AT-RvD1 (aspirin trigger-RvD1), are originated from EPA and DHA as a result of a transcellular biosynthetic route during cell-cell interactions. It is necessary to highlight that, under physiological conditions; the increase in consumption of fish oil (EPA and DHA) do not automatically implies an augmentation of resolvins levels. In non-injured tissues, the expression levels of the biosynthetic enzymes are low and they strongly increase by acute inflammation (295). These lipid-derived mediators together with lipoxins, LXA_4 and e-LXA_4, which are a AA-derived modulators, regulate different processes involved in resolution, such as neutrophil recruitment, dendritic cell migration, decrease in leukocyte infiltration, activation of phagocytosis in macrophages, reduction in the number T helper cells, blocking of TLR-mediated activation of macrophages, modulation of the cytokines production (as reduction of TNF-α in microglia) and chemokines, etc (236, 295-299).

The electrophysiological properties of macrophages depend on their state of functional activation. In fact, LPS activation mimics the TNF-α effects and high levels of TNF-α released are indicative of macrophage activation (91). Changes in the membrane potential are one of the first events on the activation process of macrophages (92, 94, 234). During the activation processes, different ion channels are involved.

First, we studied how pro-resolution lipid-derived mediators could affect the K_V currents (generated by the activation of $K_V1.3$/$K_V1.5$) in resting and LPS-activated BMDM. Potassium channels play a pivotal role in the maintenance of Ca^{2+} electrochemical gradient necessary to allow specific Ca^{2+} entry and macrophages activation (300). Previous reports show that RAW264.7 and BMDM activated with LPS macrophages present an increase in functional $K_V1.3$ channels, whereas non-stimulated RAW264.7 or BMDM macrophages do not (94, 234). It is described that $K_V1.5$ and $K_V1.3$ expression depend on the type of activation and that change between activation and immunosuppression.

Incubation of BMDM with e-LXA_4 and LXA_4, but not with RvD1, partially reverses the LPS-activation on BMDM. Incubation with e-LXA_4 decreased the amplitude, the use-dependent decay of the current at fast stimulation frequencies and the C-type inactivation of the K_V current. These results suggest that e-LXA_4 and LXA_4 are active pro-resolution mediators. Their effects are partially mediated by the $K_V1.3$ activity, since the function of $K_V1.3$ is required for the attenuation of NF-kB activity, because the e-LXA_4 effects on IKK activity and NOS-2 expression were partially reverted after selectively blocking $K_V1.3$ channels (234).

In the resolution phase, it is necessary to avoid the production of TNF-α because its effects are pro-immflamatory (295). Our hypothesis was that RvD1, as observed with e-LXA_4 and LXA_4, can reverse the activation induced by LPS, being this reversion reflected in a decrease of the $K_V1.3$ current. Duffield and colleagues reported that BMDM treated with LPS and simultaneously with RvD1 or PD1, are limited in TNF-α generation, which is the response to cell activation. They analyzed the TNF-α release ability of LPS-activated macrophages. LPS-activated BMDM were incubated with different concentrations of DHA, RvD1 and PD1. RvD1 and PD1 exhibited a markedly concentration-dependent decrease of LPS-induced TNF-α release, suggesting that both have pro-resolution activities in macrophages. Because LPS acts through TLR4 (and, to a lesser extent, through TLR2) they suggest that these compounds block TLR-mediated activation of macrophages (236). However, in our experiments, RvD1 did not reverse the $K_V1.3$ current elicited by LPS activation. This result can be due to several factors: i) RvD1 resolve the inflammatory process through a signaling cascade that do not involve K_V channels, or ii) the concentrations and the time of incubation needed exceed those used in the present study.

In order to elucidate if the effects observed are related to K_V channels, we also analyzed the acute effects of e-LXA_4 and also with RvD1. We observed that in acute perfusion, e-LXA_4 diminished the currents elicited by LPS-activated macrophages, whereas they did not affect resting macrophages. RvD1 did not modify the magnitude of the currents after acute exposition on either resting or LPS-activated macrophages. The increase in K_V current induced by LPS appeared concomitantly with its use-dependent decay and its increase in the C-type inactivation, characteristics of $K_V1.3$ (234). Under these conditions, e-LXA_4 decreased the magnitude of K_V current in LPS-stimulated BMDM but did not modify the use-dependent decrease or the C-type inactivation. These results suggest that there is no direct interaction between e-LXA and $K_V1.3$ channels. However, to ensure that the effects of e-LXA on $K_V1.3$ and $K_V1.5$ channels expressed in HEK293 cells were analyzed. No effects on any channel were observed at any concentration tested, suggesting that e-LXA_4 actions are a consequence of some effects on a signaling pathway present in macrophages but not in HEK293 cells. Our laboratory has described that the effects observed by e-LXA_4 on K_V

channels is dependent, at least in part, on ALX receptor (234). Resolvin actions are mediated by specific GPCRs (ChemR23 and GPR32, among others). Interestingly, both lipoxins and resolvins share a common receptor (ALX) (236, 301). The lack of effects of RvD1 on K_V currents can be explained if these compounds act as pro-resolving via other mechanisms

5.2.3 LXA_4 and RvD1 in K_V7.1/KCNE1 channels

In this part of the present Doctoral Thesis we studied the effects produced by LXA_4 and RvD1 on K_V7.1/KCNE1 channels expressed in COS-7 cells. We demonstrated that: i) LXA_4 decreased K_V7.1/KCNE1 current in a concentration-dependent manner, and ii) RvD1 inhibits this current, being much more potent than LXA_4.

The LXA_4 and RvD1 inhibit K_V7.1/KCNE1 current. However, LXA_4 and RvD1 effects did not modify the voltage-dependence of the K_V7.1/KCNE1 channels or the activation kinetics. Moreover, the blocking effects were almost completely washed-out when cells expressing K_V7.1/KCNE1 channels were perfused with eicosanoid-free external solution. These results suggest a direct effect between both pro-resolving compounds and K_V7.1/KCNE1 channels. In addition, as described above, LXA_4 and RvD1 activates GPR32 and ALX receptors. There is no evidence described before of the expression of these receptors in COS-7 cells. However, there are needed more experimental evidences to rule out the possibility of an indirect effect. It has been described that RvD1 produce an analgesic role. Its ability to inhibit TRP channels such as TRPA1, TRPV3 and TRPV4, has been related with the potency as analgesic attributed to RvD1 (297). Moreover, it has been shown that PUFAs or cholesterol precursors directly activate or potentiate TRPV3 channels (302). In addition, arachidonic acid is able to activate TRPV4 channels (303). Interestingly, we observed the same effects: PUFAs activate K_V7.1/KCNE1 channels and the lipid-derived compounds, LXA_4 and RvD1, inhibit K_V7.1/KCNE1 currents. Moreover, Bang and colleagues found that RvD1 blocks TRPA1, TRPV3 and TRPV4 expressed in HEK293 cells, and they suggest that RvD1 inhibits TRP currents without activating metabotropic receptor signaling (297). Although TRPs are Na^+ and Ca^{2+} channels and that their physiological implications are completely different. However, the molecular mechanism of activation or block performed by PUFAs and its derivatives can be similar.

Several evidences demonstrate that anti-inflammatory and pro-resolution mechanisms differ for control inflammation. Many of the anti-inflammatory therapeutics act by inhibiting COX-2, disrupting the endogenous pro-resolution mechanism (295). Moreover, because COX-2 is constitutively expressed in the nervous system and in the vasculature, many other processes could be indirectly altered by these anti-inflammatory compounds (238, 304). Importantly, there is evidence that aspirin, statins and pioglitazone trigger the synthesis of 15-epi-lipoxin $(LXA)_4$ in the myocardium (238, 305). An increase in the levels of these eicosanoids in the heart may produce a decrease in the I_{Ks} that may have clinical relevance.

AA and DHA are widely related with the role of preventing arrhythmias, during ischemia and reperfusion and by the sum of its effects on voltage gated channels on cardiac action potential, respectively (195, 212, 306). Furthermore, resolvins are proposed as a new class of analgesic agents, which can block abnormal pain without losing sensitivity (295). Also, COX-2 inhibitors were linked with cardiovascular risks (307).

The further investigation of PUFAs and PUFAs-derived modulators, as resolvins and lipoxins, and their targets, as potassium voltage-gated ion channels, may serve for the design of effective therapeutics not only in cardiovascular disease but also in other main prevalent disease as cancer and Alzheimer´s disease.

6. CONCLUSIONS

1. $K_V7.1$ and $K_V7.5$ subunits interact forming functional channels. $K_V7.1/K_V7.5$ heteromeric channels exhibit their own electrophysiological and pharmacological properties. They can be regulated by KCNE1 and KCNE3. Like $K_V7.5$, and opposite to $K_V7.1$ channels, $K_V7.1/K_V7.5$ heteromeric channels do not target lipid rafts. Because the lipid raft localization of ion channels is crucial for cardiovascular physiology, $K_V7.1/K_V7.5$ heteromeric channels provide efficient spatial and temporal regulation of vascular smooth muscle function. Moreover, $K_V7.1/K_V7.5$ heteromeric channels increase the diversity of structures that fine-tune blood vessels reactivity.

2. The effects of n-3 and n-6 PUFAs on the $K_V7.1$/KCNE1 current are dependent on the presence of KCNE1. These effects differ depending on the structure of the PUFA and on the time of exposure of the cells to these fatty acids. DHA and AA increase $K_V7.1$/KCNE1 current magnitude when acutely applied. However, after long term incubation of cells expressing $K_V7.1$/KCNE1, the magnitude of the current was not modified, although the kinetics and voltage-dependent characteristics were changed. DHA decreases the expression of $K_V7.1$ by increasing its degradation via proteasome. Also, the modulation of $K_V7.1$/KCNE1 channels after chronic incubation with DHA seems to be mainly due to a delocalization of $K_V7.1$ channels from lipid rafts.

3. In macrophages, long-term exposure to e-LXA_4, but not to RvD1, reversed the electrophysiological changes induced by LPS. The effects induced by e-LXA_4 were not due to a direct interaction with $K_V1.3$ or $K_V1.5$ channels.

4. LXA_4 and RvD1 inhibit $K_V7.1$/KCNE1 current, RvD1 being more potent. KCNE1 potentiates the RvD1 induced effects on $K_V7.1$. LXA_4 and RvD1 did not modify neither the voltage-dependence nor the activation of the channel and these effects were completely reversible after washed out.

1. Las subunidades $K_V7.1$ y $K_V7.5$ interaccionan formando canales heteroméricos $K_V7.1/K_V7.5$ funcionales, con un fenotipo electrofisiológico y farmacológico intermedio. Además, éstos pueden ser regulados por las subunidades accesorias KCNE1 y KCNE3. De igual manera que los canales $K_V7.5$ y, a diferencia de los $K_V7.1$, los canales $K_V7.1/K_V7.5$ se localizan fuera de las balsas lipídicas, cambiando así, la regulación de los canales en aquellos tejidos donde ambos se expresan. Los canales $K_V7.1/K_V7.5$ están involucrados en la regulación de la reactividad del músculo liso vascular, aumentando la diversidad de mecanismos implicados en esta función.
2. Los ácidos grasos poliinsaturados omega-3 y omega-6 producen efectos diferentes sobre los canales $K_V7.1$/KCNE1, ambos dependen de la subunidad reguladora KCNE1 para ejercer dichos efectos. El modo de aplicación, perfusión aguda o incubación de 48 horas, también determina el efecto observado en los canales $K_V7.1$/KCNE1. La incubación con DHA produjo una expresión a la baja de los canales, promovida por un aumento en la degradación de los canales $K_V7.1$ vía proteosoma. Además, la incubación con DHA promueve la deslocalización de los canales $K_V7.1$/KCNE1 de las balsas lipídicas.
3. La incubación de macrófagos con e-LXA_4, pero no con RvD1, revirtió los cambios electrofisiológicos promovidos por la activación de macrófagos con LPS. Los efectos producidos por e-LXA_4 no se debieron a un efecto directo sobre los canales $K_V1.3$ ó $K_V1.5$.
4. Tanto LXA_4 como RvD1 bloquearon los canales $K_V7.1$/KCNE1. Sin embargo, la potencia de RvD1 para bloquear estos canales fue mucho mayor que la de LXA_4. La presencia de la subunidad reguladora KCNE1 aumenta del efecto producido por RvD1 sobre los canales $K_V7.1$. Estos compuestos no modificaron ni la activación ni la dependencia de voltaje de los canales $K_V7.1$/KCNE1 y además, los efectos producidos por estos compuestos eran revertidos tras la perfusión de las células con solución externa carente de LXA_4 ó RvD1.

REFERENCES

1. Armstrong, C.M., Hille, B. (1998) Voltage-gated ion channels and electrical excitability. **Neuron** 20:371-380.

2. Hille, B., Armstrong, C.M., MacKinnon, R. (1999) Ion channels: from idea to reality. **Nat. Med.** 5:1105-1109.

3. Hodgkin, A.L., Katz, B. (1949) The effect of sodium ions on the electrical activity of the giant axon of the squid. **J. Physiol. (Lond)** 108:37-77.

4. Hodgkin, A.L., Huxley, A.F. (1952) A quantitative description of membrane current and its application to conduction and excitation in nerve. **J. Physiol. (Lond)** 117:500-544.

5. Katz, B., Miledi, R. (1970) Membrane noise produced by acetylcholine. **Nature** 226:962-963.

6. Sakmann B, Neher E. Single Channel Recording. New York, NY: Plenum Publishing Co., 1983.

7. Doyle, D.A., Cabral, J.M., Pfuetzner, R.A., Kuo, A., Gulbis, J.M., Cohen, S.L., Chait, B.T., MacKinnon, R. (1998) The structure of the potassium channel: molecular basis of K^+ conduction and selectivity. **Science** 280:69-77.

8. Agre, P., King, L.S., Yasui, M., Guggino, W.B., Ottersen, O.P., Fujiyoshi, Y., Engel, A., Nielsen, S. (2002) Aquaporin water channels--from atomic structure to clinical medicine. **J Physiol** 542:3-16.

9. Stott, J.B., Jepps, T.A., Greenwood, I.A. (2014) K(V)7 potassium channels: a new therapeutic target in smooth muscle disorders. **Drug Discov. Today** 19:413-424.

10. Korovkina, V.P., England, S.K. (2002) Molecular diversity of vascular potassium channel isoforms. **Clin. Exp. Pharmacol. Physiol** 29:317-323.

11. Noda, M., Ikeda, T., Suzuki, H., Takeshima, H., Takahashi, T., Kuno, M., Numa, S. (1986) Expression of functional sodium channels from cloned cDNA. **Nature** 322:826-828.

12. Tanabe, T., Takeshima, H., Mikami, A., Flockerzi, V., Takahashi, H., Kangawa, K., Kojima, M., Matsuo, H., Hirose, T., Numa, S. (1987) Primary structure of the receptor for calcium channel blockers from skeletal muscle. **Nature** 328:313-318.

13. Goulding, E.H., Ngai, J., Kramer, R.H., Colicos, S., Axel, R., Siegelbaum, S.A., Chess, A. (1992) Molecular cloning and single-channel properties of the cyclic nucleotide-gated channel from catfish olfactory neurons. **Neuron** 8:45-58.

14. Santoro, B., Liu, D.T., Yao, H., Bartsch, D., Kandel, E.R., Siegelbaum, S.A., Tibbs, G.R. (1998) Identification of a gene encoding a hyperpolarization-activated pacemaker channel of brain. **Cell** 93:717-729.

15. Kubo, Y., Baldwin, T.J., Jan, Y.N., Jan, L.Y. (1993) Primary structure and functional expression of a mouse inward rectifier potassium channel. **Nature** 362:127-133.

16. Kubo, Y., Reuveny, E., Slesinger, P.A., Jan, Y.N., Jan, L.Y. (1993) Primary structure and functional expression of a rat G-protein-coupled muscarinic potassium channel. **Nature** 364:802-806.

17. Ketchum, K.A., Joiner, W.J., Sellers, A.J., Kaczmarek, L.K., Goldstein, S.A. (1995) A new family of outwardly rectifying potassium channel proteins with two pore domains in tandem. **Nature** 376:690-695.

18. Goldstein, S.A., Wang, K.W., Ilan, N., Pausch, M.H. (1998) Sequence and function of the two P domain potassium channels: implications of an emerging superfamily. **J. Mol. Med.** 76:13-20.

19. Chen, G.Q., Cui, C., Mayer, M.L., Gouaux, E. (1999) Functional characterization of a potassium-selective prokaryotic glutamate receptor. **Nature** 402:817-821.

20. Yu, F.H., Yarov-Yarovoy, V., Gutman, G.A., Catterall, W.A. (2005) Overview of molecular relationships in the voltage-gated ion channel superfamily. **Pharmacol. Rev.** 57:387-395.

21. Hille B. Ionic channels of excitable membranes. Sunderland, Mass.: Sinauer Associates, 1992.

22. Coetzee, W.A., Amarillo, Y., Chiu, J., Chow, A., Lau, D., McCormack, T., Moreno, H., Nadal, M.S., Ozaita, A., Pountney, D., Saganich, M., Vega Saenz de Miera, E., Rudy, B. (1999) Molecular diversity of K+ channels. **Ann. N. Y. Acad. Sci.** 868:233-285.

23. Swartz, K.J. (2004) Towards a structural view of gating in potassium channels. **Nat. Rev. Neurosci.** 5:905-916.

24. Ashcroft, F.M. (2006) From molecule to malady. **Nature** 440:440-447.

25. Bezanilla, F. (2008) How membrane proteins sense voltage. **Nat. Rev. Mol. Cell Biol.** 9:323-332.

26. Zaydman, M.A., Cui, J. (2014) PIP2 regulation of KCNQ channels: biophysical and molecular mechanisms for lipid modulation of voltage-dependent gating. **Front Physiol** 5:195.

27. Loussouarn, G., Park, K.H., Bellocq, C., Baro, I., Charpentier, F., Escande, D. (2003) Phosphatidylinositol-4,5-bisphosphate, PIP2, controls KCNQ1/KCNE1 voltage-gated potassium channels: a functional homology between voltage-gated and inward rectifier K+ channels. **EMBO J** 22:5412-5421.

28. Zhang, H., Craciun, L.C., Mirshahi, T., Rohacs, T., Lopes, C.M., Jin, T., Logothetis, D.E. (2003) PIP(2) activates KCNQ channels, and its hydrolysis underlies receptor-mediated inhibition of M currents. **Neuron** 37:963-975.

29. Rodriguez-Menchaca, A.A., Adney, S.K., Tang, Q.Y., Meng, X.Y., Rosenhouse-Dantsker, A., Cui, M., Logothetis, D.E. (2012) PIP2 controls voltage-sensor movement and pore opening of Kv channels through the S4-S5 linker. **Proc. Natl. Acad. Sci. U. S. A** 109:E2399-E2408.

30. Wulff, H., Castle, N.A., Pardo, L.A. (2009) Voltage-gated potassium channels as therapeutic targets. **Nat. Rev. Drug Discov.** 8:982-1001.

31. Cox, R.H. (2005) Molecular determinants of voltage-gated potassium currents in vascular smooth muscle. **Cell Biochem. Biophys.** 42:167-195.

32. Bocksteins, E., Snyders, D.J. (2012) Electrically silent Kv subunits: their molecular and functional characteristics. **Physiology. (Bethesda.)** 27:73-84.

33. Ottschytsch, N., Raes, A., Van Hoorick, D., Snyders, D.J. (2002) Obligatory heterotetramerization of three previously uncharacterized Kv channel alpha-subunits identified in the human genome. **Proc. Natl. Acad. Sci. U. S. A** 99:7986-7991.

34. Warmke, J.W., Ganetzky, B. (1994) A family of potassium channel genes related to eag in Drosophila and mammals. **Proc. Natl. Acad. Sci. U. S. A.** 91:3438-3442.

35. Minor, D.L., Jr. (2001) Potassium channels: life in the post-structural world. **Curr. Opin. Struct. Biol.** 11:408-414.

36. Varshney, A., Mathew, M.K. (2003) A tale of two tails: cytosolic termini and K(+) channel function. **Prog. Biophys. Mol. Biol.** 83:153-170.

37. Roosild, T.P., Le, K.T., Choe, S. (2004) Cytoplasmic gatekeepers of K+-channel flux: a structural perspective. **Trends Biochem. Sci.** 29:39-45.

38. Barros, F., Dominguez, P., de la Pena, P. (2012) Cytoplasmic domains and voltage-dependent potassium channel gating. **Front Pharmacol.** 3:49.

39. Miranda, P., Manso, D.G., Barros, F., Carretero, L., Hughes, T.E., Alonso-Ron, C., Dominguez, P., de la Pena, P. (2008) FRET with multiply labeled HERG K(+) channels as a reporter of the in vivo coarse architecture of the cytoplasmic domains. **Biochim. Biophys. Acta** 1783:1681-1699.

40. Zhou, Y., Morais-Cabral, J.H., Kaufman, A., MacKinnon, R. (2001) Chemistry of ion coordination and hydration revealed by a K+ channel-Fab complex at 2.0 A resolution. **Nature** 414:43-48.

41. MacKinnon, R. (2003) Potassium channels. **FEBS Lett.** 555:62-65.

42. Long, S.B., Campbell, E.B., MacKinnon, R. (2005) Voltage sensor of Kv1.2: structural basis of electromechanical coupling. **Science** 309:903-908.

43. Roux, B., MacKinnon, R. (1999) The cavity and pore helices in the KcsA K+ channel: electrostatic stabilization of monovalent cations [see comments]. **Science** 285:100-102.

44. del Camino, D., Holmgren, M., Liu, Y., Yellen, G. (2000) Blocker protection in the pore of a voltage-gated K+ channel and its structural implications. **Nature** 403:321-325.

45. Seoh, S.A., Sigg, D., Papazian, D.M., Bezanilla, F. (1996) Voltage-sensing residues in the S2 and S4 segments of the *Shaker* K^+ channel. **Neuron** 16:1159-1167.

46. Papazian, D.M., Shao, X.M., Seoh, S.A., Mock, A.F., Huang, Y., Wainstock, D.H. (1995) Electrostatic interactions of S4 voltage sensor in Shaker K^+ channel. **Neuron** 14:1293-1301.

47. Planells Cases, R., Ferrer Montiel, A.V., Patten, C.D., Montal, M. (1995) Mutation of conserved negatively charged residues in the S2 and S3 transmembrane segments of a mammalian K+ channel selectively modulates channel gating. **Proc. Natl. Acad. Sci. U. S. A.** 92:9422-9426.

48. Schoppa, N.E., McCormack, K., Tanouye, M.A., Sigworth, F.J. (1992) The size of the gating charge in wild type and mutant *Shaker* Potassium channels. **Science** 255:1712-1715.

49. Yellen, G. (1998) Premonitions of ion channel gating [comment]. **Nat. Struct. Biol.** 5:421.

50. Bezanilla, F., Stefani, E. (1998) Gating currents. **Methods Enzymol.** 293:331-352.

51. Mannuzzu, L.M., Moronne, M.M., Isacoff, E.Y. (1996) Direct physical measure of conformational rearrangement underlying potassium channel gating. **Science** 271:213-216.

52. Cha, A., Bezanilla, F. (1997) Characterizing voltage-dependent conformational changes in the *Shaker* K^+ channel with fluorescence. **Neuron** 19:1127-1140.

53. Priest, M., Bezanilla, F. (2015) Functional Site-Directed Fluorometry. **Adv. Exp. Med. Biol.** 869:55-76.

54. Jiang, Y., Lee, A., Chen, J., Ruta, V., Cadene, M., Chait, B.T., MacKinnon, R. (2003) X-ray structure of a voltage-dependent K+ channel. **Nature** 423:33-41.

55. Zhou, M., Morais-Cabral, J.H., Mann, S., MacKinnon, R. (2001) Potassium channel receptor site for the inactivation gate and quaternary amine inhibitors. **Nature** 411:657-661.

56. Kuo, A., Gulbis, J.M., Antcliff, J.F., Rahman, T., Lowe, E.D., Zimmer, J., Cuthbertson, J., Ashcroft, F.M., Ezaki, T., Doyle, D.A. (2003) Crystal structure of the potassium channel KirBac1.1 in the closed state. **Science** 300:1922-1926.

57. Liu, Y., Holmgren, M., Jurman, M.E., Yellen, G. (1997) Gated access to the pore of a voltage-dependent K^+ channel. **Neuron** 19:175-184.

58. Webster, S.M., del Camino, D., Dekker, J.P., Yellen, G. (2004) Intracellular gate opening in Shaker K+ channels defined by high-affinity metal bridges. **Nature** 428:864-868.

59. Long, S.B., Campbell, E.B., MacKinnon, R. (2005) Crystal structure of a mammalian voltage-dependent Shaker family K+ channel. **Science** 309:897-903.

60. Isacoff, E.Y., Jan, Y.N., Jan, L.Y. (1991) Putative receptor for the cytoplasmic inactivation gate in the *Shaker* K^+ channel. **Nature** 353:86-90.

61. McCormack, K., Tanouye, M.A., Iverson, L.E., Lin, J.W., Ramaswami, M., McCormack, T., Campanelli, J.T., Mathew, M.K., Rudy, B. (1991) A role for hydrophobic residues in the voltage-dependent gating of Shaker K^+ channels. **Proc. Natl. Acad. Sci. U. S. A.** 88:2931-2935.

62. Lu, Z., Klem, A.M., Ramu, Y. (2002) Coupling between voltage sensors and activation gate in voltage-gated K+ channels. **J Gen. Physiol** 120:663-676.

63. Martinez-Marmol, R., Perez-Verdaguer, M., Roig, S.R., Vallejo-Gracia, A., Gotsi, P., Serrano-Albarras, A., Bahamonde, M.I., Ferrer-Montiel, A., Fernandez-Ballester, G., Comes, N., Felipe, A. (2013) A non-canonical di-acidic signal at the C-terminus of Kv1.3 determines anterograde trafficking and surface expression. **J Cell Sci.** 126:5681-5691.

64. Nguyen, H.M., Miyazaki, H., Hoshi, N., Smith, B.J., Nukina, N., Goldin, A.L., Chandy, K.G. (2012) Modulation of voltage-gated K+ channels by the sodium channel beta1 subunit. **Proc. Natl. Acad. Sci. U. S. A** 109:18577-18582.

65. Comes, N., Bielanska, J., Vallejo-Gracia, A., Serrano-Albarras, A., Marruecos, L., Gomez, D., Soler, C., Condom, E., Ramon, Y.C., Hernandez-Losa, J., Ferreres, J.C., Felipe, A. (2013) The voltage-dependent K(+) channels Kv1.3 and Kv1.5 in human cancer. **Front Physiol** 4:283.

66. Martinez-Marmol, R., Styrczewska, K., Perez-Verdaguer, M., Vallejo-Gracia, A., Comes, N., Sorkin, A., Felipe, A. (2017) Ubiquitination mediates Kv1.3 endocytosis as a mechanism for protein kinase C-dependent modulation. **Sci. Rep.** 7:42395.

67. Zhu, J., Yan, J., Thornhill, W.B. (2014) The Kv1.3 potassium channel is localized to the cis-Golgi and Kv1.6 is localized to the endoplasmic reticulum in rat astrocytes. **FEBS J** 281:3433-3445.

68. Jang, S.H., Byun, J.K., Jeon, W.I., Choi, S.Y., Park, J., Lee, B.H., Yang, J.E., Park, J.B., O'Grady, S.M., Kim, D.Y., Ryu, P.D., Joo, S.W., Lee, S.Y. (2015) Nuclear localization and functional characteristics of voltage-gated potassium channel Kv1.3. **J Biol. Chem.** 290:12547-12557.

69. Panyi, G., Vamosi, G., Bacso, Z., Bagdany, M., Bodnar, A., Varga, Z., Gaspar, R., Matyus, L., Damjanovich, S. (2004) Kv1.3 potassium channels are localized in the immunological synapse formed between cytotoxic and target cells. **Proc. Natl. Acad. Sci. U. S. A** 101:1285-1290.

70. Villalonga, N., Escalada, A., Vicente, R., Sanchez-Tillo, E., Celada, A., Solsona, C., Felipe, A. (2007) Kv1.3/Kv1.5 heteromeric channels compromise pharmacological responses in macrophages. **Biochem. Biophys. Res. Comm.** 352:913-918.

71. Perez-Verdaguer, M., Capera, J., Martinez-Marmol, R., Camps, M., Comes, N., Tamkun, M.M., Felipe, A. (2016) Caveolin interaction governs Kv1.3 lipid raft targeting. **Sci. Rep.** 6:22453.

72. Grunnet, M., Rasmussen, H.B., Hay-Schmidt, A., Klaerke, D.A. (2003) The voltage-gated potassium channel subunit, Kv1.3, is expressed in epithelia. **Biochim. Biophys. Acta** 1616:85-94.

73. Tian, Y., Yue, X., Luo, D., Wazir, R., Wang, J., Wu, T., Chen, L., Liao, B., Wang, K. (2013) Increased proliferation of human bladder smooth muscle cells is mediated by physiological cyclic stretch via the PI3KSGK1Kv1.3 pathway. **Mol. Med. Rep.** 8:294-298.

74. Jacob, A., Hurley, I.R., Goodwin, L.O., Cooper, G.W., Benoff, S. (2000) Molecular characterization of a voltage-gated potassium channel expressed in rat testis. **Mol. Hum. Reprod.** 6:303-313.

75. Biju, K.C., Marks, D.R., Mast, T.G., Fadool, D.A. (2008) Deletion of voltage-gated channel affects glomerular refinement and odorant receptor expression in the mouse olfactory system. **J Comp Neurol.** 506:161-179.

76. Li, Y., Wang, P., Xu, J., Desir, G.V. (2006) Voltage-gated potassium channel Kv1.3 regulates GLUT4 trafficking to the plasma membrane via a Ca2+-dependent mechanism. **Am. J Physiol Cell Physiol** 290:C345-C351.

77. Xu, J., Wang, P., Li, Y., Li, G., Kaczmarek, L.K., Wu, Y., Koni, P.A., Flavell, R.A., Desir, G.V. (2004) The voltage-gated potassium channel Kv1.3 regulates peripheral insulin sensitivity. **Proc. Natl. Acad. Sci. U. S. A** 101:3112-3117.

78. Upadhyay, S.K., Eckel-Mahan, K.L., Mirbolooki, M.R., Tjong, I., Griffey, S.M., Schmunk, G., Koehne, A., Halbout, B., Iadonato, S., Pedersen, B., Borrelli, E., Wang, P.H., Mukherjee, J., Sassone-Corsi, P., Chandy, K.G. (2013) Selective Kv1.3 channel blocker as therapeutic for obesity and insulin resistance. **Proc. Natl. Acad. Sci. U. S. A** 110:E2239-E2248.

79. Tamkun, M.M., Knoth, K.M., Walbridge, J.A., Kroemer, H., Roden, D.M., Glover, D.M. (1991) Molecular cloning and characterization of two voltage-gated K+ channel cDNAs from human ventricle. **FASEB J** 5:331-337.

80. Li, G.R., Feng, J., Yue, L., Carrier, M., Nattel, S. (1996) Evidence for two components of delayed rectifier K^+ current in human ventricular myocytes. **Circ. Res.** 78:689-696.

81. Schmitt, N., Grunnet, M., Olesen, S.P. (2014) Cardiac potassium channel subtypes: new roles in repolarization and arrhythmia. **Physiol Rev.** 94:609-653.

82. Van Wagoner, D.R., Pond, A.L., McCarthy, P.M., Trimmer, J.S., Nerbonne, J.M. (1997) Outward K+ current densities and Kv1.5 expression are reduced in chronic human atrial fibrillation. **Circ. Res.** 80:772-781.

83. Wang, Z., Fermini, B., Nattel, S. (1993) Sustained depolarization-induced outward current in human atrial myocytes. Evidence for a novel delayed rectifier K^+ current similar to Kv1.5 cloned channel currents. **Circ. Res.** 73:1061-1076.

84. Snyders, D.J., Tamkun, M.M., Bennett, P.B. (1993) A rapidly activating and slowly inactivating potassium channel cloned from human heart. Functional analysis after stable mammalian cell culture expression. **J. Gen. Physiol.** 101:513-543.

85. Fedida, D. (1993) Modulation of cardiac contractility by alpha 1 adrenoceptors. **Cardiovasc. Res.** 27:1735-1742.

86. Tamargo, J., Caballero, R., Gomez, R., Valenzuela, C., Delpon, E. (2004) Pharmacology of cardiac potassium channels. **Cardiovasc. Res.** 62:9-33.

87. Caballero, R., Gomez, R., Moreno, I., Nunez, L., Gonzalez, T., Arias, C., Guizy, M., Valenzuela, C., Tamargo, J., Delpon, E. (2004) Interaction of angiotensin II with the angiotensin type 2 receptor inhibits the cardiac transient outward potassium current. **Cardiovasc. Res.** 62:86-95.

88. Villalonga, N., Martinez-Marmol, R., Roura-Ferrer, M., David, M., Valenzuela, C., Soler, C., Felipe, A. (2008) Cell cycle-dependent expression of Kv1.5 is involved in myoblast proliferation. **Biochim. Biophys Acta** 1783:728-736.

89. Mullen, K.M., Rozycka, M., Rus, H., Hu, L., Cudrici, C., Zafranskaia, E., Pennington, M.W., Johns, D.C., Judge, S.I., Calabresi, P.A. (2006) Potassium channels Kv1.3 and Kv1.5 are expressed on blood-derived dendritic cells in the central nervous system. **Ann. Neurol.** 60:118-127.

90. Gordon, S., Martinez, F.O. (2010) Alternative activation of macrophages: mechanism and functions. **Immunity.** 32:593-604.

91. Vicente, R., Escalada, A., Coma, M., Fuster, G., Sanchez-Tillo, E., Lopez-Iglesias, C., Soler, C., Solsona, C., Celada, A., Felipe, A. (2003) Differential voltage-dependent K+ channel responses during proliferation and activation in macrophages. **J Biol. Chem** 278:46307-46320.

92. Cahalan, M.D., Chandy, K.G. (1997) Ion channels in the immune system as targets for immunosuppression. **Curr. Opin. Biotechnol.** 8:749-756.

93. Panyi, G., Vamosi, G., Bodnar, A., Gaspar, R., Damjanovich, S. (2004) Looking through ion channels: recharged concepts in T-cell signaling. **Trends Immunol.** 25:565-569.

94. Villalonga, N., David, M., Bielanska, J., Vicente, R., Comes, N., Valenzuela, C., Felipe, A. (2010) Immunomodulation of voltage-dependent K+ channels in macrophages: molecular and biophysical consequences. **J. Gen. Physiol** 135:135-147.

95. Berridge, M.J., Lipp, P., Bootman, M.D. (2000) The versatility and universality of calcium signalling. **Nat. Rev. Mol. Cell Biol.** 1:11-21.

96. Cahalan, M.D., Chandy, K.G. (2009) The functional network of ion channels in T lymphocytes. **Immunol. Rev.** 231:59-87.

97. Feske, S., Gwack, Y., Prakriya, M., Srikanth, S., Puppel, S.H., Tanasa, B., Hogan, P.G., Lewis, R.S., Daly, M., Rao, A. (2006) A mutation in Orai1 causes immune deficiency by abrogating CRAC channel function. **Nature** 441:179-185.

98. Prakriya, M., Feske, S., Gwack, Y., Srikanth, S., Rao, A., Hogan, P.G. (2006) Orai1 is an essential pore subunit of the CRAC channel. **Nature** 443:230-233.

99. Vig, M., Peinelt, C., Beck, A., Koomoa, D.L., Rabah, D., Koblan-Huberson, M., Kraft, S., Turner, H., Fleig, A., Penner, R., Kinet, J.P. (2006) CRACM1 is a plasma membrane protein essential for store-operated Ca2+ entry. **Science** 312:1220-1223.

100. Yeromin, A.V., Zhang, S.L., Jiang, W., Yu, Y., Safrina, O., Cahalan, M.D. (2006) Molecular identification of the CRAC channel by altered ion selectivity in a mutant of Orai. **Nature** 443:226-229.

101. Holmgren, M., Shin, K.S., Yellen, G. (1998) The activation gate of a voltage-gated K+ channel can be trapped in the open state by an intersubunit metal bridge. **Neuron** 21:617-621.

102. Attali, B., Romey, G., Honoré, E., Schmid-Alliana, A., Mattei, M.G., Lesage, F., Ricard, P., Barhanin, J., Lazdunski, M. (1992) Cloning, functional expression, and regulation of two K^+ channels in human T lymphocytes. **J. Biol. Chem.** 267:8650-8657.

103. Weber, C., Noels, H. (2011) Atherosclerosis: current pathogenesis and therapeutic options. **Nat. Med.** 17:1410-1422.

104. Sobirin, M.A., Kinugawa, S., Takahashi, M., Fukushima, A., Homma, T., Ono, T., Hirabayashi, K., Suga, T., Azalia, P., Takada, S., Taniguchi, M., Nakayama, T., Ishimori, N., Iwabuchi, K., Tsutsui, H. (2012) Activation of natural killer T cells ameliorates postinfarct cardiac remodeling and failure in mice. **Circ. Res.** 111:1037-1047.

105. Choo, E.H., Lee, J.H., Park, E.H., Park, H.E., Jung, N.C., Kim, T.H., Koh, Y.S., Kim, E., Seung, K.B., Park, C., Hong, K.S., Kang, K., Song, J.Y., Seo, H.G., Lim, D.S., Chang, K. (2017) Infarcted Myocardium-Primed Dendritic Cells Improve Remodeling and Cardiac Function After Myocardial Infarction by Modulating the Regulatory T Cell and Macrophage Polarization. **Circulation** 135:1444-1457.

106. Horckmans, M., Ring, L., Duchene, J., Santovito, D., Schloss, M.J., Drechsler, M., Weber, C., Soehnlein, O., Steffens, S. (2017) Neutrophils orchestrate post-myocardial infarction healing by polarizing macrophages towards a reparative phenotype. **Eur. Heart J** 38:187-197.

107. Soldovieri, M.V., Miceli, F., Taglialatela, M. (2011) Driving with no brakes: molecular pathophysiology of Kv7 potassium channels. **Physiology. (Bethesda.)** 26:365-376.

108. Brown, D.A., Passmore, G.M. (2009) Neural KCNQ (Kv7) channels. **Br. J Pharmacol.** 156:1185-1195.

109. Schenzer, A., Friedrich, T., Pusch, M., Saftig, P., Jentsch, T.J., Grotzinger, J., Schwake, M. (2005) Molecular determinants of KCNQ (Kv7) K+ channel sensitivity to the anticonvulsant retigabine. **J Neurosci.** 25:5051-5060.

110. Jentsch, T.J. (2000) Neuronal KCNQ potassium channels: physiology and role in disease. **Nat. Rev. Neurosci.** 1:21-30.

111. Yeung, S.Y., Pucovsky, V., Moffatt, J.D., Saldanha, L., Schwake, M., Ohya, S., Greenwood, I.A. (2007) Molecular expression and pharmacological identification of a role for K(v)7 channels in murine vascular reactivity. **Br. J Pharmacol.** 151:758-770.

112. Wang, Q., Curran, M.E., Splawski, I., Burn, T.C., Millholland, J.M., VanRaay, T.J., Shen, J., Timothy, K.W., Vincent, G.M., De Jager, T., Schwartz, P.J., Toubin, J.A., Moss, A.J., Atkinson, D.L., Landes, G.M., Connors, T.D., Keating, M.T. (1996) Positional cloning of a novel potassium channel gene: KVLQT1 mutations cause cardiac arrhythmias. **Nat. Genet.** 12:17-23.

113. Neyroud, N., Tesson, F., Denjoy, I., Leibovici, M., Donger, C., Barhanin, J., Faure, S., Gary, F., Coumel, P., Petit, C., Schwartz, K., Guicheney, P. (1997) A novel mutation in the potassium channel gene KVLQT1 causes the Jervell and Lange-Nielsen cardioauditory syndrome [see comments]. **Nat. Genet.** 15:186-189.

114. Charlier, C., Singh, N.A., Ryan, S.G., Lewis, T.B., Reus, B.E., Leach, R.J., Leppert, M. (1998) A pore mutation in a novel KQT-like potassium channel gene in an idiopathic epilepsy family [see comments]. **Nature Genetics** 18:53-55.

115. Kubisch, C., Schroeder, B.C., Friedrich, T., Lutjohann, B., El-Amraoui, A., Marlin, S., Petit, C., Jentsch, T.J. (1999) KCNQ4, a novel potassium channel expressed in sensory outer hair cells, is mutated in dominant deafness. **Cell** 96:437-446.

116. Haitin, Y., Attali, B. (2008) The C-terminus of Kv7 channels: a multifunctional module. **J Physiol** 586:1803-1810.

117. Wen, H., Levitan, I.B. (2002) Calmodulin is an auxiliary subunit of KCNQ2/3 potassium channels. **J Neurosci.** 22:7991-8001.

118. Yus-Najera, E., Santana-Castro, I., Villarroel, A. (2002) The identification and characterization of a noncontinuous calmodulin-binding site in noninactivating voltage-dependent KCNQ potassium channels. **J Biol. Chem.** 277:28545-28553.

119. Shahidullah, M., Santarelli, L.C., Wen, H., Levitan, I.B. (2005) Expression of a calmodulin-binding KCNQ2 potassium channel fragment modulates neuronal M-current and membrane excitability. **Proc. Natl. Acad. Sci. U. S. A** 102:16454-16459.

120. Delmas, P., Brown, D.A. (2005) Pathways modulating neural KCNQ/M (Kv7) potassium channels. **Nat. Rev. Neurosci.** 6:850-862.

121. Suh, B.C., Hille, B. (2005) Regulation of ion channels by phosphatidylinositol 4,5-bisphosphate. **Curr. Opin. Neurobiol.** 15:370-378.

122. Hernandez, C.C., Zaika, O., Tolstykh, G.P., Shapiro, M.S. (2008) Regulation of neural KCNQ channels: signalling pathways, structural motifs and functional implications. **J Physiol** 586:1811-1821.

123. Tobelaim, W.S., Dvir, M., Lebel, G., Cui, M., Buki, T., Peretz, A., Marom, M., Haitin, Y., Logothetis, D.E., Hirsch, J.A., Attali, B. (2017) Competition of calcified calmodulin N lobe and PIP2 to an LQT mutation site in Kv7.1 channel. **Proc. Natl. Acad. Sci. U. S. A** 114:E869-E878.

124. Sachyani, D., Dvir, M., Strulovich, R., Tria, G., Tobelaim, W., Peretz, A., Pongs, O., Svergun, D., Attali, B., Hirsch, J.A. (2014) Structural basis of a Kv7.1 potassium channel gating module: studies of the intracellular c-terminal domain in complex with calmodulin. **Structure.** 22:1582-1594.

125. Kwon, Y., Hofmann, T., Montell, C. (2007) Integration of phosphoinositide- and calmodulin-mediated regulation of TRPC6. **Mol. Cell** 25:491-503.

126. Park, K.H., Piron, J., Dahimene, S., Merot, J., Baro, I., Escande, D., Loussouarn, G. (2005) Impaired KCNQ1-KCNE1 and phosphatidylinositol-4,5-bisphosphate interaction underlies the long QT syndrome. **Circ. Res.** 96:730-739.

127. Kurokawa, J., Motoike, H.K., Rao, J., Kass, R.S. (2004) Regulatory actions of the A-kinase anchoring protein Yotiao on a heart potassium channel downstream of PKA phosphorylation. **Proc. Natl. Acad. Sci. U. S. A** 101:16374-16378.

128. Hoshi, N., Zhang, J.S., Omaki, M., Takeuchi, T., Yokoyama, S., Wanaverbecq, N., Langeberg, L.K., Yoneda, Y., Scott, J.D., Brown, D.A., Higashida, H. (2003) AKAP150 signaling complex promotes suppression of the M-current by muscarinic agonists. **Nat. Neurosci.** 6:564-571.

129. Zhang, J., Shapiro, M.S. (2016) Mechanisms and dynamics of AKAP79/150-orchestrated multi-protein signalling complexes in brain and peripheral nerve. **J Physiol** 594:31-37.

130. Miranda, P., Cadaveira-Mosquera, A., Gonzalez-Montelongo, R., Villarroel, A., Gonzalez-Hernandez, T., Lamas, J.A., Alvarez, d.l.R., Giraldez, T. (2013) The neuronal serum- and glucocorticoid-regulated kinase 1.1 reduces neuronal excitability and protects against seizures through upregulation of the M-current. **J Neurosci.** 33:2684-2696.

131. Dai, S., Hall, D.D., Hell, J.W. (2009) Supramolecular assemblies and localized regulation of voltage-gated ion channels. **Physiol Rev.** 89:411-452.

132. Marx, S.O., Kurokawa, J., Reiken, S., Motoike, H., D'Armiento, J., Marks, A.R., Kass, R.S. (2002) Requirement of a macromolecular signaling complex for beta adrenergic receptor modulation of the KCNQ1-KCNE1 potassium channel. **Science** 295:496-499.

133. Liin, S.I., Barro-Soria, R., Larsson, H.P. (2015) The KCNQ1 channel - remarkable flexibility in gating allows for functional versatility. **J Physiol** 593:2605-2615.

134. Wiener, R., Haitin, Y., Shamgar, L., Fernandez-Alonso, M.C., Martos, A., Chomsky-Hecht, O., Rivas, G., Attali, B., Hirsch, J.A. (2008) The KCNQ1 (Kv7.1) COOH terminus, a multitiered scaffold for subunit assembly and protein interaction. **J Biol. Chem.** 283:5815-5830.

135. Devaux, J.J., Kleopa, K.A., Cooper, E.C., Scherer, S.S. (2004) KCNQ2 is a nodal K+ channel. **J Neurosci.** 24:1236-1244.

136. David, M., Macias, A., Moreno, C., Prieto, A., Martinez-Marmol, R., Vicente, R., Felipe, A., Gonzalez, T., Tamkun, M.M., Valenzuela, C. (2012) PKC activity regulates functional effects of K_Vb1.3 on K_V1.5 channels. Identification of a cardiac K_V1.5 channelosome. **J. Biol. Chem.** 287:21416-21428.

137. Roura-Ferrer, M., Etxebarria, A., Sole, L., Oliveras, A., Comes, N., Villarroel, A., Felipe, A. (2009) Functional implications of KCNE subunit expression for the Kv7.5 (KCNQ5) channel. **Cell Physiol Biochem.** 24:325-334.

138. Grunnet, M., Jespersen, T., Rasmussen, H.B., Ljungstrom, T., Jorgensen, N.K., Olesen, S.P., Klaerke, D.A. (2002) KCNE4 is an inhibitory subunit to the KCNQ1 channel. **J Physiol** 542:119-130.

139. Abbott, G.W. (2016) KCNE4 and KCNE5: K(+) channel regulation and cardiac arrhythmogenesis. **Gene** 593:249-260.

140. McCrossan, Z.A., Abbott, G.W. (2004) The MinK-related peptides. **Neuropharmacol.** 47:787-821.

141. Schroeder, B.C., Waldegger, S., Fehr, S., Bleich, M., Warth, R., Greger, R., Jentsch, T.J. (2000) A constitutively open potassium channel formed by KCNQ1 and KCNE3. **Nature** 403:196-199.

142. Bendahhou, S., Marionneau, C., Haurogne, K., Larroque, M.M., Derand, R., Szuts, V., Escande, D., Demolombe, S., Barhanin, J. (2005) In vitro molecular interactions and distribution of KCNE family with KCNQ1 in the human heart. **Cardiovasc. Res.** 67:529-538.

143. Kroncke, B.M., Van Horn, W.D., Smith, J., Kang, C., Welch, R.C., Song, Y., Nannemann, D.P., Taylor, K.C., Sisco, N.J., George, A.L., Jr., Meiler, J., Vanoye, C.G., Sanders, C.R. (2016) Structural basis for KCNE3 modulation of potassium recycling in epithelia. **Sci. Adv.** 2:e1501228.

144. Jespersen, T., Rasmussen, H.B., Grunnet, M., Jensen, H.S., Angelo, K., Dupuis, D.S., Vogel, L.K., Jorgensen, N.K., Klaerke, D.A., Olesen, S.P. (2004) Basolateral localisation of KCNQ1 potassium channels in MDCK cells: molecular identification of an N-terminal targeting motif. **J Cell Sci.** 117:4517-4526.

145. Lerche, C., Scherer, C.R., Seebohm, G., Derst, C., Wei, A.D., Busch, A.E., Steinmeyer, K. (2000) Molecular cloning and functional expression of KCNQ5, a potassium channel subunit that may contribute to neuronal M-current diversity. **J Biol. Chem** 275:22395-22400.

146. Schroeder, B.C., Hechenberger, M., Weinreich, F., Kubisch, C., Jentsch, T.J. (2000) KCNQ5, a novel potassium channel broadly expressed in brain, mediates M-type currents. **J. Biol. Chem.** 275:24089-24095.

147. Yang, W.P., Levesque, P.C., Little, W.A., Conder, M.L., Shalaby, F.Y., Blanar, M.A. (1997) KvLQT1, a voltage-gated potassium channel responsible for human cardiac arrhythmias. **Proc. Natl. Acad. Sci. U. S. A.** 94:4017-4021.

148. Yus-Najera, E., Munoz, A., Salvador, N., Jensen, B.S., Rasmussen, H.B., Defelipe, J., Villarroel, A. (2003) Localization of KCNQ5 in the normal and epileptic human temporal neocortex and hippocampal formation. **Neurosci.** 120:353-364.

149. Mani, B.K., Robakowski, C., Brueggemann, L.I., Cribbs, L.L., Tripathi, A., Majetschak, M., Byron, K.L. (2016) Kv7.5 Potassium Channel Subunits Are the Primary Targets for PKA-Dependent Enhancement of Vascular Smooth Muscle Kv7 Currents. **Mol. Pharmacol.** 89:323-334.

150. Brueggemann, L.I., Mackie, A.R., Cribbs, L.L., Freda, J., Tripathi, A., Majetschak, M., Byron, K.L. (2014) Differential protein kinase C-dependent modulation of Kv7.4 and Kv7.5 subunits of vascular Kv7 channels. **J Biol. Chem.** 289:2099-2111.

151. Zhong, X.Z., Harhun, M.I., Olesen, S.P., Ohya, S., Moffatt, J.D., Cole, W.C., Greenwood, I.A. (2010) Participation of KCNQ (Kv7) potassium channels in myogenic control of cerebral arterial diameter. **J Physiol** 588:3277-3293.

152. Sanguinetti, M.C., Curran, M.E., Zou, A., Shen, J., Spector, P.S., Atkinson, D.L., Keating, M.T. (1996) Coassembly of K(V)LQT1 and minK (IsK) proteins to form cardiac I(Ks) potassium channel. **Nature** 384:80-83.

153. Barhanin, J., Lesage, F., Guillemare, E., Fink, M., Lazdunski, M., Romey, G. (1996) K(V)LQT1 and lsK (minK) proteins associate to form the I(Ks) cardiac potassium current. **Nature** 384:78-80.

154. Pusch, M., Magrassi, R., Wollnik, B., Conti, F. (1998) Activation and inactivation of homomeric KvLQT1 potassium channels. **Biophys. J.** 75:785-792.

155. Tristani-Firouzi, M., Sanguinetti, M.C. (1998) Voltage-dependent inactivation of the human K+ channel KvLQT1 is eliminated by association with minimal K+ channel (minK) subunits. **J. Physiol. Lond.** 510:37-45.

156. Shibasaki, T. (1987) Conductance and kinetics of delayed rectifier potassium channels in nodal cells of the rabbit heart. **J. Physiol. (Lond)** 387:227-250.

157. Sanguinetti, M.C., Jiang, C., Curran, M.E., Keating, M.T. (1995) A mechanistic link between an inherited and an acquired cardiac arrhythmia: HERG encodes the I_{Kr} potassium channel. **Cell** 81:299-307.

158. Takumi, T., Ohkubo, H., Nakanishi, S. (1988) Cloning of a membrane protein that induces a slow voltage-gated potassium current. **Science** 242:1042-1045.

159. Tinel, N., Diochot, S., Lauritzen, I., Barhanin, J., Lazdunski, M., Borsotto, M. (2000) M-type KCNQ2-KCNQ3 potassium channels are modulated by the KCNE2 subunit. **FEBS Lett.** 480:137-141.

160. Angelo, K., Jespersen, T., Grunnet, M., Nielsen, M.S., Klaerke, D.A., Olesen, S.P. (2002) KCNE5 induces time- and voltage-dependent modulation of the KCNQ1 current. **Biophys. J** 83:1997-2006.

161. Silva, J., Rudy, Y. (2005) Subunit interaction determines IKs participation in cardiac repolarization and repolarization reserve. **Circulation** 112:1384-1391.

162. Nakajo, K., Ulbrich, M.H., Kubo, Y., Isacoff, E.Y. (2010) Stoichiometry of the KC. **Proc. Natl. Acad. Sci. U. S. A** 107:18862-18867.

163. Yu, H., Lin, Z., Mattmann, M.E., Zou, B., Terrenoire, C., Zhang, H., Wu, M., McManus, O.B., Kass, R.S., Lindsley, C.W., Hopkins, C.R., Li, M. (2013) Dynamic subunit stoichiometry confers a progressive continuum of pharmacological sensitivity by KCNQ potassium channels. **Proc. Natl. Acad. Sci. U. S. A** 110:8732-8737.

164. Plant, L.D., Xiong, D., Dai, H., Goldstein, S.A. (2014) Individual IKs channels at the surface of mammalian cells contain two KCNE1 accessory subunits. **Proc. Natl. Acad. Sci. U. S. A** 111:E1438-E1446.

165. Murray, C.I., Westhoff, M., Eldstrom, J., Thompson, E., Emes, R., Fedida, D. (2016) Unnatural amino acid photo-crosslinking of the IKs channel complex demonstrates a KCNE1:KCNQ1 stoichiometry of up to 4:4. **Elife.** 5.

166. Chung, D.Y., Chan, P.J., Bankston, J.R., Yang, L., Liu, G., Marx, S.O., Karlin, A., Kass, R.S. (2009) Location of KCNE1 relative to KCNQ1 in the I(KS) potassium channel by disulfide cross-linking of substituted cysteines. **Proc. Natl. Acad. Sci. U. S. A** 106:743-748.

167. Nakajo, K., Kubo, Y. (2007) KCNE1 and KCNE3 stabilize and/or slow voltage sensing S4 segment of KCNQ1 channel. **J Gen. Physiol** 130:269-281.

168. Shamgar, L., Haitin, Y., Yisharel, I., Malka, E., Schottelndreier, H., Peretz, A., Paas, Y., Attali, B. (2008) KCNE1 constrains the voltage sensor of Kv7.1 K+ channels. **PLoS. One.** 3:e1943.

169. Xu, X., Jiang, M., Hsu, K.L., Zhang, M., Tseng, G.N. (2008) KCNQ1 and KCNE1 in the IKs channel complex make state-dependent contacts in their extracellular domains. **J. Gen. Physiol** 131:589-603.

170. Goldman, A.M., Glasscock, E., Yoo, J., Chen, T.T., Klassen, T.L., Noebels, J.L. (2009) Arrhythmia in heart and brain: KCNQ1 mutations link epilepsy and sudden unexplained death. **Sci. Transl. Med.** 1:2ra6.

171. Wang, H.S., Pan, Z., Shi, W., Brown, B.S., Wymore, R.S., Cohen, I.S., Dixon, J.E., McKinnon, D. (1998) KCNQ2 and KCNQ3 potassium channel subunits: molecular correlates of the M-channel. **Science** 282:1890-1893.

172. Wang, H.S., Brown, B.S., McKinnon, D., Cohen, I.S. (2000) Molecular basis for differential sensitivity of KCNQ and I(Ks) channels to the cognitive enhancer XE991. **Mol. Pharmacol.** 57:1218-1223.

173. Lerche, C., Bruhova, I., Lerche, H., Steinmeyer, K., Wei, A.D., Strutz-Seebohm, N., Lang, F., Busch, A.E., Zhorov, B.S., Seebohm, G. (2007) Chromanol 293B binding in KCNQ1 (Kv7.1) channels involves electrostatic interactions with a potassium ion in the selectivity filter. **Mol. Pharmacol.** 71:1503-1511.

174. Tatulian, L., Delmas, P., Abogadie, F.C., Brown, D.A. (2001) Activation of expressed KCNQ potassium currents and native neuronal M-type potassium currents by the anti-convulsant drug retigabine. **J Neurosci.** 21:5535-5545.

175. Peretz, A., Degani, N., Nachman, R., Uziyel, Y., Gibor, G., Shabat, D., Attali, B. (2005) Meclofenamic acid and diclofenac, novel templates of KCNQ2/Q3 potassium channel openers, depress cortical neuron activity and exhibit anticonvulsant properties. **Mol. Pharmacol.** 67:1053-1066.

176. Sesti, F., Tai, K.K., Goldstein, S.A. (2000) MinK endows the I(Ks) potassium channel pore with sensitivity to internal tetraethylammonium. **Biophys. J** 79:1369-1378.

177. Busch, A.E., Suessbrich, H. (1997) Role of the ISK protein in the IminK channel complex. **Trends. Pharmacol. Sci.** 18:26-29.

178. Lerche, C., Seebohm, G., Wagner, C.I., Scherer, C.R., Dehmelt, L., Abitbol, I., Gerlach, U., Brendel, J., Attali, B., Busch, A.E. (2000) Molecular impact of MinK on the enantiospecific block of I(Ks) by chromanols. **Br. J Pharmacol.** 131:1503-1506.

179. Cole, W.C., Welsh, D.G. (2011) Role of myosin light chain kinase and myosin light chain phosphatase in the resistance arterial myogenic response to intravascular pressure. **Arch. Biochem. Biophys.** 510:160-173.

180. Berwick, Z.C., Payne, G.A., Lynch, B., Dick, G.M., Sturek, M., Tune, J.D. (2010) Contribution of adenosine A(2A) and A(2B) receptors to ischemic coronary dilation: role of K(V) and K(ATP) channels. **Microcirculation.** 17:600-607.

181. Chadha, P.S., Zunke, F., Davis, A.J., Jepps, T.A., Linders, J.T., Schwake, M., Towart, R., Greenwood, I.A. (2012) Pharmacological dissection of K(v)7.1 channels in systemic and pulmonary arteries. **Br. J Pharmacol.** 166:1377-1387.

182. Ng, F.L., Davis, A.J., Jepps, T.A., Harhun, M.I., Yeung, S.Y., Wan, A., Reddy, M., Melville, D., Nardi, A., Khong, T.K., Greenwood, I.A. (2011) Expression and function of the K+ channel KCNQ genes in human arteries. **Br. J Pharmacol.** 162:42-53.

183. Ohya, S., Sergeant, G.P., Greenwood, I.A., Horowitz, B. (2003) Molecular variants of KCNQ channels expressed in murine portal vein myocytes: a role in delayed rectifier current. **Circ. Res.** 92:1016-1023.

184. Khanamiri, S., Soltysinska, E., Jepps, T.A., Bentzen, B.H., Chadha, P.S., Schmitt, N., Greenwood, I.A., Olesen, S.P. (2013) Contribution of Kv7 channels to basal coronary flow and active response to ischemia. **Hypertension** 62:1090-1097.

185. Morales-Cano, D., Moreno, L., Barreira, B., Pandolfi, R., Chamorro, V., Jimenez, R., Villamor, E., Duarte, J., Perez-Vizcaino, F., Cogolludo, A. (2015) Kv7 channels critically determine coronary artery reactivity: left-right differences and down-regulation by hyperglycaemia. **Cardiovasc. Res.** 106:98-108.

186. Priori, S.G., Wilde, A.A., Horie, M., Cho, Y., Behr, E.R., Berul, C., Blom, N., Brugada, J., Chiang, C.E., Huikuri, H., Kannankeril, P., Krahn, A., Leenhardt, A., Moss, A., Schwartz, P.J., Shimizu, W., Tomaselli, G., Tracy, C. (2013) HRS/EHRA/APHRS expert consensus statement on the diagnosis and management of patients with inherited primary arrhythmia syndromes: document endorsed by HRS, EHRA, and APHRS in May 2013 and by ACCF, AHA, PACES, and AEPC in June 2013. **Heart Rhythm.** 10:1932-1963.

187. Jackman, W.M., Friday, K.J., Anderson, J.L., Aliot, E.M., Clark, M., Lazzara, R. (1988) The long QT syndromes: a critical review, new clinical observations and a unifying hypothesis. **Prog. Cardiovasc. Dis.** 31:115-172.

188. Hedley, P.L., Jorgensen, P., Schlamowitz, S., Moolman-Smook, J., Kanters, J.K., Corfield, V.A., Christiansen, M. (2009) The genetic basis of Brugada syndrome: a mutation update. **Hum. Mutat.** 30:1256-1266.

189. Gollob, M.H., Redpath, C.J., Roberts, J.D. (2011) The short QT syndrome: proposed diagnostic criteria. **J. Am. Coll. Cardiol.** 57:802-812.

190. Jensen, M.M., Lange, S.C., Thomsen, M.S., Hansen, H.H., Mikkelsen, J.D. (2011) The pharmacological effect of positive KCNQ (Kv7) modulators on dopamine release from striatal slices. **Basic Clin. Pharmacol. Toxicol.** 109:339-342.

191. Terrenoire, C., Clancy, C.E., Cormier, J.W., Sampson, K.J., Kass, R.S. (2005) Autonomic control of cardiac action potentials: role of potassium channel kinetics in response to sympathetic stimulation. **Circ. Res.** 96:e25-e34.

192. Roden, D.M. (1993) Torsade de pointes. **Clin. Cardiol** 16:683-686.

193. Jakobsson, A., Westerberg, R., Jacobsson, A. (2006) Fatty acid elongases in mammals: their regulation and roles in metabolism. **Prog. Lipid Res.** 45:237-249.

194. De Caterina, R., Madonna, R., Zucchi, R., La Rovere, M.T. (2003) Antiarrhythmic effects of omega-3 fatty acids: from epidemiology to bedside. **Am. Heart J.** 146:420-430.

195. Leaf, A., Xiao, Y.F., Kang, J.X., Billman, G.E. (2003) Prevention of sudden cardiac death by n-3 polyunsaturated fatty acids. **Pharmacol. Ther.** 98:355-377.

196. Chaddha, A., Eagle, K.A. (2015) Cardiology Patient Page. Omega-3 Fatty Acids and Heart Health. **Circulation** 132:e350-e352.

197. Lefevre, F., Aronson, N. (2000) Ketogenic diet for the treatment of refractory epilepsy in children: A systematic review of efficacy. **Pediatrics** 105:E46.

198. Sinclair HM. The diet of Canadian Indian Eskimos. Proc Nutr Soc 1953;12:69-82(Abstract).

199. Sinclair, H.M. (1956) Deficiency of essential fatty acids and atherosclerosis, etcetera. **Lancet** 270:381-383.

200. Billman, G.E., Kang, J.X., Leaf, A. (1999) Prevention of sudden cardiac death by dietary pure omega-3 polyunsaturated fatty acids in dogs. **Circulation** 99:2452-2457.

201. Burr, M.L., Fehily, A.M., Gilbert, J.F., Rogers, S., Holliday, R.M., Sweetnam, P.M., Elwood, P.C., Deadman, N.M. (1989) Effects of changes in fat, fish, and fibre intakes on death and myocardial reinfarction: diet and reinfarction trial (DART). **Lancet** 2:757-761.

202. GISSI-Prevenzione Investigators. (1999) Dietary supplementation with n-3 polyunsaturated fatty acids and vitamin E after myocardial infarction: results of the GISSI-Prevenzione trial. Gruppo Italiano per lo Studio della Sopravvivenza nell'Infarto miocardico. **Lancet** 354:447-455.

203. Tanaka, K., Ishikawa, Y., Yokoyama, M., Origasa, H., Matsuzaki, M., Saito, Y., Matsuzawa, Y., Sasaki, J., Oikawa, S., Hishida, H., Itakura, H., Kita, T., Kitabatake, A., Nakaya, N., Sakata, T., Shimada, K., Shirato, K. (2008) Reduction in the recurrence of stroke by eicosapentaenoic acid for hypercholesterolemic patients: subanalysis of the JELIS trial. **Stroke** 39:2052-2058.

204. Tavazzi, L., Maggioni, A.P., Marchioli, R., Barlera, S., Franzosi, M.G., Latini, R., Lucci, D., Nicolosi, G.L., Porcu, M., Tognoni, G. (2008) Effect of n-3 polyunsaturated fatty acids in patients with chronic heart failure (the GISSI-HF trial): a randomised, double-blind, placebo-controlled trial. **Lancet** 372:1223-1230.

205. Kromhout, D., Giltay, E.J., Geleijnse, J.M. (2010) n-3 fatty acids and cardiovascular events after myocardial infarction. **N. Engl. J. Med.** 363:2015-2026.

206. Rauch, B., Schiele, R., Schneider, S., Diller, F., Victor, N., Gohlke, H., Gottwik, M., Steinbeck, G., Del, C.U., Sack, R., Worth, H., Katus, H., Spitzer, W., Sabin, G., Senges, J. (2010) OMEGA, a randomized, placebo-controlled trial to test the effect of highly purified omega-3 fatty acids on top of modern guideline-adjusted therapy after myocardial infarction. **Circulation** 122:2152-2159.

207. Coronel, R., Wilms-Schopman, F.J., Den Ruijter, H.M., Belterman, C.N., Schumacher, C.A., Opthof, T., Hovenier, R., Lemmens, A.G., Terpstra, A.H., Katan, M.B., Zock, P. (2007) Dietary n-3 fatty acids promote arrhythmias during acute regional myocardial ischemia in isolated pig hearts. **Cardiovasc. Res** 73:386-394.

208. Burr, M.L., Ashfield-Watt, P.A., Dunstan, F.D., Fehily, A.M., Breay, P., Ashton, T., Zotos, P.C., Haboubi, N.A., Elwood, P.C. (2003) Lack of benefit of dietary advice to men with angina: results of a controlled trial. **Eur. J Clin. Nutr.** 57:193-200.

209. Raitt, M.H., Connor, W.E., Morris, C., Kron, J., Halperin, B., Chugh, S.S., McClelland, J., Cook, J., MacMurdy, K., Swenson, R., Connor, S.L., Gerhard, G., Kraemer, D.F., Oseran, D., Marchant, C., Calhoun, D., Shnider, R., McAnulty, J. (2005) Fish oil supplementation and risk of ventricular tachycardia and ventricular fibrillation in patients with implantable defibrillators: a randomized controlled trial. **JAMA** 293:2884-2891.

210. Doolan, G.K., Panchal, R.G., Fonnes, E.L., Clarke, A.L., Williams, D.A., Petrou, S. (2002) Fatty acid augmentation of the cardiac slowly activating delayed rectifier current (IKs) is conferred by hminK. **FASEB J.** 16:1662-1664.

211. Dujardin, K.S., Dumotier, B., David, M., Guizy, M., Valenzuela, C., Hondeghem, L.M. (2008) Ultrafast sodium channel block by dietary fish oil prevents dofetilide-induced ventricular arrhythmias in rabbit hearts. **Am. J. Physiol Heart Circ. Physiol** 295:H1414-H1421.

212. Guizy, M., Arias, C., David, M., Gonzalez, T., Valenzuela, C. (2005) w-3 and w-6 polyunsaturated fatty acids block *HERG* channels. **Am J Physiol Cell Physiol** 289:C1251-C1260.

213. Guizy, M., David, M., Arias, C., Zhang, L., Cofan, M., Ruiz-Gutierrez, V., Ros, E., Lillo, M.P., Martens, J.R., Valenzuela, C. (2008) Modulation of the atrial specific Kv1.5 channel by the n-3 polyunsaturated fatty acid, alpha-linolenic acid. **J. Mol. Cell Cardiol.** 44:323-335.

214. Honoré, E., Barhanin, J., Attali, B., Lesage, F., Lazdunski, M. (1994) External blockade of the major cardiac delayed-rectifier K^+ channel (Kv1.5) by polyunsaturated fatty acids. **Proc. Natl. Acad. Sci. U. S. A** 91:1937-1941.

215. Jude, S., Bedut, S., Roger, S., Pinault, M., Champeroux, P., White, E., Le Guennec, J.Y. (2003) Peroxidation of docosahexaenoic acid is responsible for its effects on I TO and I SS in rat ventricular myocytes. **Br. J. Pharmacol.** 139:816-822.

216. Verkerk, A.O., van Ginneken, A.C., Berecki, G., Den Ruijter, H.M., Schumacher, C.A., Veldkamp, M.W., Baartscheer, A., Casini, S., Opthof, T., Hovenier, R., Fiolet, J.W., Zock, P.L., Coronel, R. (2006) Incorporated sarcolemmal fish oil fatty acids shorten pig ventricular action potentials. **Cardiovasc. Res** 70:509-520.

217. Xiao, Y.F., Gomez, A.M., Morgan, J.P., Lederer, W.J., Leaf, A. (1997) Suppression of voltage-gated L-type Ca2+ currents by polyunsaturated fatty acids in adult and neonatal rat ventricular myocytes. **Proc. Natl. Acad. Sci. U. S. A** 94:4182-4187.

218. Xiao, Y.F., Kang, J.X., Morgan, J.P., Leaf, A. (1995) Blocking effects of polyunsaturated fatty acids on Na^+ channels of neonatal rat ventricular myocytes. **Proc. Natl. Acad. Sci. U. S. A** 92:11000-11004.

219. Leifert, W.R., McMurchie, E.J., Saint, D.A. (1999) Inhibition of cardiac sodium currents in adult rat myocytes by n-3 polyunsaturated fatty acids. **J. Physiol** 520:671-679.

220. Bendahhou, S., Cummins, T.R., Agnew, W.S. (1997) Mechanism of modulation of the voltage-gated skeletal and cardiac muscle sodium channels by fatty acids. **Am J Physiol** 272:C592-C600.

221. Hallaq, H., Smith, T.W., Leaf, A. (1992) Modulation of dihydropyridine-sensitive calcium channels in heart cells by fish oil fatty acids. **Proc. Natl. Acad. Sci. U. S. A** 89:1760-1764.

222. Kang, J.X., Leaf, A. (1996) Evidence that free polyunsaturated fatty acids modify Na^+ channels by directly binding to the channel proteins. **Proc. Natl. Acad. Sci. U. S. A** 93:3542-3546.

223. Xiao, Y.F., Sigg, D.C., Leaf, A. (2005) The antiarrhythmic effect of n-3 polyunsaturated fatty acids: modulation of cardiac ion channels as a potential mechanism. **J Membr. Biol.** 206:141-154.

224. Borjesson, S.I., Hammarstrom, S., Elinder, F. (2008) Lipoelectric modification of ion channel voltage gating by polyunsaturated fatty acids. **Biophys. J** 95:2242-2253.

225. Moreno, C., de la Cruz, A., Oliveras, A., Kharche, S.R., Guizy, M., Comes, N., Stary, T., Ronchi, C., Rocchetti, M., Baro, I., Loussouarn, G., Zaza, A., Severi, S., Felipe, A., Valenzuela, C. (2015) Marine n-3 PUFAs modulate IKs gating, channel expression, and location in membrane microdomains. **Cardiovasc. Res.** 105:223-232.

226. Liin, S.I., Silvera, E.M., Barro-Soria, R., Skarsfeldt, M.A., Larsson, J.E., Starck, H.F., Parkkari, T., Bentzen, B.H., Schmitt, N., Larsson, H.P., Elinder, F. (2015) Polyunsaturated fatty acid analogs act antiarrhythmically on the cardiac IKs channel. **Proc. Natl. Acad. Sci. U. S. A** 112:5714-5719.

227. Liin, S.I., Karlsson, U., Bentzen, B.H., Schmitt, N., Elinder, F. (2016) Polyunsaturated fatty acids are potent openers of human M-channels expressed in Xenopus laevis oocytes. **Acta Physiol (Oxf)** 218:28-37.

228. Khanapure, S.P., Garvey, D.S., Janero, D.R., Letts, L.G. (2007) Eicosanoids in inflammation: biosynthesis, pharmacology, and therapeutic frontiers. **Curr. Top. Med. Chem.** 7:311-340.

229. Merched, A.J., Ko, K., Gotlinger, K.H., Serhan, C.N., Chan, L. (2008) Atherosclerosis: evidence for impairment of resolution of vascular inflammation governed by specific lipid mediators. **FASEB J** 22:3595-3606.

230. Serhan, C.N., Chiang, N., Van Dyke, T.E. (2008) Resolving inflammation: dual anti-inflammatory and pro-resolution lipid mediators. **Nat. Rev. Immunol.** 8:349-361.

231. Calder, P.C. (2006) n-3 polyunsaturated fatty acids, inflammation, and inflammatory diseases. **Am. J Clin. Nutr.** 83:1505S-1519S.

232. Ortega-Gomez, A., Perretti, M., Soehnlein, O. (2013) Resolution of inflammation: an integrated view. **EMBO Mol. Med.** 5:661-674.

233. Brancaleone, V., Gobbetti, T., Cenac, N., le, F.P., Colom, B., Flower, R.J., Vergnolle, N., Nourshargh, S., Perretti, M. (2013) A vasculo-protective circuit centred on Lipoxin A4 and aspirin-triggered 15-epi-lipoxin A4 operative in murine microcirculation. **Blood**.

234. Moreno, C., Prieto, P., Macias, A., Pimentel-Santillana, M., de la Cruz, A., Traves, P.G., Bosca, L., Valenzuela, C. (2013) Modulation of voltage-dependent and inward-rectifyier potassium channels by 15-epi-lipoxin A_4 in activated murine macrophages: implications in the innate immunity. **J. Immunol.** 191:6136-6146.

235. Serhan, C.N., Yacoubian, S., Yang, R. (2008) Anti-inflammatory and proresolving lipid mediators. **Annu. Rev. Pathol.** 3:279-312.

236. Duffield, J.S., Hong, S., Vaidya, V.S., Lu, Y., Fredman, G., Serhan, C.N., Bonventre, J.V. (2006) Resolvin D series and protectin D1 mitigate acute kidney injury. **J Immunol.** 177:5902-5911.

237. Lima-Garcia, J.F., Dutra, R.C., da, S.K., Motta, E.M., Campos, M.M., Calixto, J.B. (2011) The precursor of resolvin D series and aspirin-triggered resolvin D1 display anti-hyperalgesic properties in adjuvant-induced arthritis in rats. **Br. J Pharmacol.** 164:278-293.

238. Bazan, N.G., Calandria, J.M., Serhan, C.N. (2010) Rescue and repair during photoreceptor cell renewal mediated by docosahexaenoic acid-derived neuroprotectin D1. **J Lipid Res.** 51:2018-2031.

239. Kain, V., Ingle, K.A., Colas, R.A., Dalli, J., Prabhu, S.D., Serhan, C.N., Joshi, M., Halade, G.V. (2015) Resolvin D1 activates the inflammation resolving response at splenic and ventricular site following myocardial infarction leading to improved ventricular function. **J Mol. Cell Cardiol.** 84:24-35.

240. Yates, C.M., Calder, P.C., Ed, R.G. (2014) Pharmacology and therapeutics of omega-3 polyunsaturated fatty acids in chronic inflammatory disease. **Pharmacol. Ther.** 141:272-282.

241. Peña, J.M., MacFadyen, J., Glynn, R.J., Ridker, P.M. (2012) High-sensitivity C-reactive protein, statin therapy, and risks of atrial fibrillation: an exploratory analysis of the JUPITER trial. **Eur. Heart J.** 33:531-537.

242. Greenwood, I.A., Ohya, S. (2009) New tricks for old dogs: KCNQ expression and role in smooth muscle. **Br. J Pharmacol.** 156:1196-1203.

243. Abbott, G.W., Goldstein, S.A. (2001) Potassium channel subunits encoded by the KCNE gene family: physiology and pathophysiology of the MinK-related peptides (MiRPs). **Mol. Interv.** 1:95-107.

244. Schwake, M., Athanasiadu, D., Beimgraben, C., Blanz, J., Beck, C., Jentsch, T.J., Saftig, P., Friedrich, T. (2006) Structural determinants of M-type KCNQ (Kv7) K+ channel assembly. **J Neurosci.** 26:3757-3766.

245. Joshi, S., Balan, P., Gurney, A.M. (2006) Pulmonary vasoconstrictor action of KCNQ potassium channel blockers. **Respir. Res.** 7:31.

246. Joshi, S., Sedivy, V., Hodyc, D., Herget, J., Gurney, A.M. (2009) KCNQ modulators reveal a key role for KCNQ potassium channels in regulating the tone of rat pulmonary artery smooth muscle. **J Pharmacol. Exp. Ther.** 329:368-376.

247. Harrison, R., Burr, M., Elton, P. (1999) GISSI-Prevenzione trial. **Lancet** 354:1554-1555.

248. Chen, M., Divangahi, M., Gan, H., Shin, D.S., Hong, S., Lee, D.M., Serhan, C.N., Behar, S.M., Remold, H.G. (2008) Lipid mediators in innate immunity against tuberculosis: opposing roles of PGE2 and LXA4 in the induction of macrophage death. **J. Exp. Med.** 205:2791-2801.

249. Cogolludo, A., Frazziano, G., Briones, A.M., Cobeno, L., Moreno, L., Lodi, F., Salaices, M., Tamargo, J., Perez-Vizcaino, F. (2007) The dietary flavonoid quercetin activates BKCa currents in coronary arteries via production of H2O2. Role in vasodilatation. **Cardiovasc. Res.** 73:424-431.

250. Oliveras, A., Roura-Ferrer, M., Sole, L., de la Cruz, A., Prieto, A., Etxebarria, A., Manils, J., Morales-Cano, D., Condom, E., Soler, C., Cogolludo, A., Valenzuela, C., Villarroel, A., Comes, N., Felipe, A. (2014) Functional assembly of Kv7.1/Kv7.5 channels with emerging properties on vascular muscle physiology. **Arterioscler. Thromb. Vasc. Biol.** 34:1522-1530.

251. Zaza, A., Rocchetti, M., Brioschi, A., Cantadori, A., Ferroni, A. (1998) Dynamic Ca2+-induced inward rectification of K+ current during the ventricular action potential. **Circ. Res.** 82:947-956.

252. Kang, D., La, J.H., Kim, E.J., Park, J.Y., Hong, S.G., Han, J. (2006) An endogenous acid-sensitive K+ channel expressed in COS-7 cells. **Biochem. Biophys. Res. Commun.** 341:1231-1236.

253. Jiang, B., Sun, X., Cao, K., Wang, R. (2002) Endogenous Kv channels in human embryonic kidney (HEK-293) cells. **Mol. Cell Biochem.** 238:69-79.

254. Macias, A., de la Cruz, A., Prieto, A., Peraza, D.A., Tamkun, M.M., Gonzalez, T., Valenzuela, C. (2014) PKC inhibition results in a Kv1.5 + Kvbeta1.3 pharmacology closer to Kv1.5 channels. **Br. J Pharmacol.** 171:4914-4926.

255. Hamill, O.P., Marty, A., Neher, E., Sakmann, B., Sigworth, F.J. (1981) Improved patch clamp techniques for high-resolution current recording from cells and cell-free membrane patches. **Pflügers Arch.** 391:85-100.

256. Marchioli, R., Barzi, F., Bomba, E., Chieffo, C., Di, G.D., Di, M.R., Franzosi, M.G., Geraci, E., Levantesi, G., Maggioni, A.P., Mantini, L., Marfisi, R.M., Mastrogiuseppe, G., Mininni, N., Nicolosi, G.L., Santini, M., Schweiger, C., Tavazzi, L., Tognoni, G., Tucci, C., Valagussa, F. (2002) Early protection against sudden death by n-3 polyunsaturated fatty acids after myocardial infarction: time-course analysis of the results of the Gruppo Italiano per lo Studio della Sopravvivenza nell'Infarto Miocardico (GISSI)-Prevenzione. **Circulation** 105:1897-1903.

257. Moreno, C., Oliveras, A., de la Cruz, A., Bartolucci, C., Munoz, C., Salar, E., Gimeno, J.R., Severi, S., Comes, N., Felipe, A., Gonzalez, T., Lambiase, P., Valenzuela, C. (2015) A new KCNQ1 mutation at the S5

segment that impairs its association with KCNE1 is responsible for short QT syndrome. **Cardiovasc. Res.** 107:613-623.

258. Arias, C., Guizy, M., David, M., Marzian, S., Gonzalez, T., Decher, N., Valenzuela, C. (2007) Kvb1.3 reduces the degree of stereoselective bupivacaine block of Kv1.5 channels. **Anesthesiol.** 107:641-651.

259. Franqueza, L., Longobardo, M., Vicente, J., Delpon, E., Tamkun, M.M., Tamargo, J., Snyders, D.J., Valenzuela, C. (1997) Molecular determinants of stereoselective bupivacaine block of hKv1.5 channels. **Circ. Res.** 81:1053-1064.

260. Martinez-Marmol, R., Villalonga, N., Sole, L., Vicente, R., Tamkun, M.M., Soler, C., Felipe, A. (2008) Multiple Kv1.5 targeting to membrane surface microdomains. **J. Cell Physiol** 217:667-673.

261. Vicente, R., Villalonga, N., Calvo, M., Escalada, A., Solsona, C., Soler, C., Tamkun, M.M., Felipe, A. (2008) Kv1.5 association modifies Kv1.3 traffic and membrane localization. **J. Biol. Chem.** 283:8756-8764.

262. Aiken, S.P., Lampe, B.J., Murphy, P.A., Brown, B.S. (1995) Reduction of spike frequency adaptation and blockade of M- current in rat CA1 pyramidal neurones by linopirdine (DuP 996), a neurotransmitter release enhancer. **Br. J. Pharmacol.** 115:1163-1168.

263. Stewart, A.P., Gomez-Posada, J.C., McGeorge, J., Rouhani, M.J., Villarroel, A., Murrell-Lagnado, R.D., Edwardson, J.M. (2012) The Kv7.2/Kv7.3 heterotetramer assembles with a random subunit arrangement. **J Biol. Chem.** 287:11870-11877.

264. Hernandez, C.C., Falkenburger, B., Shapiro, M.S. (2009) Affinity for phosphatidylinositol 4,5-bisphosphate determines muscarinic agonist sensitivity of Kv7 K+ channels. **J Gen. Physiol** 134:437-448.

265. Maguy, A., Hebert, T.E., Nattel, S. (2006) Involvement of lipid rafts and caveolae in cardiac ion channel function. **Cardiovasc. Res.** 69:798-807.

266. O'Connell, K.M., Martens, J.R., Tamkun, M.M. (2004) Localization of ion channels to lipid Raft domains within the cardiovascular system. **Trends Cardiovasc. Med.** 14:37-42.

267. Dart, C. (2010) Lipid microdomains and the regulation of ion channel function. **J Physiol** 588:3169-3178.

268. Babiychuk, E.B., Smith, R.D., Burdyga, T., Babiychuk, V.S., Wray, S., Draeger, A. (2004) Membrane cholesterol regulates smooth muscle phasic contraction. **J Membr. Biol.** 198:95-101.

269. Roura-Ferrer, M., Sole, L., Oliveras, A., Dahan, R., Bielanska, J., Villarroel, A., Comes, N., Felipe, A. (2010) Impact of KCNE subunits on KCNQ1 (Kv7.1) channel membrane surface targeting. **J. Cell Physiol** 225:692-700.

270. Roura-Ferrer, M., Sole, L., Oliveras, A., Villarroel, A., Comes, N., Felipe, A. (2012) Targeting of Kv7.5 (KCNQ5)/KCNE channels to surface microdomains of cell membranes. **Muscle Nerve** 45:48-54.

271. Preston, P., Wartosch, L., Gunzel, D., Fromm, M., Kongsuphol, P., Ousingsawat, J., Kunzelmann, K., Barhanin, J., Warth, R., Jentsch, T.J. (2010) Disruption of the K+ channel beta-subunit KCNE3 reveals an important role in intestinal and tracheal Cl- transport. **J Biol. Chem.** 285:7165-7175.

272. Abbott, G.W., Tai, K.K., Neverisky, D.L., Hansler, A., Hu, Z., Roepke, T.K., Lerner, D.J., Chen, Q., Liu, L., Zupan, B., Toth, M., Haynes, R., Huang, X., Demirbas, D., Buccafusca, R., Gross, S.S., Kanda, V.A., Berry, G.T. (2014) KCNQ1, KCNE2, and Na+-coupled solute transporters form reciprocally regulating complexes that affect neuronal excitability. **Sci. Signal.** 7:ra22.

273. Liu, Y., Liu, D., Heath, L., Meyers, D.M., Krafte, D.S., Wagoner, P.K., Silvia, C.P., Yu, W., Curran, M.E. (2001) Direct activation of an inwardly rectifying potassium channel by arachidonic acid. **Mol. Pharmacol.** 59:1061-1068.

274. Brouwer, I.A., Zock, P.L., Camm, A.J., Bocker, D., Hauer, R.N., Wever, E.F., Dullemeijer, C., Ronden, J.E., Katan, M.B., Lubinski, A., Buschler, H., Schouten, E.G. (2006) Effect of fish oil on ventricular tachyarrhythmia and death in patients with implantable cardioverter defibrillators: the Study on Omega-3 Fatty Acids and Ventricular Arrhythmia (SOFA) randomized trial. **JAMA** 295:2613-2619.

275. Vicente, R., Escalada, A., Villalonga, N., Texido, L., Roura-Ferrer, M., Martin-Satue, M., Lopez-Iglesias, C., Soler, C., Solsona, C., Tamkun, M.M., Felipe, A. (2006) Association of Kv1.5 and Kv1.3 contributes to the major voltage-dependent K+ channel in macrophages. **J Biol. Chem** 281:37675-37685.

276. Vicente, R., Coma, M., Busquets, S., Moore-Carrasco, R., Lopez-Soriano, F.J., Argiles, J.M., Felipe, A. (2004) The systemic inflammatory response is involved in the regulation of K(+) channel expression in brain via TNF-alpha-dependent and -independent pathways. **FEBS Lett.** 572:189-194.

277. Chadha, P.S., Jepps, T.A., Carr, G., Stott, J.B., Zhu, H.L., Cole, W.C., Greenwood, I.A. (2014) Contribution of kv7.4/kv7.5 heteromers to intrinsic and calcitonin gene-related peptide-induced cerebral reactivity. **Arterioscler. Thromb. Vasc. Biol.** 34:887-893.

278. Schwake, M., Jentsch, T.J., Friedrich, T. (2003) A carboxy-terminal domain determines the subunit specificity of KCNQ K+ channel assembly. **EMBO Rep.** 4:76-81.

279. Howard, R.J., Clark, K.A., Holton, J.M., Minor, D.L., Jr. (2007) Structural insight into KCNQ (Kv7) channel assembly and channelopathy. **Neuron** 53:663-675.

280. Wickenden, A.D., Zou, A., Wagoner, P.K., Jegla, T. (2001) Characterization of KCNQ5/Q3 potassium channels expressed in mammalian cells. **Br. J Pharmacol.** 132:381-384.

281. Kunzelmann, K., Hubner, M., Schreiber, R., Levy-Holzman, R., Garty, H., Bleich, M., Warth, R., Slavik, M., von, H.T., Greger, R. (2001) Cloning and function of the rat colonic epithelial K+ channel KVLQT1. **J Membr. Biol.** 179:155-164.

282. Kapetanovic, I.M., Yonekawa, W.D., Kupferberg, H.J. (1995) The effects of D-23129, a new experimental anticonvulsant drug, on neurotransmitter amino acids in the rat hippocampus in vitro. **Epilepsy Res.** 22:167-173.

283. Rostock, A., Tober, C., Rundfeldt, C., Bartsch, R., Engel, J., Polymeropoulos, E.E., Kutscher, B., Loscher, W., Honack, D., White, H.S., Wolf, H.H. (1996) D-23129: a new anticonvulsant with a broad spectrum activity in animal models of epileptic seizures. **Epilepsy Res.** 23:211-223.

284. Corbin-Leftwich, A., Mossadeq, S.M., Ha, J., Ruchala, I., Le, A.H., Villalba-Galea, C.A. (2016) Retigabine holds KV7 channels open and stabilizes the resting potential. **J Gen. Physiol** 147:229-241.

285. Wuttke, T.V., Seebohm, G., Bail, S., Maljevic, S., Lerche, H. (2005) The new anticonvulsant Retigabine favors voltage-dependent opening of the Kv7.2 (KCNQ2) channel by binding to its activation gate. **Mol. Pharmacol.**

286. Yeung, S.Y., Greenwood, I.A. (2005) Electrophysiological and functional effects of the KCNQ channel blocker XE991 on murine portal vein smooth muscle cells. **Br. J Pharmacol.** 146:585-595.

287. Zhou, P., Zhang, Y., Xu, H., Chen, F., Chen, X., Li, X., Pi, X., Wang, L., Zhan, L., Nan, F., Gao, Z. (2015) P-retigabine: an N-propargyled retigabine with improved brain distribution and enhanced antiepileptic activity. **Mol. Pharmacol.** 87:31-38.

288. Hoshi, T., Tian, Y., Xu, R., Heinemann, S.H., Hou, S. (2013) Mechanism of the modulation of BK potassium channel complexes with different auxiliary subunit compositions by the omega-3 fatty acid DHA. **Proc. Natl. Acad. Sci. U. S. A** 110:4822-4827.

289. Xiao, Y.F., Ke, Q., Wang, S.Y., Auktor, K., Yang, Y., Wang, G.K., Morgan, J.P., Leaf, A. (2001) Single point mutations affect fatty acid block of human myocardial sodium channel alpha subunit Na+ channels. **Proc. Natl. Acad. Sci. U. S. A** 98:3606-3611.

290. Hoshi, T., Xu, R., Hou, S., Heinemann, S.H., Tian, Y. (2013) A point mutation in the human Slo1 channel that impairs its sensitivity to omega-3 docosahexaenoic acid. **J Gen. Physiol** 142:507-522.

291. Balijepalli, R.C., Delisle, B.P., Balijepalli, S.Y., Foell, J.D., Slind, J.K., Kamp, T.J., January, C.T. (2007) Kv11.1 (ERG1) K+ channels localize in cholesterol and sphingolipid enriched membranes and are modulated by membrane cholesterol. **Channels** 1:263-272.

292. Moreno, C., de la Cruz, A., Valenzuela, C. (2016) In-Depth Study of the Interaction, Sensitivity, and Gating Modulation by PUFAs on K+ Channels; Interaction and New Targets. **Front Physiol** 7:578.

293. Serhan, C.N., Clish, C.B., Brannon, J., Colgan, S.P., Chiang, N., Gronert, K. (2000) Novel functional sets of lipid-derived mediators with antiinflammatory actions generated from omega-3 fatty acids via cyclooxygenase 2-nonsteroidal antiinflammatory drugs and transcellular processing. **J Exp. Med.** 192:1197-1204.

294. Chiang, N., Arita, M., Serhan, C.N. (2005) Anti-inflammatory circuitry: lipoxin, aspirin-triggered lipoxins and their receptor ALX. **Prostaglandins Leukot. Essent. Fatty Acids** 73:163-177.

295. Ji, R.R., Xu, Z.Z., Strichartz, G., Serhan, C.N. (2011) Emerging roles of resolvins in the resolution of inflammation and pain. **Trends Neurosci.** 34:599-609.

296. Connor, K.M., SanGiovanni, J.P., Lofqvist, C., Aderman, C.M., Chen, J., Higuchi, A., Hong, S., Pravda, E.A., Majchrzak, S., Carper, D., Hellstrom, A., Kang, J.X., Chew, E.Y., Salem, N., Jr., Serhan, C.N., Smith, L.E. (2007) Increased dietary intake of omega-3-polyunsaturated fatty acids reduces pathological retinal angiogenesis. **Nat. Med.** 13:868-873.

297. Bang, S., Yoo, S., Yang, T.J., Cho, H., Kim, Y.G., Hwang, S.W. (2010) Resolvin D1 attenuates activation of sensory transient receptor potential channels leading to multiple anti-nociception. **Br. J Pharmacol.** 161:707-720.

298. Arita, M., Yoshida, M., Hong, S., Tjonahen, E., Glickman, J.N., Petasis, N.A., Blumberg, R.S., Serhan, C.N. (2005) Resolvin E1, an endogenous lipid mediator derived from omega-3 eicosapentaenoic acid, protects against 2,4,6-trinitrobenzene sulfonic acid-induced colitis. **Proc. Natl. Acad. Sci. U. S. A** 102:7671-7676.

299. Rajasagi, N.K., Reddy, P.B., Suryawanshi, A., Mulik, S., Gjorstrup, P., Rouse, B.T. (2011) Controlling herpes simplex virus-induced ocular inflammatory lesions with the lipid-derived mediator resolvin E1. **J Immunol.** 186:1735-1746.

300. Chandy, K.G., Wulff, H., Beeton, C., Pennington, M., Gutman, G.A., Cahalan, M.D. (2004) K+ channels as targets for specific immunomodulation. **Trends Pharmacol. Sci.** 25:280-289.

301. Krishnamoorthy, S., Recchiuti, A., Chiang, N., Yacoubian, S., Lee, C.H., Yang, R., Petasis, N.A., Serhan, C.N. (2010) Resolvin D1 binds human phagocytes with evidence for proresolving receptors. **Proc. Natl. Acad. Sci. U. S. A** 107:1660-1665.

302. Hu, H.Z., Xiao, R., Wang, C., Gao, N., Colton, C.K., Wood, J.D., Zhu, M.X. (2006) Potentiation of TRPV3 channel function by unsaturated fatty acids. **J Cell Physiol** 208:201-212.

303. Watanabe, H., Vriens, J., Prenen, J., Droogmans, G., Voets, T., Nilius, B. (2003) Anandamide and arachidonic acid use epoxyeicosatrienoic acids to activate TRPV4 channels. **Nature** 424:434-438.

304. Ghilardi, J.R., Svensson, C.I., Rogers, S.D., Yaksh, T.L., Mantyh, P.W. (2004) Constitutive spinal cyclooxygenase-2 participates in the initiation of tissue injury-induced hyperalgesia. **J Neurosci.** 24:2727-2732.

305. Birnbaum, Y., Ye, Y., Lin, Y., Freeberg, S.Y., Nishi, S.P., Martinez, J.D., Huang, M.H., Uretsky, B.F., Perez-Polo, J.R. (2006) Augmentation of myocardial production of 15-epi-lipoxin-a4 by pioglitazone and atorvastatin in the rat. **Circulation** 114:929-935.

306. Kim, D., Clapham, D.E. (1989) Potassium channels in cardiac cells activated by arachidonic acid and phospholipids. **Science** 244:1174-1176.

307. Funk, C.D., FitzGerald, G.A. (2007) COX-2 inhibitors and cardiovascular risk. **J Cardiovasc. Pharmacol.** 50:470-479.

8. APPENDIX 1: SUPPLEMENTAL MATERIAL

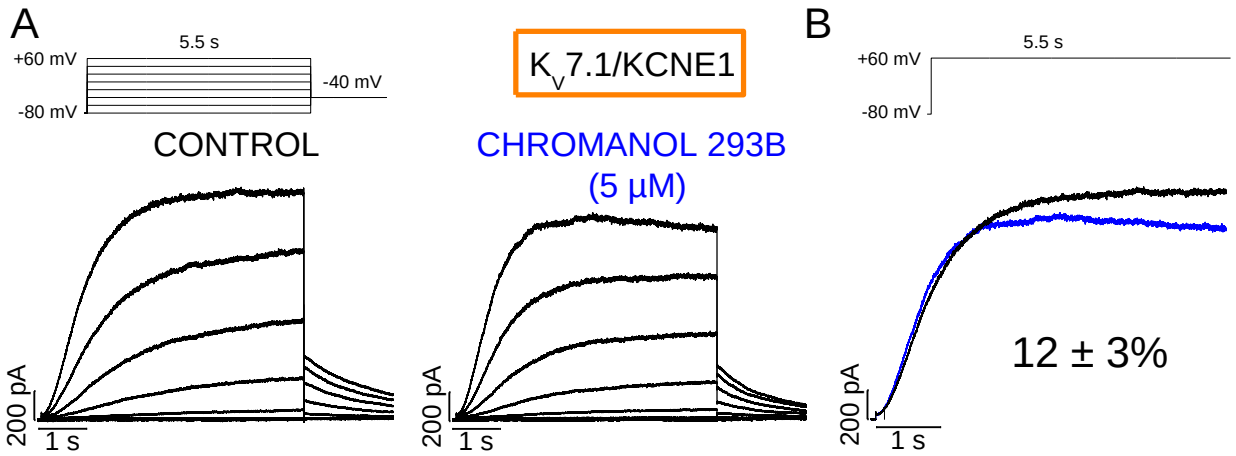

Figure S1: Chromanol 293B effects on K_V7.1/KCNE1 currents. **A:** Representative current records from COS-7 cells co-transfected with K_V7.1/KCNE1. Currents were evoked applying the protocol shown on the top of the figure in the absence or in the presence of 5 µM chromanol 293B. **B:** Representative traces obtained after applying 5.5 s pulses of +60 mV from a holding potential of -80 mV, in the absence (black trace) and in the presence of 5 µM chromanol 293B (blue trace). The percentage of block is shown. Data are shown as the mean ± SEM. *: $P < 0.05$, n= 3

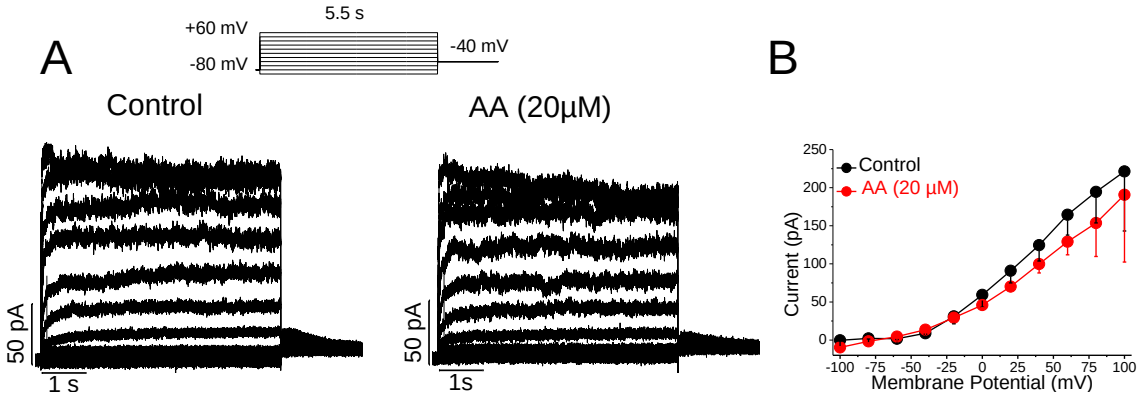

Figure S2: Voltage-dependent effects produced by AA on $K_V7.1$ current. A: Current traces obtained after applying the pulse protocol shown in the top in the absence and in the presence of AA (20 µM). **B:** I-V relationships obtained under control conditions and after perfusion with AA. Data are shown as the mean ± SEM. *: P < 0.05, n= 3

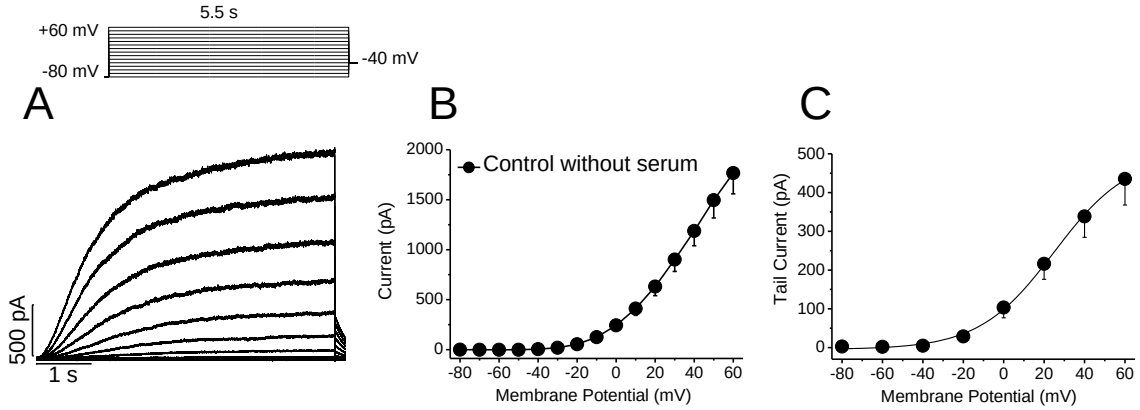

Figure S3: Control conditions in serum-free medium of K_V7.1/KCNE1 currents. A: K_V7.1/KCNE1 original traces recorded after applying depolarizing 5.5-s pulses from a holding potential of -80 mV to +60 mV in 10 mV steps. **B:** I-V relationships obtained measuring the current after 5.5s **C:** Activation curves obtained after representing the maximum tail current amplitude versus the previous step potential. Data are shown as the mean ± SEM, n= 18.

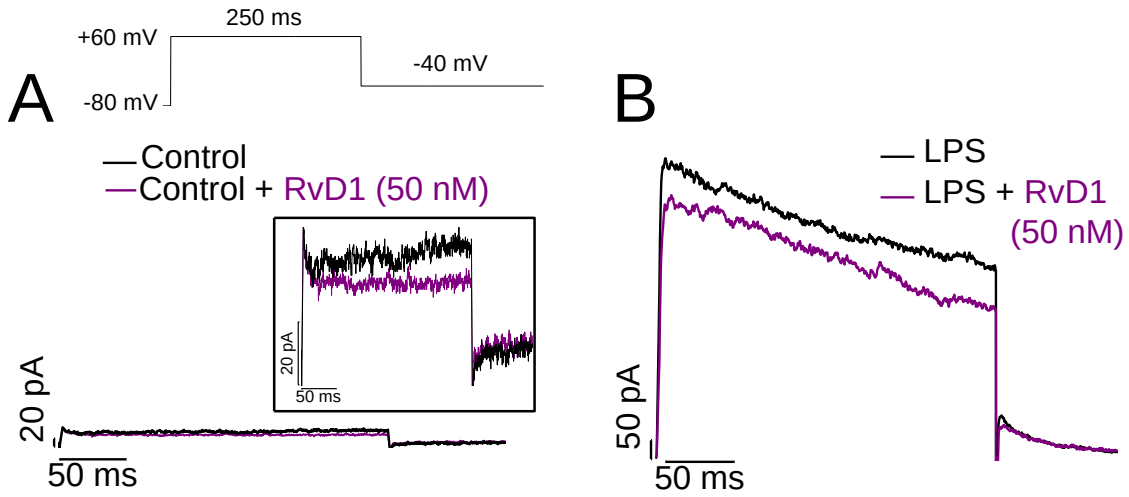

Figure S4: Effects of acute treatment with RvD1 (50nM) on K_V currents in control and LPS-activated BMDM. Representative currents traces of K_V currents recorded from control (resting) and LPS-activated BMDM. Currents were elicited by applying the protocol shown on the top **A:** control (resting) BMDM in the absence and in the presence of RvD1 (50 nM). Inset show the currents bigger to better observation. **B:** LPS-activated BMDM in the absence and in the presence of RvD1 (50 nM). n = 5-6 per group

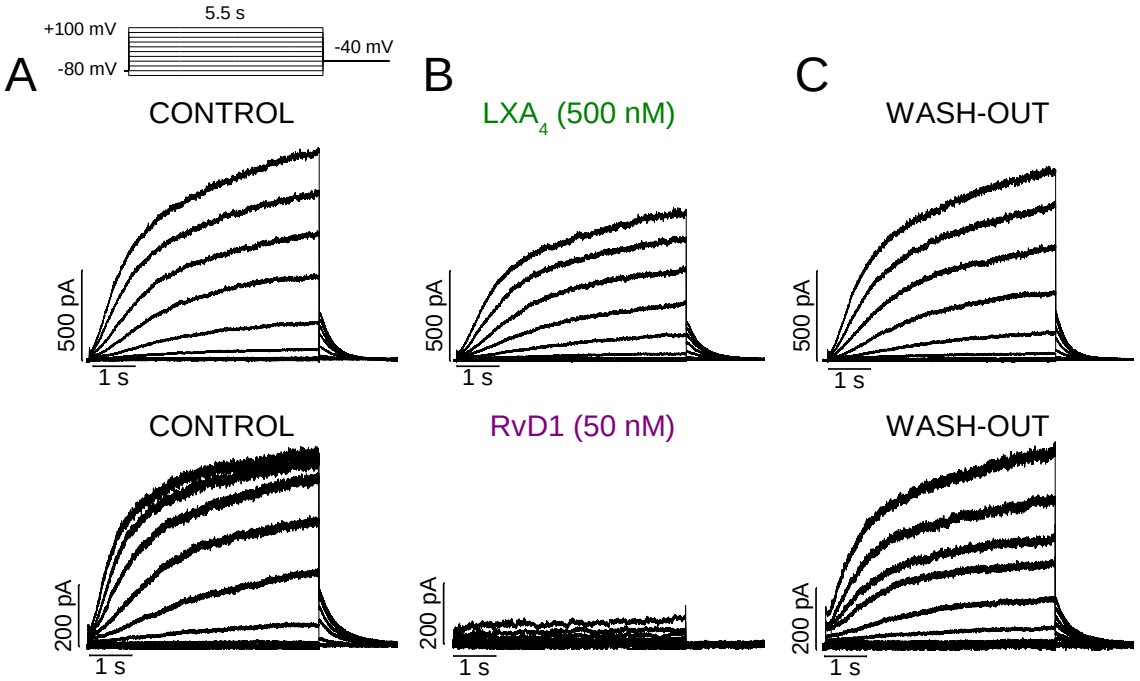

Figure S5: Representative traces of LXA_4 and RvD1 wash-out on $K_V7.1$/KCNE1 current. Current traces were obtained after applying the pulse protocol shown in the top. **A:** $K_V7.1$/KCNE1 current in control conditions, **B:** LXA_4 (top) and RvD1 (bottom) effects on $K_V7.1$/KCNE1 channels **C:** Wash-out effects for both, Activation curves of LXA_4 (top) and RvD1 (bottom) on $K_V7.1$/KCNE1 currents.

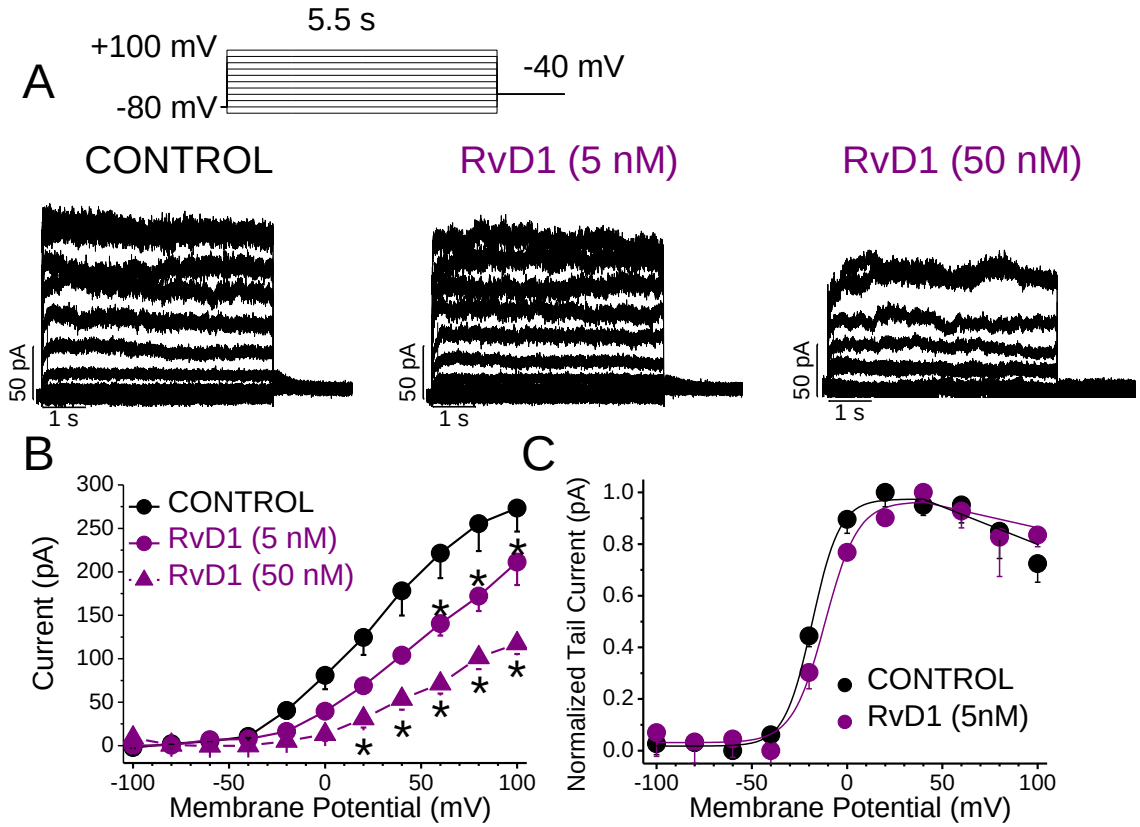

Figure S6: Voltage-dependent effects of RvD1 on $K_V7.1$ channels. **A:** Current traces obtained after applying the pulse protocol shown in the top, in the absence and in the presence of 5 and 50 nM RvD1. **B:** I-V relationships obtained after plotting the current at the end of 5.5-s *vs.* membrane potential, in the absence and in the presence of RvD1 (5 and 50 nM). **C:** Activation curves of $K_V7.1$ current obtained after representing the maximum tail current amplitude *vs.* the previous step potential, recorded in the absence and in the presence of 5 nM RvD1. Data are shown as the mean ± SEM. *P < 0.05, n = 4-6.

9. APPENDIX 2: PUBLICATIONS

9.1 ORIGINAL PAPERS

Modulation of voltage-dependent and inward rectifier potassium channels by 15-Epi-Lipoxin-A4 in activated murine macrophages: implications in innate immunity

Moreno C*, Prieto P*, Macías A*, Pimentel-Santillana M*, de la Cruz A, Través PG, Boscá L, Valenzuela C

Potassium channels modulate macrophage physiology. Blockade of voltage-dependent potassium channels (K_V) by specific antagonists decreases macrophage cytokine production and inhibits proliferation. In the presence of aspirin, acetylated cyclooxygenase-2 loses the activity required to synthesize PGs but maintains the oxygenase activity to produce 15R-HETE from arachidonate. This intermediate product is transformed via 5-LOX into epimeric lipoxins, termed 15-epi-lipoxins (15-epi-lipoxin A4 [e-LXA4]). K_V have been proposed as anti-inflammatory targets. Therefore, we studied the effects of e-LXA4 on signaling and on K_V and inward rectifier potassium channels (Kir) in mice bone marrow-derived macrophages (BMDM). Electrophysiological recordings were performed in these cells by the whole-cell patch-clamp technique. Treatment of BMDM with e-LXA4 inhibited LPS-dependent activation of NF-κB and IκB kinase β activity, protected against LPS activation-dependent apoptosis, and enhanced the accumulation of the Nrf-2 transcription factor. Moreover, treatment of LPS-stimulated BMDM with e-LXA4 resulted in a rapid decrease of K_V currents, compatible with attenuation of the inflammatory response. Long-term treatment of LPS-stimulated BMDM with e-LXA4 significantly reverted LPS effects on K_V and Kir currents. Under these conditions, e-LXA4 decreased the calcium influx versus that observed in LPS-stimulated BMDM. These effects were partially mediated via the lipoxin receptor (ALX), because they were significantly reversed by a selective ALX receptor antagonist. We provide evidence for a new mechanism by which e-LXA4 contributes to inflammation resolution, consisting of the reversion of LPS effects on K_V and Kir currents in macrophages. **J Immunol.** 2013 Dec 15;191(12):6136-46. (*: MC, PP, MA and PM authors contributed equally to this work). **Reviewed in Nature Chemical Biology,** February 2014.

Functional assembly of K_V7.1/K_V7.5 channels with emerging properties on vascular muscle physiology

Oliveras A, Roura-Ferrer M, Sole L, de la Cruz A, Prieto A, Etxebarria A, Manils J, Morales-Cano D, Condom E, Soler C, Cogolludo A, Valenzuela C, Villarroel A, Comes N, Felipe A.

OBJECTIVE:

Voltage-dependent K(+) (K_V) channels from the K_V7 family are expressed in blood vessels and contribute to cardiovascular physiology. Although K_V7 channel blockers trigger muscle contractions, K_V7 activators act as vasorelaxants. K_V7.1 and K_V7.5 are expressed in many vessels. K_V7.1 is under intense investigation because K_V7.1 blockers fail to modulate smooth muscle reactivity. In this study, we analyzed whether K_V7.1 and K_V7.5 may form functional heterotetrameric channels increasing the channel diversity in vascular smooth muscles.

APPROACH AND RESULTS:

K_V7.1 and K_V7.5 currents elicited in arterial myocytes, oocyte, and mammalian expression systems suggest the formation of heterotetrameric complexes. K_V7.1/K_V7.5 heteromers, exhibiting different pharmacological characteristics, participate in the arterial tone. K_V7.1/K_V7.5 associations were confirmed by coimmunoprecipitation, fluorescence resonance energy transfer, and fluorescence recovery after photobleaching experiments. K_V7.1/K_V7.5 heterotetramers were highly retained at the endoplasmic reticulum. Studies in HEK293 cells, heart, brain, and smooth and skeletal muscles demonstrated that the predominant presence of K_V7.5 stimulates release of K_V7.1/K_V7.5 oligomers out of lipid raft microdomains. Electrophysiological studies supported that KCNE1 and KCNE3 regulatory subunits further increased the channel diversity. Finally, the analysis of rat isolated myocytes and human blood vessels demonstrated that K_V7.1 and K_V7.5 exhibited a differential expression, which may lead to channel diversity.

CONCLUSIONS:

K_V7.1 and K_V7.5 form heterotetrameric channels increasing the diversity of structures which fine-tune blood vessel reactivity. Because the lipid raft localization of ion channels is crucial for cardiovascular physiology, K_V7.1/K_V7.5 heteromers provide efficient spatial and temporal regulation of smooth muscle function. Our results shed light on the debate about the contribution of K_V7 channels to vasoconstriction and hypertension. **Arterioscler Thromb Vasc Biol.** 2014 Jul;34(7):1522-30

PKC inhibition results in a K_V1.5+K_Vβ1.3 pharmacology closer to K_V1.5 channels.

Macias A, de la Cruz A, Prieto A, Peraza DA, Tamkun MM, González T, Valenzuela C.

BACKGROUND AND PURPOSE:

The K_Vβ1.3 subunit modifies the gating and pharmacology of K_V1.5 channels in a PKC-dependent manner, decreasing channel sensitivity to bupivacaine- and quinidine-mediated blockade. Cardiac K_V1.5 channels associate with receptor for activated C kinase 1 (RACK1), the K_Vβ1.3 subunit and different PKC isoforms, resulting in the formation of a functional channelosome. The aim of the present study was to investigate the effects of PKC inhibition on bupivacaine and quinidine block of K_V1.5 + K_Vβ1.3 channels.

EXPERIMENTAL APPROACH:

HEK293 cells were transfected with K_V1.5 + K_Vβ1.3 channels, and currents were recorded using the whole-cell configuration of the patch-clamp technique. PKC inhibition was achieved by incubating the cells with either calphostin C or bisindolylmaleimide II and the effects of bupivacaine and quinidine were analysed.

KEY RESULTS:

The voltage-dependent inactivation of K_V1.5 + K_Vβ1.3 channels and their pharmacological behaviour after PKC inhibition with calphostin C were similar to those displayed by K_V1.5 channels alone. Indeed, the IC50 values for bupivacaine were similar in cells whose PKC was inhibited with calphostin C or bisindolylmaleimide II. Similar results were also observed in the presence of quinidine.

CONCLUSIONS AND IMPLICATIONS:

The finding that the voltage-dependence of inactivation and the pharmacology of Kv 1.5 + Kv β1.3 channels after PKC inhibition resembled that observed in Kv 1.5 channels suggests that both processes are dependent on PKC-mediated phosphorylation. These results may have clinical relevance in diseases that are characterized by alterations in kinase activity. **Br J Pharmacol.** 2014 Nov;171(21):4914-26.

Marine n-3 PUFAs modulate IKs gating, channel expression, and location in membrane microdomains.

Moreno C*, de la Cruz A*, Oliveras A, Kharche SR, Guizy M, Ronchi C, Comes N, Rocchetti M, Starý T, Baró I, Loussouarn G, Zaza A, Severi S, Felipe A, Valenzuela C

AIMS:

Polyunsaturated fatty n-3 acids (PUFAs) have been reported to exhibit antiarrhythmic properties.However, the mechanisms of action remain unclear.We studied the electrophysiological effects of eicosapentaenoic acid (EPA) and docosahexaenoic acid (DHA) on IKs, and on the expression and location of Kv7.1 and KCNE1.

METHODS AND RESULTS:

Experiments were performed using patch-clamp, western blot, and sucrose gradient techniques in COS7 cells transfected with Kv7.1/KCNE1 channels. Acute perfusion with both PUFAs increased Kv7.1/KCNE1 current, this effect being greater for DHA than for EPA. Similar results were found in guinea pig cardiomyocytes. Acute perfusion of either PUFA slowed the activation kinetics and EPA shifted the activation curve to the left. Conversely, chronic EPA did not modify Kv7.1/KCNE1 current magnitude and shifted the activation curve to the right. Chronic PUFAs decreased the expression of Kv7.1, but not of KCNE1, and induced spatial redistribution of Kv7.1 over the cell membrane. Cholesterol depletion with methyl-b-cyclodextrin increased Kv7.1/KCNE1 current magnitude. Under these conditions, acute EPA produced similar effects than those induced in non-cholesterol-depleted cells. A ventricular action potential computational model suggested antiarrhythmic efficacy of acute PUFA application under IKr block.

CONCLUSIONS:

We provide evidence that acute application of PUFAs increasesKv7.1/KCNE1 through a probably direct effect, and shows antiarrhythmic efficacy under I_{Kr} block. Conversely, chronic EPA application modifies the channel activity through a change in the Kv7.1/KCNE1 voltage-dependence, correlated with a redistribution of Kv7.1 over the cell membrane. This loss of function may be pro-arrhythmic. This shed light on the controversial effects of PUFAs regarding arrhythmias. **Cardiovasc Res.** 2015 Feb 1;105(2):223-32. (*: Both authors contributed equally to this work)

A new KCNQ1 mutation at the S5 segment that impairs its association with KCNE1 is responsible for short QT syndrome.

Moreno C*, Oliveras A*, de la Cruz A, Bartolucci C, Muñoz C, Salar E, Gimeno JR, Severi S, Comes N, Felipe A, González T, Lambiase P, Valenzuela C.

AIMS:

KCNQ1 and KCNE1 encode K_V7.1 and KCNE1, respectively, the pore-forming and the accessory subunits of the slow delayed rectifier potassium current, I_{Ks}. KCNQ1 mutations are associated with long and short QT syndrome. The aim of this study was to characterize the biophysical and cellular phenotype of a KCNQ1 missense mutation, F279I, found in a 23-year-old man with a corrected QT interval (QTc) of 356 ms and a family history of sudden cardiac death.

METHODS AND RESULTS:

Experiments were performed using perforated patch-clamp, western blot, co-immunoprecipitation, biotinylation, and immunocytochemistry techniques in HEK293, COS-7 cells and in cardiomyocytes transfected with WT K_V7.1/KCNE1 or F279I K_V7.1/KCNE1 channels. In the absence of KCNE1, F279I K_V7.1 current exhibited a lesser degree of inactivation than WT Kv7.1. Also, functional analysis of F279I K_V7.1 in the presence of KCNE1 revealed a negative shift in the activation curve and an acceleration of the activation kinetics leading to a gain of function in I_{Ks}. The co-assembly between F279I K_V7.1 channels and KCNE1 was markedly decreased compared with WT K_V7.1 channels, as revealed by co-immunoprecipitation and Föster Resonance Energy Transfer experiments. All these effects contribute to the increase of I_{Ks} when channels incorporate F279I K_V7.1 subunits, as shown by a computer model simulation of these data that predicts a shortening of the action potential (AP) consistent with the patient phenotype.

CONCLUSION:

The F279I mutation induces a gain of function of I_{Ks} due to an impaired gating modulation of K_V7.1 induced by KCNE1, leading to a shortening of the cardiac AP. **Cardiovasc Res. 2015** Sep 1;107(4):613-23. (*: Both authors contributed equally to this work)

Activating transcription factor 6 derepression mediates neuroprotection in Huntington disease.

Naranjo JR, Zhang H, Villar D, González P, Dopazo XM, Morón-Oset J, Higueras E, Oliveros J C, Arrabal M D, Prieto A, Cercós P, González T, De la Cruz A, Casado-Vela J, Rábano A, Valenzuela C, Gutierrez-Rodriguez M, Li J-Y, Mellström B.

Deregulated protein and Ca^{2+} homeostasis underlie synaptic dysfunction and neurodegeneration in Huntington disease (HD); however, the factors that disrupt homeostasis are not fully understood. Here, we determined that expression of downstream regulatory element antagonist modulator (DREAM), a multifunctional Ca^{2+}-binding protein, is reduced in murine in vivo and in vitro HD models and in HD patients. DREAM downregulation was observed early after birth and was associated with endogenous neuroprotection. In the R6/2 mouse HD model, induced DREAM haplodeficiency or blockade of DREAM activity by chronic administration of the drug repaglinide delayed onset of motor dysfunction, reduced striatal atrophy, and prolonged life span. DREAM-related neuroprotection was linked to an interaction between DREAM and the unfolded protein response (UPR) sensor activating transcription factor 6 (ATF6). Repaglinide blocked this interaction and enhanced ATF6 processing and nuclear accumulation of transcriptionally active ATF6, improving prosurvival UPR function in striatal neurons. Together, our results identify a role for DREAM silencing in the activation of ATF6 signaling, which promotes early neuroprotection in HD. **J Clin Invest.** 2016 Feb;126(2):627-38. **Reviewed in Nature Reviews Drug Discovery (2016; 15: 169).**

Fludarabine inhibits K_V1.3 currents in human B lymphocytes.

de la Cruz A*, Vera-Zambrano*, Peraza D, Pérez-Chacon G, Zapata J, Valenzuela C and Gonzalez T

Fludarabine (F-ara-A) is a purine analog commonly used in the treatment of indolent B cell malignancies that interferes with different aspects of DNA and RNA synthesis. K_V1.3 K+ channels are membrane proteins involved in the maintenance of K+ homeostasis and the resting potential of the cell, thus controlling signaling events, proliferation and apoptosis in lymphocytes. Here we show that F-ara-A inhibits K_V currents in human B lymphocytes. Our data indicate that K_V1.3 is expressed in both BL2 and Dana B cell lines, although total K_V1.3 levels were higher in BL2 than in Dana cells. However, K_V currents in the plasma membrane were similar in both cell lines and were abrogated by the specific K_V1.3 channel inhibitor PAP-1, indicating that K_V1.3 accounts for most of the K_V currents in these cell lines. F-ara-A, at a concentration (3.5 μM) similar to that achieved in the plasma of fludarabine phosphate-treated patients (3 μM), inhibited K_V1.3 currents by 61 ± 6.3% and 52.3 ± 6.3% in BL2 and Dana B cells, respectively. The inhibitory effect of F-ara-A was concentration-dependent and showed an IC_{50} value of 0.36 ± 0.04 μM and a n_H value of 1.07 ± 0.15 in BL2 cells and 0.34 ± 0.13 μM (IC_{50}) and 0.77 ± 0.11 (n_H) in Dana cells. F-ara-A inhibition of plasma membrane K_V1.3 was observed irrespective of its cytotoxic effect on the cells, BL2 cells being sensitive and Dana cells resistant to F-ara-A cytotoxicity. Interestingly, PAP-1, at concentrations as high as 10 μM, did not affect the viability of BL2 and Dana cells, indicating that blockage of K_V1.3 in these cells is not toxic. Finally, F-ara-A had no effect on ectopically expressed K_V1.3 channels, suggesting an indirect mechanism of current inhibition. In summary, our results describe the inhibitory effect of F-ara-A on the activity of K_V1.3 channel. Although K_V1.3 inhibition is not sufficient to induce cell death, further research is needed to determine whether it might still contribute to F-ara-A cytotoxicity in sensitive cells or be accountable for some of the clinical side effects of the drug.

Front Pharmacol. 2017 Mar 31;8:177. (*: Both authors contributed equally to this work)

9.2 REVIEWS

Stereoselective interactions between local anesthetics and ion channels

Valenzuela C, Moreno C, de la Cruz A, Macias A, Prieto A, González T.

Abstract: Local anesthetics are useful probes of ion channel function and structure. Stereoselective interactions are especially interesting because they can reveal three-dimensional relationships between drugs and channels with otherwise identical biophysical and physicochemical properties. Furthermore, stereoselectivity suggests direct and specific receptor-mediated action, and identification of such stereospecific interactions may have important clinical consequences. The fact that drug targets are able to discriminate between the enantiomers present in a racemic drug is the consequence of the ordered asymmetric macromolecular units that form living cells. However, almost 25% of the drugs used in the clinical practice are racemic mixtures, and their individual enantiomers frequently differ in both their pharmacodynamic and pharmacokinetic profiles. Moreover, their effects can be similar to or different from the pharmacological effect of the drug and may contribute to the undesired effects of the drug. In other cases, the pharmacological effects induced by the two enantiomers on the molecular target are opposite. In the present manuscript, we will review the stereoselective effects of bupivacaine-like local anesthetics on cardiac sodium and potassium channels. **Chirality.** 2012 Nov;24(11):944-50.

Effects of n-3 polyunsaturated fatty acids on cardiac ion channels.

Moreno C, Macías A, de la Cruz A, Prieto A, González T, Valenzuela C.

Dietary n-3 polyunsaturated fatty acids (PUFAs) have been reported to exhibit antiarrhythmic properties, and these effects have been attributed to their capability to modulate ion channels. In the present review, we will focus on the effects of PUFAs on a cardiac sodium channel (Na(v)1.5) and two potassium channels involved in cardiac atrial and ventricular repolarization (K(v)) (K(v)1.5 and K(v)11.1). n-3 PUFAs of marine (docosahexaenoic, DHA and eicosapentaenoic acid, EPA) and plant origin (alpha-linolenic acid, ALA) block K(v)1.5 and K(v)11.1 channels at physiological concentrations. Moreover, DHA and EPA decrease the expression levels of K(v)1.5, whereas ALA does not. DHA and EPA also decrease the magnitude of the currents elicited by the activation of Na(v)1.5 and calcium channels. These effects on sodium and calcium channels should theoretically shorten the cardiac action potential duration (APD), whereas the blocking actions of n-3 PUFAs on K(v) channels would be expected to produce a lengthening of cardiac action potential. Indeed, the effects of n-3 PUFAs on the cardiac APD and, therefore, on cardiac arrhythmias vary depending on the method of application, the animal model, and the underlying cardiac pathology. **Front Physiol.** 2012 Jul 9;3:245.

Polyunsaturated fatty acids modify the gating of Kv channels.

Moreno C, Macías A, Prieto A, de la Cruz A, Valenzuela C

Polyunsaturated fatty acids (PUFAs) have been reported to exhibit antiarrhythmic properties, which are attributed to their capability to modulate ion channels. This PUFAs ability has been reported to be due to their effects on the gating properties of ion channels. In the present review, we will focus on the role of PUFAs on the gating of two Kv channels, Kv1.5 and Kv11.1. Kv1.5 channels are blocked by n-3 PUFAs of marine [docosahexaenoic acid (DHA) and eicosapentaenoic acid] and plant origin (alpha-linolenic acid, ALA) at physiological concentrations. The blockade of Kv1.5 channels by PUFAs steeply increased in the range of membrane potentials coinciding with those of Kv1.5 channel activation, suggesting that PUFAs-channel binding may derive a significant fraction of its voltage sensitivity through the coupling to channel gating. A similar shift in the activation voltage was noted for the effects of n-6 arachidonic acid (AA) and DHA on Kv1.1, Kv1.2, and Kv11.1 channels. PUFAs-Kv1.5 channel interaction is time-dependent, producing a fast decay of the current upon depolarization. Thus, Kv1.5 channel opening is a prerequisite for the PUFA-channel interaction. Similar to the Kv1.5 channels, the blockade of Kv11.1 channels by AA and DHA steeply increased in the range of membrane potentials that coincided with the range of Kv11.1 channel activation, suggesting that the PUFAs-Kv channel interactions are also coupled to channel gating. Furthermore, AA regulates the inactivation process in other Kv channels, introducing a fast voltage-dependent inactivation in non-inactivating Kv channels. These results have been explained within the framework that AA closes voltage-dependent potassium channels by inducing conformational changes in the selectivity filter, suggesting that Kv channel gating is lipid dependent. **Front Pharmacol.** 2012 Sep 10;3:163.

In-depth study of the interaction, sensitivity and gating modulation by PUFAs on K+ channels; interaction and new targets.

Moreno C, de la Cruz A, Valenzuela C.

Voltage gated potassium channels (K_V) are membrane proteins that allow selective flow of K+ ions in a voltage-dependent manner. These channels play an important role in several excitable cells as neurons, cardiomyocytes, and vascular smooth muscle. Over the last 20 years, it has been shown that omega-3 polyunsaturated fatty acids (PUFAs) enhance or decrease the activity of several cardiac KV channels. PUFAs-dependent modulation of potassium ion channels has been reported to be cardioprotective. However, the precise cellular mechanism underlying the cardiovascular benefits remained unclear in part because new PUFAs targets and signaling pathways continue being discovered. In this review, we will focus on recent data available concerning the following aspects of the K_V channel modulation by PUFAs: (i) the exact residues involved in PUFAs-K_V channels interaction; (ii) the structural PUFAs determinants important for their effects on KV channels; (iii) the mechanism of the gating modulation of KV channels and, finally, (iv) the PUFAs modulation of a few new targets present in smooth muscle cells (SMC), KCa1.1, K2P, and KATP channels, involved in vascular relaxation. **Front Physiol.** 2016 Nov 24;7:578.

9.3 PUBLICATIONS IN PROGRESS

D242N, a KV7.1 LQTS mutation uncovers a key residue for IKs voltage dependence.

Moreno C*, Oliveras A*, Bartolucci C, Muñoz C, de la Cruz A, Peraza DA, Gimeno JR, Martín-Martínez M, Severi S, Felipe A, Lambiase PD, González T, Valenzuela C.

J Mol Cell Cardiol (JMCC10487-R1, En revisión)

Fludarabine inhibits K_V1.3 currents in chronic lymphocytic leukemia cells: implications to fludarabine refractoriness. Perez-Chacon G*, Peraza DA*, Vera-Zambrano A, de la Cruz A, Acosta-Iborra B, Martinez-Laperche C, Muñoz-Calleja C, Buño I, Valenzuela C, Zapata JM, Gonzalez T.

Kinase C inhibition decreases Kv1.5 recycling.

Macias A*, de la Cruz A*, Prieto A, González T, Valenzuela C. (*: Both authors contributed equally to this work)

Retigabine stabilizes the open state of K_V7.1/ K_V7.5 channels.

De la Cruz A, Oliveras A, Felipe A, Valenzuela C.

Modulation of K_V7.1-KCNE1 induced by n-3 and n-6 PUFAs metabolites

de la Cruz A, Peraza DA, García C, Lillo MP, Valenzuela C.